SYNTHESIS AND CHARACTERIZATION OF NOVEL UNNATURAL PEPTIDE INHIBITORS OF THROMBIN ACTIVATION OF PLATELET AGGREGATION

by

Fernanda Ferraccioli Marques Burke

A dissertation submitted in partial fulfillment
of the requirements for the degree of
Doctor of Philosophy
(Medicinal Chemistry)
in the University of Michigan
2007

Doctoral Committee:

Professor Henry I. Mosberg, Chair
Professor Ronald W. Woodard
Associate Professor Barry E. Bleske
Associate Professor George A. Garcia

To my devoted family and my loyal friends who have supported me, guided me, inspired me, cared for me and loved me throughout.

ACKNOWLEDGEMENTS

I wish to extend my sincere gratitude to a number of individuals who have not only played a role in my scientific development, but have helped me grow as a person of strength and character. I would like to start by thanking my parents, Telma and Celestino Marques. I am tremendously privileged to have parents that have given their all to and are as invested in my educational achievements as I am. You have been instrumental in my journey from infancy, and I know this is as much a victory for you as it is for me. I feel enormously proud to have achieved our dream. I would also like to thank my brother, Dr. Bruno Marques, for being a loyal and supportive big brother. I did not anticipate that our career choices would provide me with not only a friend, but also a peer and a mentor. Your readiness to share your every experience, both successes and failures, with me in order to help me along the way has been invaluable.

I would like to extend my gratitude to my advisor, Dr. Henry I. Mosberg, for his unwavering support and commitment through the progression of my research project and academic career. Your expert guidance and sensible advice have immensely contributed to the success of this project and to my scientific readiness. Before coming to the University of Michigan, I knew that I wanted to work in Dr. Mosberg's laboratory, and I was very fortunate to have this opportunity.

I wish to thank the members of my Doctoral Committee (Dr. Ronald W. Woodard, Dr. George A, Garcia, and Dr. Barry E. Bleske) for their willingness to share

their time and their valuable suggestions in the preparation of this research effort and dissertation. This project was generously funded by the Pharmacological Sciences Training Program, the Mr. and Mrs. Edward S. Blake Fellowship, the Sheila B. Creswell Fellowship in Medicinal Chemistry, and the Fred W. Lyons Fellowship.

I reserve special thanks for Kate Kojiro and John Omnaas for their everlasting patience and their invaluable counsel and assistance. I feel extremely privileged to have gotten to learn from two of the most knowledgeable and practical researchers in the College of Pharmacy. I have personally benefited from their camaraderie, friendship, and unique personalities. I would also like to acknowledge the students and researchers of the Mosberg group who have shared their time and expertise with me through out the past five years. You have created a wonderful environment where work has been both productive and enjoyable.

Moving to Ann Arbor has been a wonderful personal experience as I have met a brilliant group of people. The Medicinal Chemistry students are diverse and dynamic, and I have tremendously enjoyed getting to know each individual. I have learned a vast deal from our interactions, and that has greatly enriched my graduate school experience. I have made lifelong friendships that have gotten me through the best and worse of times. I would like to thank two friends in particular, Dr. Parag Aggarwal and Kelly L. Damm, who are outstanding people and talented scientists. I do not use the term “friendship” lightly, but you both have been integral to my success and happiness through the years.

Lastly, I am immeasurably thankful to my husband and best friend, Joe Burke. Your unconditional love, care, and support have allowed me to become a stronger and more resilient person. Having you by my side throughout this challenging experience has

made every bump and bruise bearable and the future always bright. I thank you not only for the emotional support, but also the technical assistance necessary to bring my ideas to life. We make a great team, and I am certain that this is just the first milestone of a lifetime filled with success, happiness, joy, and laughter for us.

TABLE OF CONTENTS

LIST OF FIGURES

Figure

LIST OF TABLES

Table

LIST OF APPENDICES

Appendix

LIST OF ABBREVIATIONS

ACE	angiotensin-converting enzyme
AcOH	acetic acid
ACS	acute coronary syndrome
ADP	adenosine diphosphate
AGG	platelet aggregation assay
AMI	acute myocardial infarction
APC	activated protein kinase C
APTT	activated partial thromboplastin time
AT	antithrombin
AUC	area under the curve
Boc	*tert*-butyloxycarbonyl
*t*Bu	*tert*-butyl
˚C	degrees centigrade
Ca^{2+}	calcium ion
$CaCl_2$	calcium chloride
Cbz (Z)	benzyloxycarbonyl
CNBr	cyanogen bromide
C_p	plasma concentration of a drug
Da	Dalton
DCM	dichloromethane
Dde	*N*-[1-(4,4-dimethyl-2,6-dioxocyclohex-1-ylidene)ethyl]
DIC	diisopropylcarbodiimide
DIEA	diisopropylethylamine
DMF	dimethylformamide

D_2O	deuterium oxide
DTI	direct thrombin inhibitor
DVT	deep vein thrombosis
ESI-MS	electron spray ionization mass spectrometer
Et	ethyl
EtOAc	ethyl acetate
5-FAM	5-carboxyfluorescein
Fmoc	9-fluorenylmethyloxycarbonyl
Fmoc-OSu	*N*-(9-fluorenylmethoxycarbonyloxy) succinimide
g	grams
GP	glycoprotein
HBr	hydrobromic acid
HBTU	O-benzotriazole-*N*,*N*,*N'*,*N*'-tetramethyl-uronium-hexafluoro-phosphate
HCII	heparin cofactor II
HCl	hydrochloric acid
HEPES	(4-(2-hydroxyethyl)-1-piperazineethanesulfonic acid
^{1}H-NMR	proton nuclear magnetic resonance spectroscopy
HOBt	1-hydroxybenzotriazole
hr	hour
Hz	hertz
IC_{100}	concentration at 100% inhibition
IND	investigative new drug
IP	intraperitoneal
IPTG	isopropyl-beta-D-thiogalactopyranoside
KCl	potassium chloride
KH_2PO_4	monobasic potassium phosphate
K_i	inhibition binding constant
KSI	ketosteroid isomerase
L	liter

LC-MS	liquid chromatography mass spectrometer
LMWH	low-molecular weight heparin
log D_{pH7}	octanol:water partition coefficient
M	molar (moles per liter)
MeOH	methanol
MES	2-(*N*-morpholino)-ethane sulphonic acid
mg	milligram
µg	microgram
mL	milliliter
µL	microliter
mmol	millimole
mol	mole
Mg^{2+}	magnesium ion
Mtr	4-methoxy-2,3,6-trimethylbenzenesulfonyl
Mtr-Cl	4-methoxy-2,3,6-trimethylbenzenesulfonyl chloride
N	normal (equivalent per liter)
N_2	nitrogen
NaCl	sodium chloride
Na_2CO_3	sodium carbonate
$NaHCO_3$	sodium bicarbonate
NaH_2PO_4	monobasic sodium phosphate
NaOH	sodium hydroxide
NE	no effect
NH_4OH	ammonium hydroxide
NI	no inhibition
nm	nanometer
NMP	*N*-methylpyrrolidinone
PAL-PEG-PS	peptide amide linker polyethylene glycol polystyrene
PAR	protease-activated receptor
$rPAR1_{EC}$	recombinant PAR1 exodomain
$rPAR4_{EC}$	recombinant PAR4 exodomain

Pbf	2,2,4,6,7-pentamethyldihydrobenzofuran-5-sulfonyl
PBS	phosphate buffered saline
*p*Na	*para*-nitroanalide
PPP	platelet poor plasma
PRP	platelet rich plasma
PS	protein S
PT	prothrombin time
rOicPaF(*p*-Me)	D-Arg-Oic-Pro-D-Ala-Phe(*p*-Me)-NH_2
rOicPaF(*p*-Me)K-biotin	D-Arg-Oic-Pro-D-Ala-Phe(*p*-Me)-Lys(biotin)-NH_2
RP-HPLC	reverse phase-high performance liquid chromatography
RPPGF	arginine-proline-proline-glycine-phenylalanine
S-S	disulfide bond
S-Et-S	ethylene dithioether
SEM	standard error of the mean
SERPIN	plasma serine protease inhibitor
$t_{1/2}$	half life
TCT	thrombin clotting time
TF	tissue factor
TFA	trifluoroacetic acid
TFPI	tissue factor pathway inhibitor
TLC	thin layer chromatography
TM	thrombomodulin
Tris	tris(hydroxymethyl)aminomethane
Trt	trityl
turbo-TMB	turbo-3,3',5,5'-tetramethylbenzidine
v/v	volume (mL)/volume (mL)
VTE	venous thromboembolism
w/v	weight (gram)/volume (mL)

ABSTRACT

Inhibitors of the activation of platelet aggregation have promise as important therapeutic agents for the management of acute coronary syndrome. Platelet activation by thrombin occurs by binding to and cleavage of the extracellular N-terminal domains of protease-activated receptors 1 and 4 (PAR1 and PAR4). The proteolysis of the PARs exposes new tethered ligands that then signal through transmembrane domains to initiate platelet activation. A pentapeptide cleavage product of bradykinin with the sequence Arg-Pro-Pro-Gly-Phe (RPPGF) serves as an inhibitor of α- and γ-thrombin-induced platelet aggregation.

Analogs of RPPGF were prepared that result in improved inhibition of thrombin activation of platelets. Specific amino acid residues required for activity against platelet aggregation have been identified, and a lead compound, D-Arg-Oic-Pro-D-Ala-Phe(*p*-Me)-NH_2 (**27**), has been developed. Compound **27**, which completely inhibits threshold γ-thrombin-induced platelet aggregation at a concentration of 16 μM, represents an important lead compound in the development of inhibitors of thrombin-mediated platelet aggregation.

The mechanism of action of compound **27** was studied, and there is a clear interaction with the active site of thrombin, as well as preliminary results that indicate analog **27** is binding to PAR1. In addition, due to its composition of unnatural amino acid residues, **27** is orally available with 12.7% bioavailability in rat models. In order to

improve upon this bioavailability, a new series of peptides with modified N- and C-termini, di-substituted phenylalanine, and methylated arginine analogs designed to reduce the net charge and/or increase the lipophilicity of the peptide was prepared.

These modifications were well tolerated and a new lead compound was discovered. Compound **48** (D-Arg-Oic-Pro-D-Ala-Phe(*p*-Me)-NH-Et) has the same amino acid sequence as analog **27**, but possesses an ethyl group at the amide of the C-terminus. This compound is a 3-fold more potent inhibitor of thrombin and platelet aggregation than is **27** (K_i = 2.1 μM, IC_{100} = 5 μM). This dissertation has shown the benefits of substituting unnatural amino acid residues into the sequence of a naturally occurring peptide as a means of modulating activity and developing analogs with desirable pharmacokinetic profiles. Compounds **27** and **48** demonstrate promise to become the first orally administered direct thrombin inhibitor.

CHAPTER I

INTRODUCTION

The development of safe and effective treatment options for thrombotic disorders has proven elusive for over half a century. The problem certainly lies in the complexity of the hemostatic system, which maintains the balance between thrombus formation and blood flow primarily through the action of a serine protease known as thrombin. Inhibition of this enzyme would be beneficial for the treatment and prevention of a multitude of diseases including acute myocardial infarction, the leading cause of death in the United States. Currently available treatments are plagued with side effects, dosage maintenance difficulties, and undesirable delivery methods. Consequently, there is great medicinal potential for the design and synthesis of a novel anticoagulant agent that is both potent and selective with minimal side effects.

MEDICAL BENEFITS OF ANTICOAGULANT THERAPY. Perhaps the most promising application of a novel anticoagulant agent would be as a means of preventing acute coronary syndrome (ACS). ACS refers to a number of conditions that arise from myocardial ischemia, which most often develops as a result of reduced blood supply due to ruptured atherosclerotic plaque in the coronary artery of the heart[1, 2]. ACS covers a spectrum of clinical conditions ranging from unstable angina to acute myocardial

infarction. Acute myocardial infarction (AMI) is the leading cause of death for both men and women in the United States comprising 36.3% of all deaths in 2004[3]. AMI refers to the rapid development of myocardial necrosis often resulting from plaque rupture with thrombus formation in a coronary vessel. This leads to an acute reduction of blood supply to a portion of the myocardium[1, 2]. Every year an estimated 1.7 million Americans suffer a heart attack of which approximately 90% result from an acute thrombus that obstructs an atherosclerotic coronary artery[1, 4]. Therefore, by modulating the activity of the hemostatic system, we can attempt to treat and prevent these serious and often fatal medical conditions.

Venous thromboembolism (VTE) is a collective term used to describe a number of medical conditions that result from abnormal thrombosis including deep vein thrombosis (DVT) and pulmonary embolism. The incidence rate of VTE in Caucasians exceeds 1 in 1,000 persons in the United States with the risk of occurrence increasing to 1 in 100 for those over the age of 75 years[5-7]. VTE is caused by three major factors: blood hypercoagulability (excessive clotting), blood-flow stasis (immobility), and vessel wall damage (atherosclerosis)[5]. Anticoagulant treatment is absolutely required in order to maintain proper blood circulation in patients with predisposition for these conditions, those who have suffered from trauma and/or immobilization, and those on certain medications including hormone replacement therapy[8]. Current available treatments require constant clinical monitoring due to the variation in individual response to the drugs[9]. A new generation of anticoagulants could potentially revolutionize the treatment options for thrombotic disorders.

The third major cause of death in the Western world is stroke with 700,000 cases each year in the United States[10, 11]. Stroke occurs when the blood supply to a region of the brain is interrupted leading to sudden loss of neuronal function and subsequent cell death. Approximately 15-25% of all strokes are associated with abnormalities in the cardiovascular system causing the formation of a secondary embolus that reaches the cerebral circulation resulting in ischemia and neuronal damage[12, 13]. Cardioembolic strokes are often treatable with anticoagulants following atrial fibrillation, intracardial thrombus or endocarditis[14]. Consequently, the development of a safe and effective anticoagulant has the potential of treating stroke by reducing the incidence of detached thrombi in patients with high risk factors such as race, hypertension, diabetes, and high cholesterol levels[15].

HEMOSTASIS. A thorough understanding of the hemostatic system is essential in order to design and develop a new anticoagulant agent. The hemostatic system refers to the complex assembly in which serine proteases gather at the cell membrane receptors where they arrange into complexes with cofactors leading to a series of regulated enzymatic reactions[16, 17]. The final product is a hemostatic thrombus or plug that halts the bleeding at the site of damaged endothelium. The hemostatic system spurs into action through the activation of two distinct responses: the activation of the factor VII-tissue factor complex and the aggregation of circulating platelets[16, 17]. The two responses combined produce the hemostatic plug, which is composed of aggregated platelets and deposited fibrin. The regulation of these distinct responses requires coordination between the platelet and coagulation activation pathways, and such coordination is achieved through the

employment of the plasma protease, thrombin[18]. Thrombin is the vital link between these two systems.

THROMBIN AND THE COAGULATION SYSTEM. Thrombin, a serine protease containing 308 amino acids, is the main effector protease of the coagulation system, which includes a series of zymogen transformations culminating in the conversion of soluble fibrinogen into insoluble fibrin[19]. Biological amplification is achieved by converting substrates (zymogens) into active serine proteases, which then serve as enzymes in the next reaction in the cascade. The series of reactions that comprise blood coagulation is initiated by the activation of the factor VIIa-tissue factor complex that in turn activates factor IX to IXa in the presence of factor VIII (see Figure 1). Factors IXa and VIIIa assemble in a complex known as tenase in order to activate factor X to factor Xa[16, 20]. Factor Xa assembles with factor V in the prothrombinase complex to convert prothrombin into thrombin. Thrombin then converts soluble fibrinogen to a fibrin clot. If there is a need for more thrombin, thrombin can activate factor XI to factor XIa that then activates factor IX, amplifying the system. Thrombin generates fibrin deposits at sites of bleeding, contributing to the fibrinous portion of the hemostatic plug[21].

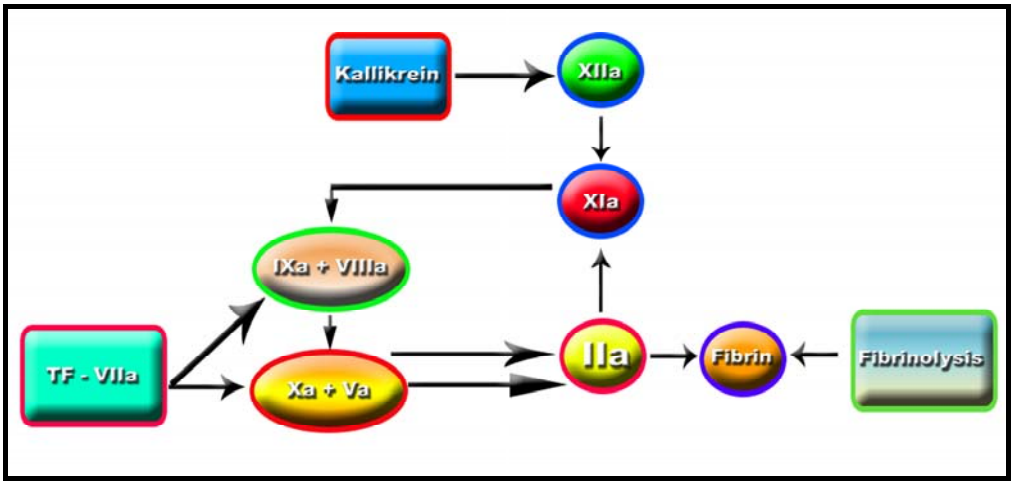

Figure 1: Review of the hemostatic system[16].

As alluded to above, thrombin is a serine protease activated by the cleavage of prothrombin in a series of proteolytic activations of several zymogens. After cleavage, the newly formed enzyme has an overall ellipsoid-like structure, and is composed of a small A-chain and a catalytic B-chain[20, 22]. The catalytic triad of thrombin consists of the characteristic residues His, Asp, and Ser that are located at the canyon-like cleft of the catalytic pocket[20, 23]. However, thrombin's catalytic activity is not only dictated by the catalytic site, but also by recognition sites involved in regulating the specificity of the enzyme for its various substrates. There are two recognition sites that play central roles in the function of thrombin: the fibrinogen recognition site (exosite I) and the heparin-binding site (exosite II). Exosite I consists of the loop Arg^{67}-Ile^{82} of the B-chain and helps in the recognition of the substrate fibrinogen along with thrombomodulin and protease-activated receptor 1 (PAR1)[19, 20]. Exosite II is the glycosaminoglycan binding site of thrombin located at the C-terminus of the B-chain, which binds to glycoprotein Ib and heparin, a thrombin inhibitor[19, 20]. Understanding of the interactions between thrombin and its substrate is crucial in the identification and design of novel medicinal agents that

would interact and modulate the activity of the enzyme. Figure 2 illustrates the active site of thrombin along with both recognition sites.

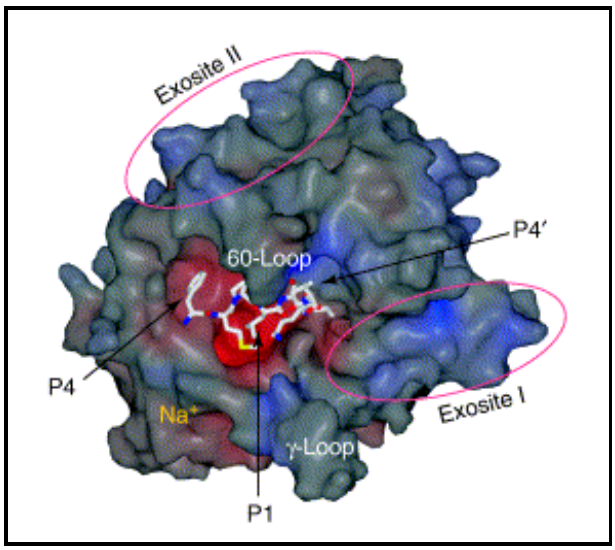

Figure 2: Surface representation of thrombin with HCII bound at the active site. The colors represent the electrostatic potential with blue representing positive charge and red denoting negative charge[19].

An important aspect of thrombin action in the hemostatic system is that it has both anticoagulant and pro-coagulant activity. In the absence of injury or stimulation, endothelial cells in the intravascular compartment are an anticoagulant surface that ensures the fluidity of the circulating blood as well as limit intravascular coagulation[16, 24]. Two systems are primarily responsible for regulating thrombin anti- and pro-coagulant activity. The first system, protein C and protein S, provides an indirect approach to the regulation of thrombin activity. Protein C, a vitamin-K dependent protein, is activated by thrombin on endothelial cell membranes by binding of both proteins to an endothelial cell protein, thrombomodulin[16, 24-26]. Activated protein C (APC) acts as an inhibitor of factors Va and VIIIa, two cofactors of thrombin, thus decreasing the rate of thrombin formation[16, 24]. Protein S acts as a cofactor for APC, serving as APC's receptor to localize its inhibitory activity[25]. Initially, thrombin

generation in the intravascular compartment results in protein C activation, limiting the amount of thrombin formed. Thus thrombin initially acts as an anticoagulant. However, the anticoagulant function of thrombin is limited by a finite number of thrombomodulin binding sites. If the amount of thrombin exceeds the number of thrombomodulin binding sites, then thrombin becomes a physiologic pro-coagulant enzyme[26]. Figure 3 depicts the activation and inhibitory action of the protein C and protein S anticoagulant system.

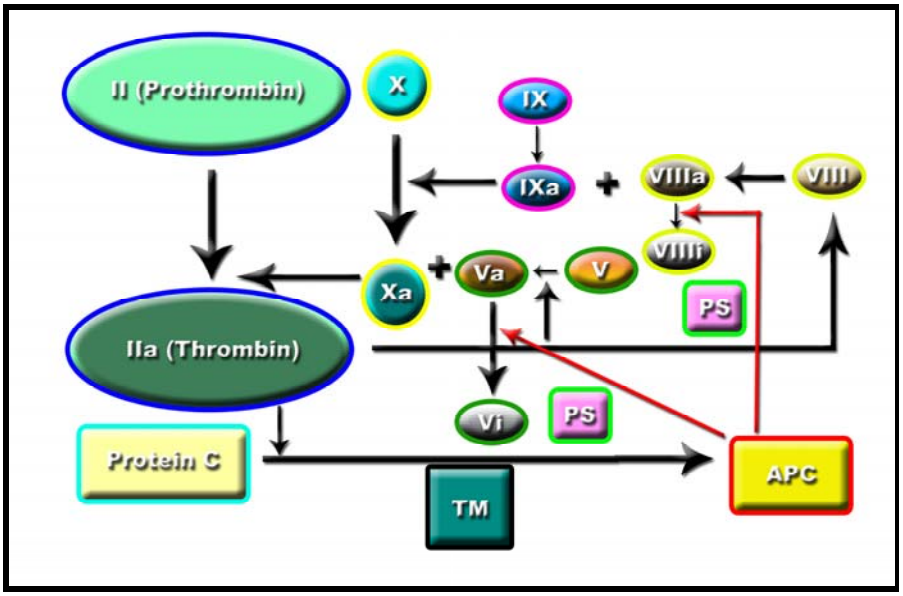

Figure 3: The protein C and protein S anticoagulant system[16].

The second anticoagulant system that regulates thrombin activity is the plasma serine protease inhibitor (SERPIN) simply known as antithrombin (AT). This protein operates by directly interacting with the active site of thrombin as well as the other major coagulation enzymes (factors Xa, VIIa, IXa, XIa, XIIa, and plasma kallikrein)[19, 25]. AT primarily inhibits factors Xa and VIIa, obstructing the formation of both the tenase and prothrombase complexes, the two critically important kinetic platforms for physiologic activation of the coagulation system. A cofactor for antithrombin activity is heparin,

which renders the inhibitor 1,000-fold more potent when it is present[16, 25]. Thrombin is also regulated by a second SERPIN, heparin cofactor II. This latter protein is a specific thrombin inhibitor whose activity is potentiated by the glycosaminoglycan, dermatan sulfate.

Thrombin also has an important role in platelet activation and aggregation by initiating a wide range of platelet responses such as shape change, release of granules, mobilization of adhesion molecules (P-selectin) to the platelet surface, and activation of glycoprotein (GP) IIb/IIIa and GP Ib[27-29]. Thrombin has two substrates on human platelets, protease-activated receptors 1 and 4, that when stimulated lead to platelet activation. Thrombin's interaction with these proteins is an enzyme-substrate interaction like the enzyme's interaction with other proteins. Platelets play a key role in the development of acute myocardial syndrome and coronary artery occlusion due to their ability to aggregate in large numbers at the site of injury[2, 30].

PAR FAMILY AND ITS INTRACELLULAR SIGNALING. The protease-activated receptors (PARs) were identified as G protein-coupled receptors that use an unusual mechanism to convert an extracellular proteolytic cleavage event into a transmembrane signal. These receptors carry their own ligand, which remains cryptic until the receptor is cleaved by thrombin[31-33]. Figure 4 depicts the activation of the PAR family by thrombin. This family includes four receptors known as PAR1, PAR2, PAR3, and PAR4, three of which (PAR1, PAR3, and PAR4) are cleaved by thrombin while PAR2 is cleaved by trypsin and tryptase[34]. PAR2 is a receptor expressed in the gastrointestinal tract that

once activated leads to smooth muscle contraction and release of prostaglandin suggesting a role in gastric motility[35].

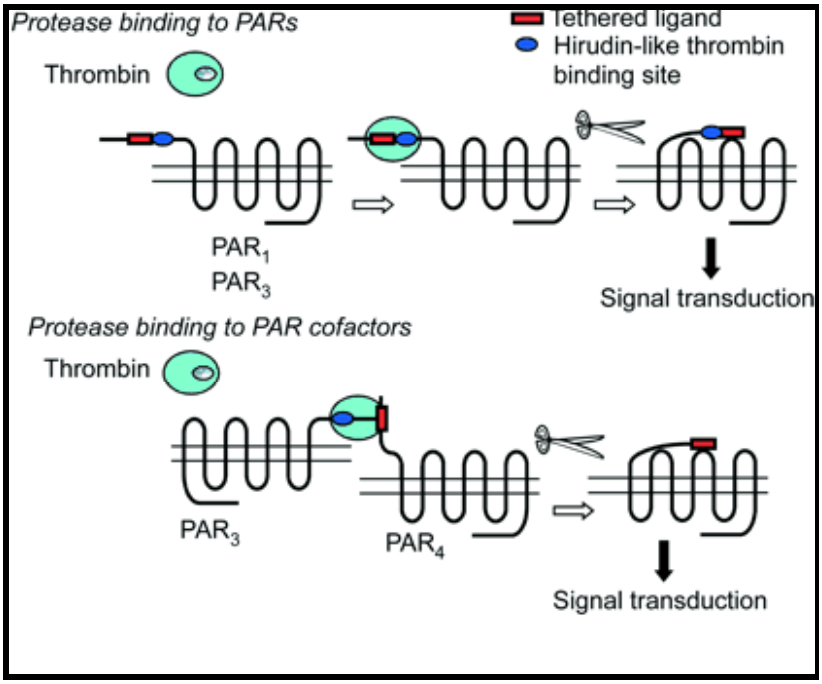

Figure 4: Mechanism of PAR1 and PAR4 activation by thrombin[34, 36].

PAR1 and PAR4 are found on the surface of human platelets and are the main mediators of thrombosis, while PAR3 serves solely as a facilitator of the cleavage of PAR4 in murine cells[27, 34, 37-39]. PAR4 differs from PAR1 in the lack of a downstream hirudin-like domain that is important for the interaction with the anion-binding exosite I of thrombin[40, 41]. Since PAR4 does not contain this consensus sequence for thrombin binding, PAR1 binds more tightly to thrombin and 100-fold lower concentration of the latter is necessary for activation compared to PAR4[34, 40-42]. On the other hand, PAR3 contains the consensus sequence for thrombin binding, indicating that it can bind to the enzyme and when paired with PAR4 may help modulate its activity[33, 43]. It has been shown that PAR1 and PAR4 do not play redundant roles during platelet activation, but

rather complement each other's response. PAR1 generates the initial response at nanomolar concentrations of thrombin while PAR4 maintains the signal once the concentration has diminished[39, 44].

In addition to the presence or absence of the upstream thrombin binding domain, the amino acid sequence surrounding the cleavage site of PAR1 and PAR4 are also completely different. The PAR1 cleavage site resides at the Arg^{41}-Ser^{42} peptide bond and leads to the unveiling of a new N-terminus with a starting sequence of ^{42}SFLLRN^{47} (Figure 5). This sequence represents the tethered ligand that binds intramolecularly to the second extracellular loop of the receptor[44]. In contrast, PAR4 is cleaved by thrombin at the Arg^{47}-Gly^{48} peptide bond revealing an N-terminus segment with the sequence ^{48}GYPGQV^{53} that serves as the PAR4 tethered ligand[44].

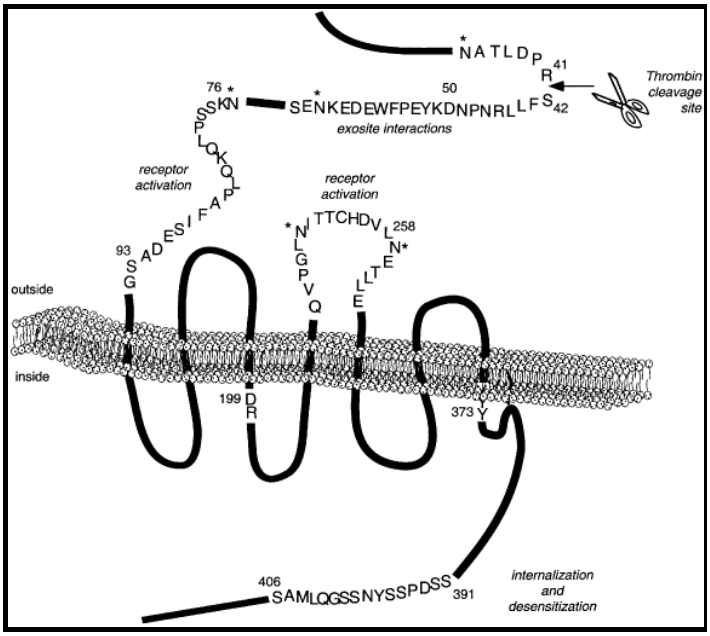

Figure 5: Structure and features of PAR1 highlighting domains thought to be involved in receptor activation and interactions with thrombin[34].

The stimulation of PAR1/PAR4 at the surface of platelets produces an intracellular response that is initiated by the cleavage of the receptor by thrombin. Once

activated, PARs can couple to several G proteins thereby triggering a signaling cascade resulting in marked changes in the phenotype of the platelet, including cell shape, secretion, integrin activation, metabolism, transcription, and cell motility[32, 43]. PAR1 couples to several G proteins (G_q, G_i, and $G_{12/13}$) and the cascade responsible for the changes in the cellular phenotype is depicted in Figure 6. PAR signaling upregulates adhesion molecules expression and triggers the production of active neutrophils and monocytes[31]. This event leads to the binding, rolling, and final attachment of platelets and leukocytes to the endothelium surface, which may trigger further production of thrombin (positive feedback loop) due to the presence of leukocyte tissue factors on the surface of these cells[31]. Thrombin also increases the permeability of the endothelium surface; therefore, PAR activation triggers edema formation[31]. This system could certainly trigger intravascular thrombosis and local tissue damage from leukocyte products[31]. Consequently, the inhibition of the PAR1/PAR4 system would be highly beneficial for the treatment of several conditions that are propagated by platelet activation leading to aggregation and subsequent occlusion of the vascular system, e.g. acute coronary syndrome, thrombotic embolism, and/or stroke.

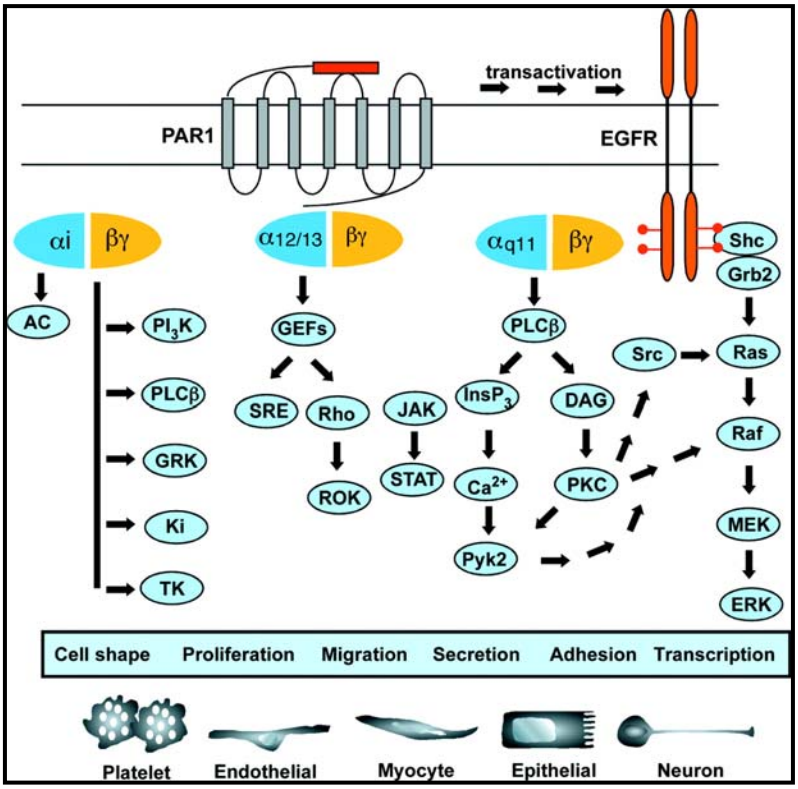

Figure 6: Thrombin receptor (PAR1) signaling[36].

The cleavage of PAR1 and PAR4 are irreversible proteolytic events that if left unregulated could result in physiological damage. Therefore, mechanisms are in place for modulating the inactivation of these receptors. The first pathway involves cellular processing that leads to internalization through coated pits in the plasma membrane and succeeding degradation by lysosomes[45]. The second pathway relies on the action of plasmin, which is found at high concentrations on the surface of activated platelets[46, 47]. Plasmin apparently recognizes the activated receptor and cleaves at a cluster of arginine and lysine residues of the tethered ligand thereby deactivating the receptor[47]. The two mechanisms may be cell specific, but are both efficient means of inactivation of PAR1 and PAR4.

CURRENT TREATMENTS FOR THROMBOSIS. Two main approaches have been employed to prevent and treat thromboembolic disorders: hindering thrombin formation and inhibiting the enzyme's activity. Since the 1940s, vitamin-K antagonists such as coumarin, dicoumarol, and warfarin have been the most commonly administered anticoagulants for the treatment of a variety of thrombotic conditions. These agents work by inhibiting several clotting factors of the coagulation system since they interfere with vitamin-K dependent post-translational protein modifications that are essential for their function[5]. Therefore, vitamin K antagonists work indirectly by inhibiting the proper synthesis of coagulation factors that are necessary to activate thrombin[48]. Warfarin's activity is plagued with inconsistency due to the irregularity of vitamin-K levels in individual patients. In addition, it has a narrow therapeutic range requiring constant monitoring in order to achieve the most effective dosage[48].

A more direct approach to prevent thrombotic disorder involves heparin, a sulfated glycosaminoglycan produced by mast cells, that acts by activating antithrombin, which in turn inhibits thrombin and coagulation factor Xa[49-51]. Heparin produces a conformational change in the endogenous inhibitor that leads to 1,000-fold increase in the rate of antithrombin activity[48-50]. There are several drawbacks to the use of heparin including poor subcutaneous absorption, variable effect due to binding to multiple plasma proteins, and the development of thrombocytopenia (decrease in normal levels of platelets)[5, 48, 52]. Smaller fragments of the anticoagulant, known as low-molecular weight heparin (LMWH), have been synthesized in an effort to improve the bioavailability and hinder interactions with plasma proteins. LMWHs demonstrate greater duration of anticoagulant activity and their response appears to correlate with body weight permitting

administration of a fixed dose[52]. However, the large size of even these fractions of heparin is still a concern since LMWHs must be administered subcutenously limiting their use for outpatient therapy[48, 52].

The need to develop an anticoagulant with a high efficacy-to-safety profile has lead researchers to explore other means of achieving their goal of efficiently inhibiting thrombin with minimal side effects. A new approach involves targeting both the active site and the substrate recognition sites of the enzyme and developing what is known as direct thrombin inhibitors (DTIs). The advantages of this new class of anticoagulants are that they act independently of antithrombin, they do not bind to plasma proteins, and they pose no risk of developing thrombocytopenia since DTIs are designed to interact with the enzyme only[48]. Hirudin, a 65-amino acid polypeptide extracted from medicinal leeches, is a bivalent DTI that interacts with both exosite I and the active site of thrombin, as confirmed by both kinetics and x-ray crystallography[9, 53-55]. Hirudin is an extremely potent and selective thrombin inhibitor with a K_i value of 20 fM that forms a nearly irreversible bond with the enzyme[54].

Various analogs of hirudin have been synthesized in order to reduce the size of the inhibitor and to improve the reversibility of the interaction between drug and enzyme. Bivalirudin is a synthetic analog composed of 20-amino acid residues that acts as a selective and reversible inhibitor of thrombin. In this analog, both size and reversibility are circumvented due to the smaller size and the presence of an amino-terminal D-Phe-Pro-Arg-Pro sequence, that once bound to the enzyme, is cleaved freeing up the active site (i.e. it acts as a substrate)[56-58]. Bivalirudin has been approved by the FDA for use as

an anticoagulant for the treatment of unstable angina. However, problems with parenteral delivery and rapid clearance have limited its use for a wider range of conditions.

A second class of DTIs has produced several promising agents with favorable delivery, clearance, and safety profiles as compared to current treatments. These univalent DTIs interact solely with the active site of thrombin in a non-covalent fashion and are often small molecules. The most notable compound is melagatran, which represents a new class of thrombin inhibitors that are reversible, potent, and have a molecular mass of 500 Da or less[5, 48, 58-60]. With a K_i value of 2 pM, melagatran is a very potent DTI that has some additional functions including its ability to inhibit thrombin-induced platelet aggregation and it has a wide therapeutic window without unwanted bleeding[5, 59]. However, melagatran is unsuitable for oral administration due to low oral bioavailability in man, which is associated with the presence of three charged groups in the molecule (see Figure 7)[61, 62].

A prodrug of melagatran (ximelagatran) was synthesized with a hydroxyl group attached to the amidine and an ethyl group attached to the carboxylic acid as shown in Figure 7. Despite its 185-fold decrease in antithrombin activity, ximelagatran is readily converted to melagatran after intestinal absorption and has the potential to be the first oral direct thrombin inhibitor[61, 62]. Ximelagatran is currently in Phase III Clinical Trials where adverse side effects have been discovered involving increased levels of alanine transaminase in the liver after long-term treatment[63-65]. More analogs of this prodrug are currently in development driven by the promise of designing the first orally available anticoagulant.

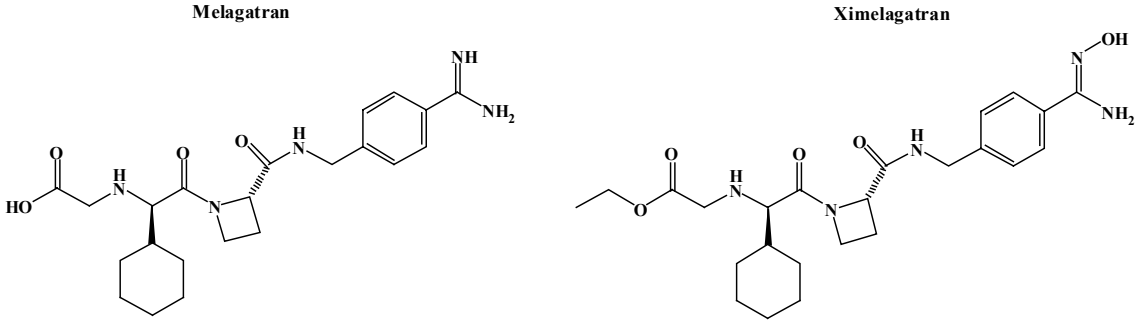

Figure 7: Structure of melagatran and its prodrug ximelagatran.

In parallel to the development of direct thrombin inhibitors, research has focused on another method to selectively target the hemostatic system without interfering with the coagulation process. A new class of inhibitors has been designed to interact with protease-activated receptors at the surface of platelets. Most of the work thus far has focused on PAR1, also known as the thrombin receptor, and several ways of inhibiting the signaling at the receptor are being explored. The first and most commonly used approach is to design antagonists that compete for binding with the tethered ligand[66-68]. Development of PAR1 antagonists began with structural analogs of SFLLRNP (the portion of the tethered ligand that interacts with the second extracellular loop of the receptor) and have since evolved into small molecules with low nanomolar K_i values and potential for oral delivery[68-74].

An alternative and novel method of inhibiting PAR1 would be to interfere with the docking of thrombin and subsequent cleavage of the receptor. This mechanism of action would provide a way to inhibit the activation of not only PAR1, but also other members of the PAR family (e.g. PAR3/PAR4) since the potential compound would not be designed after the tethered ligand, which varies for each individual receptor. Our research focuses on designing and synthesizing such compounds and elucidating this

novel mechanism of action. The starting point of our design was previously reported work that claimed that plasma kininogens and their cleavage product, bradykinin, both possessed antithrombin activity and bound to the surface of platelets preventing thrombin from binding to the receptor[75-79].

BRADYKININ AND RPPGF PEPTIDE. Bradykinin, a nonapeptide, is released from the plasma protein high and low molecular weight kininogen through the action of plasma kallikrein[76]. Bradykinin increases vascular permeability, dilates blood vessels, contracts non-vascular smooth muscle, and causes pain[77]. The short-lived vasodilator is further degraded by angiotensin-converting enzyme (ACE) to produce a pentapeptide with sequence Arg-Pro-Pro-Gly-Phe (RPPGF)[79]. This pentapeptide, along with kininogen and bradykinin, inhibits thrombin-induced platelet activation and aggregation by interacting with the active site of thrombin at high concentrations (K_i = 1.7 mM)[80, 81]. RPPGF also binds to the extracellular fragment of PAR1 thereby preventing thrombin from binding and cleaving PAR1 leading to the inhibition of platelet aggregation[80]. Therefore, RPPGF is a formidable lead in the development of a potent inhibitor of platelet aggregation.

Modifications made to the sequence of RPPGF are the main focus of Chapter II and the first portion of Chapter IV of this written work. The structure activity driven changes led to the design and synthesis of an analog with 135-fold improvement in the activity against thrombin-induced platelet aggregation. This novel lead peptide, compound **48** [D-Arg-Oic-Pro-D-Ala-Phe(*p*-Me)-NH-Et], is active at 5 μM concentration

and shows promise as an orally dosed anticoagulant as described in the final portion of Chapter IV.

ORAL DELIVERY AND PEPTIDE THERAPEUTICS. The long-term objective of this project is to develop an orally bioavailable drug for treatment of individuals with thrombin disorders including acute coronary syndromes. Many of the agents routinely used as anticoagulant and/or antiplatelet agents, such as heparin and bivalirudin, are administered subcutaneously or intravenously[48]. The only oral anticoagulant currently approved to treat thrombotic disorders is warfarin, but as previously described it displays inconsistencies in dosing and response in patients requiring constant monitoring in order to maintain proper levels of the drug[48]. Other oral agents attack specific platelet targets like the ADP receptor (clopidogrel) or platelet cyclooxygenase (aspirin)[82-84]. The market for an oral anticoagulant remains unexploited at the present time, and the drugs in development, though promising, still display undesirable side effects.

Since our compounds are peptides, there are major challenges that must be overcome in order to design a molecule that will be both active and orally bioavailable. The most prominent problems hindering oral peptide therapeutics is the extreme sensitivity to serum proteases (peptides are readily degraded before having an opportunity to reach their target), and the often large size of the molecules, which limits absorption via passive diffusion[85, 86]. The stability and longevity of peptides can be improved by introduction of unnatural amino acid residues or modifications to the backbone structure, and the bioavailability may be improved by the development of peptide delivery systems[85, 87, 88].

New peptide therapies are currently being developed for a variety of conditions including metabolic and immune disorders, neurological conditions, cardiovascular disease, HIV, and cancer[89]. A major success story is the design of Humalog, the first biosynthetic hormone optimized by DNA technology for the treatment of diabetes, which has developed into a blockbuster drug for Eli Lilly[90]. There are also several peptides in late-stage clinical trials including enfuvirtide (Fuzeon), a viral fusion inhibitor that blocks the virus before it enters CD4 cells[91]. The prospective for new peptide therapeutics has not reached its full potential, as there are still some hurdles to be overcome in both delivery and stability, but the success of the current peptide drugs does illustrate the possible future of these agents.

This dissertation demonstrates that unnatural modifications can make an impact not only on the potency of the peptides, but can also influence the stability and bioavailability of these molecules. A variety of substitutions to the naturally occurring pentapeptide (RPPGF) have been explored and a mechanism of action for the new lead compound has been elucidated.

RESEARCH OBJECTIVE. By utilizing an indirect approach to inhibit the hemostatic system, it is possible to modulate thrombus formation by targeting a family of receptors at the surface of platelets known as protease-activated receptors (PARs) that are activated by proteolytic cleavage by thrombin. The initial hypothesis for this research effort focused on interfering with the interaction between thrombin and the PARs. To accomplish this, analogs were designed to bind to the extracellular domain of the PARs thereby making it difficult for thrombin to dock to and cleave the receptor. The

consequent selective inhibition of the intramolecular activation step of the protease-activated receptor should result in moderation of platelet activation and aggregation without interfering with the enzymatic activity of thrombin in the coagulation process. This selective inhibition would be expected to result in fewer side effects since thrombin could continue to function in the coagulation system.

The thrombin inhibitory domain of bradykinin, the pentapeptide RPPGF, was exploited as a possible template for the peptides presented in this report. However, the inhibitory concentration of RPPGF is too high (K_i = 1.7 mM) and further substitutions to the sequence must be considered in order to achieve inhibition at a concentration low enough to warrant its consideration as a drug for the management of acute coronary syndrome. Chapter II describes the design and synthesis of a library of peptides with modifications at positions 4 and 5 leading to the discovery of a novel analog that is 42-fold more potent than RPPGF against thrombin-induced platelet aggregation.

The structure activity relationship study presented in Chapter II accomplished the first aim of the project, which was to produce a more potent analog of RPPGF. However, in the final portion of Chapter II, the issue of selectivity between direct thrombin inhibition and activity against platelet aggregation through the protease-activated receptors is raised. The lead peptide is more potent, but there is no selectivity as shown in the clotting assay results (measures the effect of molecules on the intrinsic and extrinsic pathways of the coagulation system). The mechanism of action of our analogs was thus explored in order to determine which mechanism is prominent in modulating the inhibition of platelet aggregation. Chapter III illustrates the many techniques employed to

determine whether the most potent peptides in our library are acting by inhibiting thrombin or through binding to PAR1 and PAR4.

Finally, with Chapter IV we attempt to address the long-term goal of our project, which is to develop an orally available anticoagulant agent. Since the lead compound from the structure-activity relationship studies in Chapter II was found to be 12.7% orally bioavailable in rats, a new series of peptides was designed and synthesized to improve the pharmacokinetic profile. By assuming initially that the lead peptide is being absorbed through passive diffusion in the gastrointestinal tract, modifications were introduced to increase the lipophilicity and decrease the net charge of the peptides. The substituents selected were small and lipophilic (methyl and ethyl moieties) since the aim was to maintain the size and potency of the lead compound. From this final series, a new lead analog was discovered that is 3-fold more potent than the previous lead described in Chapters II and III. This compound is very promising since it represents a 135-fold improvement over RPPGF, and it possesses all unnatural amino acid residues along with other synthetic modifications, which are believed to contribute to its stability and oral bioavailability.

In summary, this thesis presents a promising and novel class of anticoagulants with improved activity as well as stability and oral absorption. By synthesizing a peptide consisting of unnatural amino acid residues, we have developed a candidate that is currently patented and under FDA evaluation for an Investigative New Drug (IND) application and Phase I clinical trial for a single intravenous infusion for the treatment of myocardial infarction and high-risk active angina.

CHAPTER II

STRUCTURE ACTIVITY RELATIONSHIP STUDIES TO OPTIMIZE RESIDUES AT POSITION 4 AND 5

Previous work employing a combinatorial approach and rational drug design based on the RPPGF bradykinin fragment indicated that the change of configuration of arginine to D-arginine and replacement of Pro^2 by Oic (octahydroindole-2-carboxylic acid), known to improve potency of bradykinin antagonists, while maintaining proline in the third position of the sequence, led to pronounced improvements in potency, and resulted in the lead compound, D-Arg-Oic-Pro-Gly-Phe-NH_2 (TH146)[92-94]. The analogs of TH146 discussed throughout this dissertation were synthesized as linear sequences with an amide group at the C-terminus. Both features were determined to be essential for activity against platelet aggregation. A small series of peptides attempting to constrict the structure of TH146 through the cyclization of the linear peptide (compounds **59** thru **64**) was developed early on in the project. All of the cyclic compounds were inactive in the functional assay indicating that maintaining the flexibility of TH146 was necessary for activity (this feature will be discussed further in Chapter III).

With the above features delineated, the natural next step to further develop RPPGF analogs with increased potency for inhibition of thrombin-induced platelet aggregation was to substitute residues at positions 4 and 5. The current effort aims to optimize these remaining positions of TH146 by preparing analogs with substitutions at

Xxx^4 and Xxx^5. The results of these substitutions are summarized in Tables 1 and 2, where data are reported as the minimal concentration of the inhibitor necessary to completely block threshold γ–thrombin-induced platelet aggregation (IC_{100})[80, 81, 92]. Several previously synthesized and reported compounds are also included for comparison. A summary of the platelet aggregation data for all the compounds tested throughout this dissertation can be found in Appendix F.

SAR STUDIES. Table 1 presents data for compounds with replacements for Gly at position 4 of D-Arg-Oic-Pro-Gly-Phe-NH_2 (TH146). Since glycine can assume conformations allowed for L- and D-amino acids, alanine, the most conservative substitution for glycine, was examined in both L- and D- configurations (compounds **1** and **2**, respectively). As seen in Table 1, the D-Ala^4 containing analog, compound **2**, which showed 100% inhibition of platelet aggregation at 56 μM, is 10-fold more potent than compound **1** and 2.5-fold more potent than TH146 in γ-thrombin induced platelet aggregation assay.

The successful results observed for peptide **2**, encouraged us to explore further D-amino acid substitutions in position 4. Among the remaining D-amino acid substituted analogs, compound **3**, D-Arg-Oic-Pro-D-Asn-Phe-NH_2 showed a modest improvement over TH146 with 100% inhibition of platelet aggregation at 83 μM, slightly less potent than **2**. The remaining analogs in this series had comparable activity independent of the chemical nature of the residue's side chain. Consequently, the trend observed in these peptides was that the requirement for residue 4 seemed to be primarily related to the configuration of the amino acid residue, rather than the actual side chain size and charge.

A possible explanation is that the D-stereochemistry moves the side chain "out of the way" while helping to orient the rest of the molecule. This assumption would be consistent with the improved activity displayed by **2**, with the small alanine side chain.

TABLE 1

Position 4 modifications of TH146

Compounds	**Sequence**	**Inhibition of Threshold Platelet Aggregation**
		μM ± S.E.M
RPPGF[#]	Arg-Pro-Pro-Gly-Phe	680 ± 280
TH146	D-Arg-Oic-Pro-Gly-Phe-NH_2	140 ± 20
1*	D-Arg-Oic-Pro-Ala-Phe-NH_2	550 ± 166
2*	D-Arg-Oic-Pro-D-Ala-Phe-NH_2	56 ± 16
3*	D-Arg-Oic-Pro-D-Asn-Phe-NH_2	83 ± 17
4*	D-Arg-Oic-Pro-D-Lys-Phe-NH_2	133 ± 33
5*	D-Arg-Oic-Pro-D-Phe-Phe-NH_2	133 ± 33
6*	D-Arg-Oic-Pro-D-Pro-Phe-NH_2	167 ± 33
7*	D-Arg-Oic-Pro-D-Leu-Phe-NH_2	300 ± 100
9*	D-Arg-Oic-Pro-D-Asp-Phe-NH_2	567 ± 233
10	D-Arg-Oic-Pro-D-Gln-Phe-NH_2	400 ± 100
11	D-Arg-Oic-Pro-D-Abu-Phe-NH_2	275 ± 75
12	D-Arg-Oic-Pro-D-Orn-Phe-NH_2	250 ± 87
13	D-Arg-Oic-Pro-D-Nle-Phe-NH_2	275 ± 75

Data presented are the mean ± S.E.M. of $n > 3$ independent experiments. The values given represent the minimal concentration of peptide necessary to inhibit 100 % of threshold γ–thrombin-induced platelet aggregation (IC_{100}). [#] From Hasan et al.[80]. * Detones compounds synthesized by Kate Kojiro and Ping He.

In parallel with the examination of varying Xxx^4, we also introduced several substitutions at Xxx^5 of the lead compound TH146. The data for the D-Arg-Oic-Pro-Gly-Xxx^5-NH_2 series are presented in Table 2. It can be clearly seen that L-amino acids are preferred over D-amino acids in this series. This trend is exemplified by the sharp decrease in activity of compound **18**, with D-phenylalanine at position 5 (IC_{100} = 833 μM), in comparison to TH146 (IC_{100} = 140 μM). In addition, it appears that a larger aromatic side chain is preferred while aliphatic and polar groups are not well tolerated

(compounds **15**, **16**, **20**, and **22** were all inactive in the functional assay). The most potent compound in this series, compound **14**, replaces Phe^5 with $2\text{-}Nal^5$ (3-(2-naphthyl)-L-alanine) in D-Arg-Oic-Pro-Gly-Xxx^5-NH_2 resulting in a 3-fold improvement in activity over TH146 (IC_{100} = 50 μM).

TABLE 2

Position 5 modifications of TH146

Compounds	**Sequence**	**Inhibition of Threshold Platelet Aggregation**
		μM ± S.E.M
RPPGF[#]	Arg-Pro-Pro-Gly-Phe	680 ± 280
TH146	D-Arg-Oic-Pro-Gly-Phe-NH_2	140 ± 20
14*	D-Arg-Oic-Pro-Gly-2-Nal-NH_2	50 ± 0
15*	D-Arg-Oic-Pro-Gly-Glu-NH_2	NE
16*	D-Arg-Oic-Pro-Gly-Nle-NH_2	NE
17	D-Arg-Oic-Pro-Gly-Phe(*p*-F)-NH_2	200 ± 0
18*	D-Arg-Oic-Pro-Gly-D-Phe-NH_2	833 ± 144
19*	D-Arg-Oic-Pro-Gly-Trp-NH_2	350 ± 87
20*	D-Arg-Oic-Pro-Gly-His-NH_2	NE
21*	D-Arg-Oic-Pro-Gly-1-Nal-NH_2	200 ± 0
22	D-Arg-Oic-Pro-Gly-Arg-NH_2	NE
23	D-Arg-Oic-Pro-Gly-Tyr-NH_2	300 ± 100

Data presented are the mean ± S.E.M. of $n > 3$ independent experiments. The values given represent the minimal concentration of peptide necessary to inhibit 100 % of threshold γ -thrombin-induced platelet aggregation (IC_{100}). NE represents no effect or ≥ 1000 μM activity. [#] From Hasan et al.[80]. * Denotes compounds synthesized by Kate Kojiro, John Omnaas, and Ping He.

Interestingly, there is a 4-fold decrease in activity when 1-Nal is substituted at position 5 as relative to $2\text{-}Nal^5$. A possible explanation for the difference in potency generated by these two close analogs is that the position at which the bulky naphthyl moiety is attached to the backbone influences the direction of the second ring of the side chain. In Appendix D, the 2-D representation of 1-Nal and 2-Nal are shown to describe the slight but yet important distinction between the positioning of the secondary ring of the aromatic system. This observation will become key in designing future series of

analogs with substituted phenylalanine residues that will be discussed in more detail later in this chapter and in Chapter IV.

The substitution of Phe^5 with 2-Nal in compound **14** encouraged the synthesis of a series of analogs with 2-Nal in position 5, re-examining several D-amino acid replacements in position 4, in order to assess whether the potency would be affected by this substitution. The results for this series of compounds are summarized in Table 3. Compound **57** [D-Arg-Oic-Pro-D-Gln-2-Nal-NH_2] (IC_{100} = 83 μM) showed almost a 5-fold increase in activity over compound **10** [D-Arg-Oic-Pro-D-Gln-Phe-NH_2] (IC_{100} = 400 μM). The remaining compounds, including the best compounds from the Phe series, showed only a slight improvement in activity when 2-Nal was positioned as the fifth amino acid residue.

TABLE 3

Position 4 analogs of [2-Nal^5]TH146

Compounds	**Sequence**	**Inhibition of Threshold Platelet Aggregation**
		μM ± S.E.M
RPPGF[#]	Arg-Pro-Pro-Gly-Phe	680 ± 280
TH146	D-Arg-Oic-Pro-Gly-Phe-NH_2	140 ± 20
14*	D-Arg-Oic-Pro-Gly-2-Nal-NH_2	50 ± 0
25	D-Arg-Oic-Pro-D-Ala-2-Nal-NH_2	100 ± 35
52	D-Arg-Oic-Pro-D-Phe-2-Nal-NH_2	83 ± 17
53	D-Arg-Oic-Pro-D-Ser-2-Nal-NH_2	56 ± 16
54	D-Arg-Oic-Pro-D-Thr-2-Nal-NH_2	75 ± 14
55	D-Arg-Oic-Pro-D-His-2-Nal-NH_2	75 ± 25
56	D-Arg-Oic-Pro-β-Ala-2-Nal-NH_2	675 ± 197
57	D-Arg-Oic-Pro-D-Gln-2-Nal-NH_2	83 ± 17

Data presented are the mean ± S.E.M. of $n > 3$ independent experiments. The values given represent the minimal concentration of peptide necessary to inhibit 100 % of threshold γ–thrombin-induced platelet aggregation (IC_{100}). [#] From Hasan et al.[80]. * Denotes compound synthesized by Ping He.

Following the results from our three initial series, we attempted to combine the best substitutions observed in the singly modified Xxx^4 and Xxx^5 series, but

unfortunately the effects do not appear to be additive. On the contrary, as shown in Table 3, the projected best analog, compound **25** is only slightly more potent than TH146 (IC_{100} = 100 μM). The explanation for the observed result may be related to the imposed steric and conformational changes with a less flexible backbone (due to D-alanine at position 4) and the bulky side chain of 2-Nal. The substitutions made at position 4 continued to display little influence on potency.

Thus, we chose to examine other possible aromatic replacements for 2-Nal at position 5. As shown in Table 4, we introduced several variations of Phe that, like the successful 2-Nal[5] substitution, were larger, aromatic, and lipophilic. In the initial analogs of the D-Arg-Oic-Pro-D-Ala-Xxx[5]-NH_2 series, we chose to use Phe derivatives as a means of probing the requirements for interaction with the target receptor. Phe is present in the original lead compound, RPPGF, and, as seen in Table 2, the aromatic nature of Phe[5] appears to be essential for inhibition of platelet activation. In addition, the substitutions were made at the *para* position of the aromatic ring since that would be representative of the 9th position of the 2-naphthyl aromatic system allowing for the further examination of the spatial requirements for this residue. As a first set of modifications, we chose to use small (methyl), intermediate (chloro), and large (phenyl) lipophilic substituents at the *para* position of the phenyl ring of phenylalanine.

TABLE 4

Position 5 analogs of [D-Ala^4]TH146

Compounds	**Sequence**	**Inhibition of Threshold Platelet Aggregation**
		μM ± S.E.M
RPPGF[#]	Arg-Pro-Pro-Gly-Phe	680 ± 280
TH146	D-Arg-Oic-Pro-Gly-Phe-NH_2	140 ± 20
2*	D-Arg-Oic-Pro-D-Ala-Phe-NH_2	56 ± 16
26	D-Arg-Oic-Pro-D-Ala-Bip-NH_2	200 ± 100
27 (FM19)	D-Arg-Oic-Pro-D-Ala-Phe(*p*-Me)-NH_2	16 ± 4
28	D-Arg-Oic-Pro-D-Ala-Phe(*p*-Cl)-NH_2	44 ± 11

Data presented are the mean ± S.E.M. of $n > 3$ independent experiments. The values given represent the minimal concentration of peptide necessary to inhibit 100 % of threshold γ -thrombin-induced platelet aggregation (IC_{100}). [#] From Hasan et al.[80]. * Denotes compound synthesized by Kate Kojiro.

Within this initial small sample of synthesized analogs, there was a clear preference for the smaller substituent at the *para* position of Phe. This finding is not too surprising since analog **14** (2-Nal[5]) showed slight improved potency relative to TH146, but the size of the secondary ring created a possible problem. Compound **27** containing the *p*-methylphenylalanine, whose structure is shown in Figure 8, was 3.5-fold more potent than compound **2**, 42-fold more potent than RPPGF, and had a 7-fold increase in potency compared to TH146 in γ-thrombin induced platelet aggregation. The structure activity relationship described has been recently published in *Chemical Biology and Drug Design*[95] .

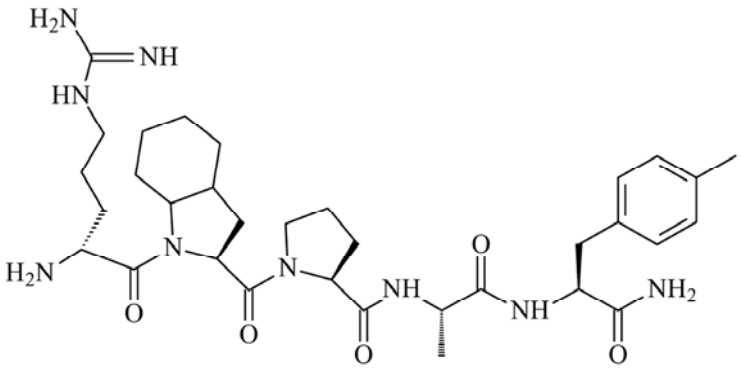

D-Arg-Oic-Pro-*D*-Ala-pMePheNH$_2$ [rOicPaF(p-Me)-NH$_2$]

Figure 8: The chemical structure of compound **27**.

Following the discovery of analog **27**, a new site for modification was introduced that provided for an extension of the D-Arg-Oic-Pro-D-Ala-Xxx^5-NH$_2$ series. Peptides were designed in which a variety of Phe derivatives with a wide range of chemical structure and position of the ring substitution was examined. A small series of analogs that possessed the *p*-methylphenylalanine at the fifth position with modifications at the fourth position with residues that had shown activity in previous series (D-Arg-Oic-Pro-D-Xxx^4-Phe(*p*-Me)-NH$_2$) was also created. Table 5 summarizes the results observed for these compounds. From these extended series, three new potential lead compounds, **29** [D-Arg-Oic-Pro-D-Ser-Phe(*p*-Me)-NH$_2$], **33** [D-Arg-Oic-Pro-D-Ala-Phe(*p*-Br)-NH$_2$], and **36** [D-Arg-Oic-Pro-D-Ala-Phe(*p*-I)-NH$_2$] were identified. All three compounds shared similar potency in the thrombin-induced platelet aggregation assay, which is used as a primary screening method for the activity of the compounds.

TABLE 5

Modifications at positions 4 and 5 in comparison to compound **27**

Compounds	Sequence	Fold Decrease in the Inhibition of Platelet Aggregation Potency vs. 27
27 (FM19)	D-Arg-Oic-Pro-D-Ala-Phe(*p*-Me)-NH_2	1*
24	D-Arg-Oic-Pro-Gly-Phe(*p*-Me)-NH_2	7
28	D-Arg-Oic-Pro-D-Ala-Phe(*p*-Cl)-NH_2	2.75
29	D-Arg-Oic-Pro-D-Ser-Phe(*p*-Me)-NH_2	0.81
30	D-Arg-Oic-Pro-D-Asn-Phe(*p*-Me)-NH_2	4
31	D-Arg-Oic-Pro-D-Ala-Hfe-NH_2	8
32	D-Arg-Oic-Pro-D-Ala-Phe(*p*-NH_2)-NH_2	8
33	D-Arg-Oic-Pro-D-Ala-Phe(*p*-Br)-NH_2	1.1
34	D-Arg-Oic-Pro-D-Ala-Phe(*p*-*t*Bu)-NH_2	2
35	D-Arg-Oic-Pro-D-Ala-Phe(*p*-CN)-NH_2	2
36	D-Arg-Oic-Pro-D-Ala-Phe(*p*-I)-NH_2	1
37	D-Arg-Oic-Pro-D-Ala-Phe(2-Me)-NH_2	2
38	D-Arg-Oic-Pro-D-Ala-Phe(3-Me)-NH_2	4
39	D-Arg-Oic-Pro-D-Ala-Phe(*p*-NO_2)-NH_2	3
40	D-Arg-Oic-Pro-D-Ala-Phg-NH_2	2
41	D-Arg-Oic-Pro-D-Ala-Phe(*p*-COOH)-NH_2	35

The data represent the fold increase in concentration of the peptide necessary to inhibit threshold γ-thrombin-induced platelet aggregation when compared to compound **27** (FM19) (*IC_{100} = 16±4 μM). The error for this study is in the range of 1-3 fold due to the variable nature of the platelet aggregation assay.

Most of the modifications at the *para* postion of Phe^5 were well tolerated as demonstrated by the 1-3 fold decrease in activity as compared to analog **27** for the majority of the peptides. However, a few substituents such as polar groups (compounds **32** and **41)** and the elongated aromatic side chain of homophenylalanine (Hfe) in **31** produced much less potent analogs (8 fold and higher decrease in potency). The additional carbon bond in Hfe not only extends the side chain by one methylene group, but it also influences the position of the aromatic ring by introducing an extra rotational angle to the side chain. Both differences may explain the changes in activity for analog **31**. There is definite evidence that a small alkyl group (*p*-Me^5) and halogens (*p*-Br^5 and *p*-

I^5) are preferred at the fifth position and that D-serine can be exchanged for D-alanine at position 4.

SELECTIVITY BETWEEN ANTI-PLATELET ACTIVATION AND CLOTTING ACTIVITY. The discovery of compound **27** and its equipotent analogs (**29**, **33**, and **36**) fulfilled our first goal of producing a more active analog of RPPGF and TH146. However, we were also interested in producing analogs with improved selectivity between inhibition of the clotting properties of thrombin and platelet aggregation mediated by the PAR family. In order to test for selectivity, the clinical anticoagulation tests (APTT, PT and TCT) were employed to measure the ability of our lead compound to interfere with the clotting cascade. The activated partial thromboplastin time (APTT) was used to assess the affect on the intrinsic pathway (from an internal injury) while the prothrombin time (PT) probed the extrinsic pathway (external injury)[16]. The third test, the thrombin clotting time (TCT), determined the inhibition of the final step of the coagulation system where thrombin cleaves fibrinogen to produce insoluble fibrin. The combination of these three tests allowed for the complete assessment of the extent to which our compound is inhibiting the clotting cascade.

Like RPPGF and TH146, compound **27** also displays direct inhibition of thrombin as evident by the results of the clinical coagulation assays (APTT, PT and TCT). The clinical studies demonstrated that at 1.56 μM, 1.56 μM, or 0.78 μM of **27**, there was a significant prolongation ($p < 0.05$) of the APTT, PT, or TCT, respectively. Compound **27** is a 10-40 fold more potent inhibitor of thrombin clotting properties than is TH146, which was deemed a direct inhibitor of thrombin at higher concentrations than **27**[92]. The

data displayed in Figure 9 indicate that the improved antiplatelet activity of compound **27** may be partially linked to its direct interaction with thrombin. Consequently, this compound is more potent, but it is not selective for the target receptor.

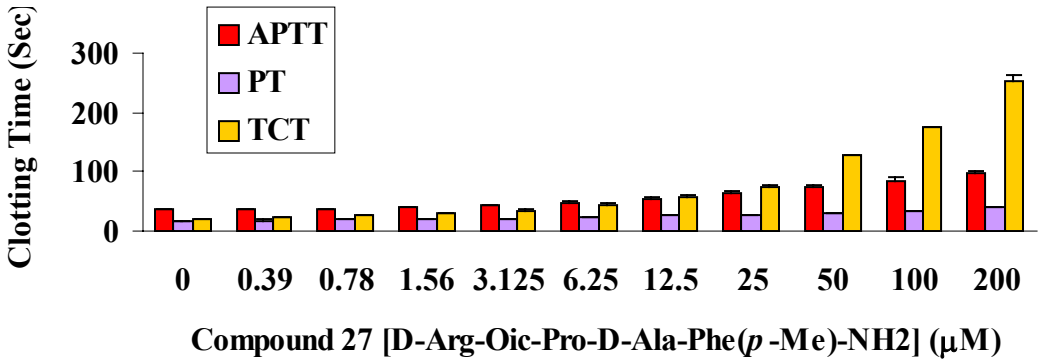

Figure 9: Influence of **27** on coagulation assays. Normal human plasma was incubated with increasing concentration of **27** and the APTT (red bars), PT (purple bars), or TCT (yellow bars) was determined as described under *Materials and Methods*. The data represent the mean ± standard deviation of at least three independent experiments.

In order to further explore the requirements for interaction with the receptor and the selectivity of their anti-coagulant activity, compound **27** and its analogs (**29**, **33**, and **36**) were used in order to examine the mechanism of action of this class of compounds. In the subsequent chapter (Chapter III), we employed *in vitro* and *in vivo* assays to probe the interaction of these compounds with thrombin and both PAR1 and PAR4 exodomains.

CHAPTER III

BIOCHEMICAL CHARACTERIZATION OF LEAD ANALOGS AND ELUCIDATION OF THE MECHANISM OF ACTION

IN VITRO CHARACTERIZATION OF ANALOGS. As described in Chapter II, our structure-activity relationship studies of TH146 led to four good candidates for further study, compounds **27**, **29**, **33**, and **36**. In the present chapter, we examine these lead analogs more extensively to assess their possible selectivity as thrombin induced PAR activation inhibitors. The previously described clinical anticoagulant assays (APTT, PT, and TCT) were used to assess the anti-clotting activity of the three new analogs along with **27** and, the results are summarized in Table 6.

Similar activity as compound **27** was observed for compound **29** on the clotting time of normal human plasma using the APTT, PT, and TCT assays (3.13 μM, 1.56 μM, and 0.39 μM, respectively) suggesting that this analog is inhibiting both the extrinsic and intrinsic clotting pathways as well as directly interfering with fibrin formation. The remaining two analogs (compounds **33** and **36**) were less potent inhibitors of the intrinsic and extrinsic pathways (4-16 fold less potent), but displayed activity in the thrombin clotting time assay comparable to compound **27** (0.78 μM). The data indicate that even though all four analogs have a significant inhibitory effect against α-thrombin, the modifications seem to have different effects on how each compound modulates the clotting cascade. This suggests that analogs **33** and **36** are inhibiting fibrin formation

(TCT assay), but are not interfering with the upstream mechanisms. On the other hand, **27** and **29** are able to inhibit not only the final step of the clotting cascade, but are also inhibiting the pathways leading to thrombin formation (from prothrombin as described in Chapter I). The interaction of all four compounds with other clotting factors involved in the intrinsic and extrinsic pathways was tested, and the data is presented later in this chapter.

TABLE 6

Influence of peptide analogs on coagulation assays.

Compounds	**Sequence**	**Minimal Concentration for Prolongation ($p < 0.05$)**		
		APTT	PT	TCT
			μM	
27	D-Arg-Oic-Pro-D-Ala-Phe(*p*-Me)-NH_2	1.56	1.56	0.78
29	D-Arg-Oic-Pro-D-Ser-Phe(*p*-Me)-NH_2	3.13	1.56	0.39
33	D-Arg-Oic-Pro-D-Ala-Phe(*p*-Br)-NH_2	12.5	6.25	0.78
36	D-Arg-Oic-Pro-D-Ala-Phe(*p*-I)-NH_2	25	6.25	0.78

Normal human plasma was incubated with increasing concentration of **27** and the APTT, PT, or TCT was determined as described under *Materials and Methods*. The data represent the mean ± standard deviation of at least three independent experiments.

Since RPPGF and TH146 were shown to interact with the active site of thrombin, the peptide analogs' ability to inhibit α-thrombin cleavage of a substrate was measured. The assay used Sar-Pro-Arg-*p*-nitroaniline as the substrate in the presence of a pre-determined threshold concentration of α-thrombin (2 nM) necessary for detectable cleavage[92]. This assay works by measuring the change in absorbance due to the presence of free *p*-nitroaniline as a product of thrombin cleavage of the substrate. All four analogs inhibited the enzymatic activity of both α-thrombin and γ-thrombin with K_i values ranging from 5.9-7.3 μM and 42-59.2 μM, respectively (Table 7). These data indicate that all four compounds are approximately 15-fold better inhibitors of thrombin cleavage

of substrates than is TH146 (K_i = 91.7 μM). To be certain that the analogs' anticoagulant activity was due to their ability to inhibit thrombin, other enzymes in the coagulation system were tested with the corresponding chromogenic substrate (see *Materials and Methods* section). Factors Xa, XIa, and VIIa were selected since they are important enzymes in the coagulation cascade that lead to the activation of thrombin. None of the four lead peptides inhibited the enzymatic activity of these clotting factors. Therefore, these peptide analogs are binding discriminately to the active site of thrombin.

TABLE 7

Effect of peptide analogs on enzymatic activity of thrombin and related coagulation enzymes.

Compounds	α-IIa	γ-Iia	FXa	FXIa	FVIIa	FVIIa+TF
			Ki (μM ± S.D.)			
27	5.9 ± 1	54.35 ± 16	NI	NI	NI	NI
29	6.8 ± 0.9	42.23 ± 6	NI	NI	NI	NI
33	7.3 ± 2	48.72 ± 7	NI	NI	NI	NI
36	6.4 ± 1	59.24 ± 13	NI	NI	NI	NI

The enzymatic activity assays were performed as described under *Materials and Methods*. The presented are mean ± standard deviation of three independent experiments. NI: no inhibition.

To further elucidate the mechanism of action of our peptides at the cellular level, the calcium mobilization assay was utilized to probe the effect of each analog on the downstream signaling of α-thrombin in normal human fibroblast cells[92]. During platelet activation, thrombin cleavage of PAR1 is known to induce calcium mobilization in cells through the intracellular action of G_q. G_q activates phospholipase Cβ[54], triggering phosphoinositide hydrolysis resulting in calcium influx and activation of protein kinase C[31, 35, 96]. Therefore, by using a calcium ion indicator (Fura2), calcium mobilization can be monitored as a reporter of platelet activation[39, 97, 98]. First the threshold concentration of α-thrombin necessary to stimulate maximal calcium influx (2 nM α-thrombin) was

determined. Then a range of concentrations of each peptide was incubated with the cells prior to the addition of threshold α-thrombin. The results are displayed in Figure 10 as a plot of concentration of peptide versus percent calcium influx.

When 80 μM of either compound **27** or **29** was present, there was 97% inhibition of thrombin-induced calcium mobilization. As the concentration of these peptides was decreased to 3 μM, there was a corresponding decrease in the inhibition of calcium mobilization to 69% and 59%, respectively. At 0.38 μM compound **27** and **29**, there was full recovery of α-thrombin-induced calcium mobilization. IC_{50} values for the inhibition of calcium influx for compounds **27** and **29** were 12 μM and 15 μM, respectively. Consistent with the results observed in the *in vitro* APTT, PT, and TCT assays, compounds **27** and **29** were more potent inhibitors of calcium mobilization in cells than were the other two analogs (compounds **33** and **36**).

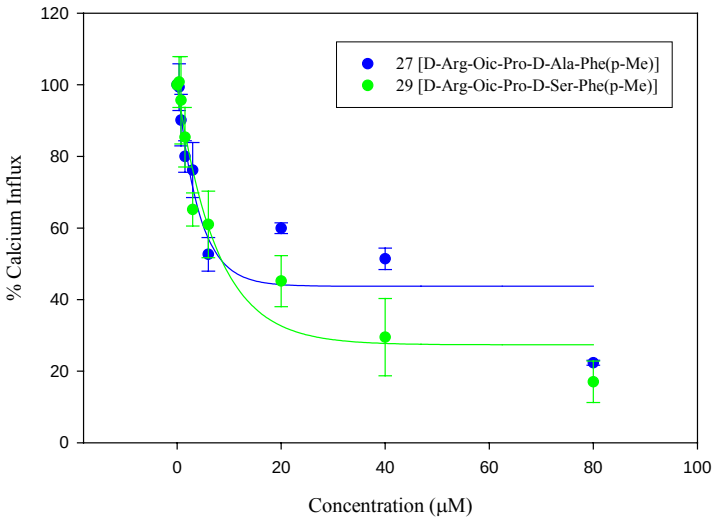

Figure 10: The effect of peptides on α-thrombin induced calcium mobilization.
Data represents the influence of a range of concentrations of **27** and **29** on threshold α-thrombin-induced calcium mobilization in normal human lung fibroblast cells. Calcium mobilization studies were performed as described under *Materials and Methods*. Values for each concentration of peptide were determined by calculating the area under the curve and are expressed as percentage of calcium influx. The data represent the mean ± standard deviation of three independent experiments.

Previous work published by Hasan et al.[81] suggested that RPPGF inhibits PAR1 proteolysis by both interacting with the active site of thrombin and by binding directly to the extracellular domain (approximately 71 amino acid residues of the N-terminus located outside of the cell) of the receptor. Thus far, our data suggest that the peptide analogs are clearly interacting with thrombin and inhibiting its enzymatic activity both *in vitro* and in cells, but are these peptides interacting with our target receptors, PAR1 and PAR4, at the surface of platelets? To answer this question, an experiment to measure whether compound **27** interferes with the binding of 15 μM RPPGFK-biotin to the exodomain of PAR1 was performed and the results are shown in Figure 11. Biotin was used as the labeling agent for these experiments, and its presence was detected by streptavidin horseradish peroxidase conjugate system.

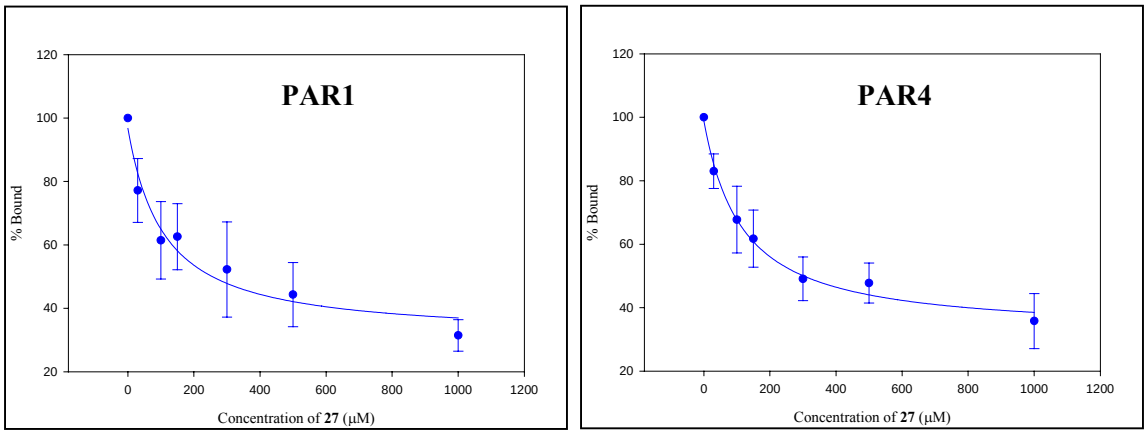

Figure 11: Inhibition of RPPGFK-biotin binding to $rPAR1_{EC}$ by **27**. The competition-binding assay was performed as described in *Materials and Methods*. The data are normalized to wells containing no inhibitor that represents 100% of binding and are represented as the mean ± standard deviation of at least three independent experiments. 1 mM TH146 was used as a positive control to ensure that the experiment worked properly.

At 30 μM, 300 μM, and 1000 μM, compound **27** displaced 23%, 52%, and 69% of RPPGFK-biotin, respectively (Figure 11). The data indicate that **27** inhibited the

binding of 15 μM RPPGFK-biotin to the extracellular domain of PAR1 with an IC_{50} of 275 μM. The results show that compound **27** is about 2-fold less potent than TH146 at inhibiting the binding of the labeled compound to PAR1 (IC_{50} = 160 μM for TH146)[92]. The same type of experiment was applied to PAR4 and at 30 μM, 300 μM, and 1000 μM, compound **27** behaved in a similar manner (IC_{50} = 300 μM). The results from the competition binding experiments are suggestive of the interaction with the receptor. However, when comparing the inhibition of the lead compound to TH146 it was observed that compound **27** is less potent at displacing RPPGFK-biotin as seen in the increased IC_{50} value[92]. In the physiological assay (platelet aggregation) peptide **27** is 7-fold more potent than TH146. So if the activity is achieved through binding to the receptor and consequent inhibition of platelet aggregation, a different outcome would be expected (lower IC_{50} value for **27** relative to TH146 since the latter is a weaker inhibitor of platelet aggregation).

The results of the competition-binding assay compelled us to question the specificity and accuracy of the assay. In order to test if the binding was sequence specific, the next experiment involved synthesizing two compounds with the same amino acid composition as **27**, but with different sequences (Phe(*p*-Me)-Oic-D-Arg-Pro-D-Ala-NH_2 and D-Ala-Pro-D-Arg-Oic-Phe(*p*-Me)-NH_2). The results shown by Nieman et al.[92] indicated that the binding of TH146 to PAR1 and PAR4 exodomains was sequence-dependent; however, when the "scrambled" analogs of **27** were tested, both were inactive in the platelet aggregation assay, but they competed with RPPGFK-biotin for binding to PAR1 and PAR4 with potencies comparable to **27**. Consequently, other "scrambled peptides" were synthesized and the experimental conditions were optimized, but similar

results were observed. Thus, there was still a need to find a different way to observe whether our new lead compound was interacting with the exodomain of PAR1 and PAR4.

In order to resolve the issues encountered with the competition assay, we decided to biotinylate compound **27** (**27**K-biotin [D-Arg-Oic-Pro-D-Ala-Phe(*p*-Me)-Lys(biotin)-NH_2]) as a means of directly assessing the binding of our lead compound to PAR1 and PAR4. Recombinant PAR1 exodomain ($rPAR1_{EC}$) was prepared as described by Hasan et al.[81], and the binding protocol was used as previously described by Nieman et al.[92]. $rPAR1_{EC}$ was incubated overnight at 4°C in 0.1 M Na_2CO_3, pH 9.6, to link the receptor to the wells of a 96-well microtiter plate. After incubation, the wells were washed five times with 10 mM NaH_2PO_4, 150 mM NaCl, pH 7.4, and containing 0.05% Tween 20. The wells were then blocked with 0.2% bovine serum albumin in PBS with 0.05% Tween 20 for one hour at 37°C. After blocking and washing of the wells, the bound $rPAR1_{EC}$ was incubated with various concentrations of **27**K-biotin in the presence (non-specific binding) and absence (total binding) of 150-fold excess of unlabeled **27**. The specific binding curve (green line) for **27**K-biotin based on the time course of binding to PAR1 is shown in Figure 12.

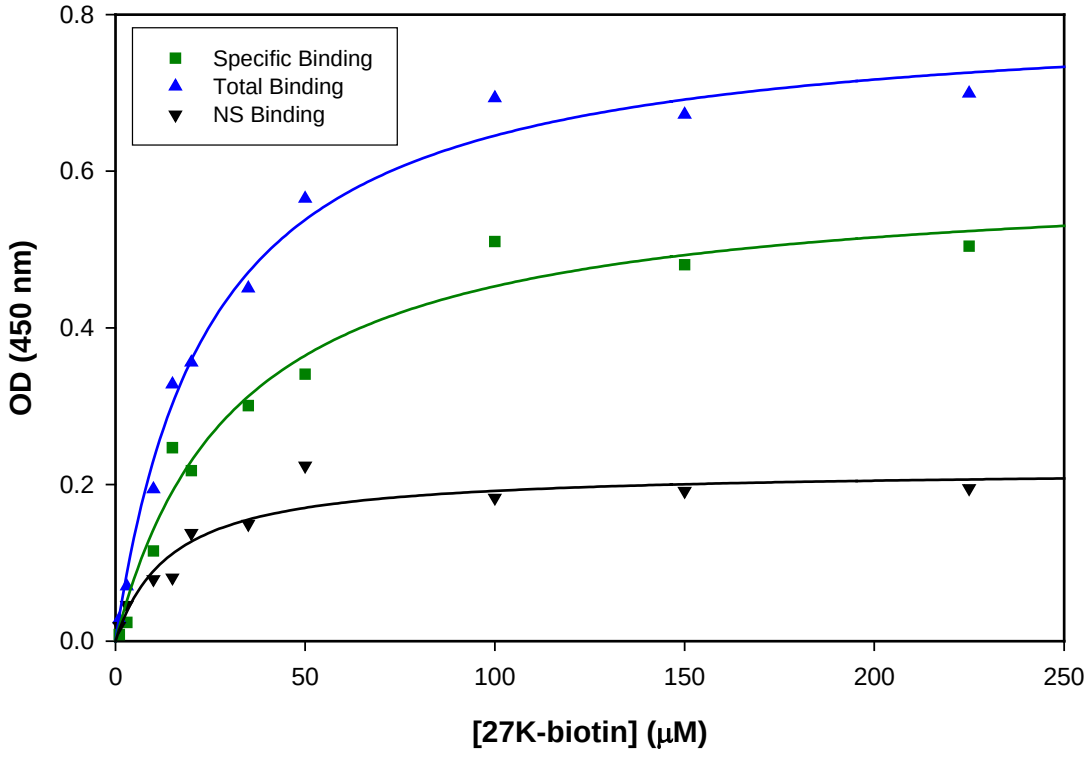

Figure 12: Compound **27**K-biotin binding to rPAR1$_{EC}$ linked to microtiter plates. The binding assay was performed as described in *Materials and Methods*. The data are represented as the mean ± standard deviation of three independent experiments.

The results of the direct binding studies demonstrate that compound **27** is specifically binding to the exodomain of PAR1 (green line in Figure 12). However, the results from this experiment was once again questioned when the competition-binding experiments were performed in the presence of negative controls such as "scrambled peptides" and D-Glu-Oic-Pro-D-Ala-Phe(*p*-Me)-NH_2 (inactive compound due to the lack of positively charged D-arginine in position 1). The "scrambled peptides" were able to compete with **27**K-biotin while D-Glu-Oic-Pro-D-Ala-Phe(*p*-Me)-NH_2 was not. A possible explanation for the discrepancy in the data is that the binding experiments are not particularly representative of the environment necessary for compound **27** to interact

with the receptor at the cellular level. By linking the $rPAR1_{EC}$ to the wells in the presence of 0.1 M Na_2CO_3 buffer, a negatively charged surface is created that may be responsible for the binding of peptides due solely on the presence of the positively charged D-arginine residue.

In order to further investigate the mechanism of action of the lead compound, Dr. Schmaier's laboratory is currently working on a cell-based assay using HeLa cells that were engineered to express PAR1 and PAR4 in order to assess the binding of compound **27** to the receptors in a more natural setting. The receptors are expressed at the surface of the cells to mimic their expression in normal platelets. The 5-carboxyfluorescein labeled compound **27** (**27**K-FAM [D-Arg-Oic-Pro-D-Ala-Phe(*p*Me)-Lys(5-FAM)-NH_2]) was synthesized in order to be used in flow cytometry studies to determine if the peptide is specifically binding to the receptors in cells. The labeled compound has maintained the characteristics of compound **27** as determined by the activity in the platelet aggregation assay (28 ± 6 μM). Therefore, the analog is a good candidate for probing the interaction of the peptide and PAR1 and PAR4 in cells.

IN VIVO STUDIES WITH COMPOUND 27. The in depth *in vitro* experiments have provided insight into the mechanism of action of the peptide analogs, in particular compound **27**. The data indicate that the lead compound is inhibiting platelet aggregation through the inhibition of thrombin both *in vitro* and in cells. The natural progression was to analyze the effects of the lead compound *in vivo*. The animal studies were performed by Mark Warnock in Dr. Schmaier's lab. These studies were carried out to determine the pharmacokinetic profile of compound **27** as well as its ability to affect the coagulation

system in an animal model[92]. The data from the pharmacokinetic studies performed in dogs showed that compound **27** has a prolonged half life ($t_{1/2\alpha}$) of 32.6 ± 3.2 min and slower clearance of 8.1 ± 5.1 ml/min/kg when compared to TH146 ($t_{1/2\alpha}$ = 3.1 ± 0.3 min and clearance of 66 ± 32 ml/min/kg), and the plasma half life of **27** is an order of magnitude longer than the natural peptide RPPGF[92]. The studies showed that compound **27** prevents thrombosis in the mouse. Analog **27**, at 0.4 mg/kg IP, produces a significant prolongation ($p<0.005$) in the time to occlusion of the mouse right carotid artery in the Rose Bengal model for arterial thrombosis[92].

Following up on these promising initial results, our collaborator, Dr. John Hilfinger from Therapeutic Systems Research Laboratories, Inc., performed oral absorption and intestinal stability studies through the analysis of rat plasma and intestinal samples using LC/MS/MS. The data suggest that our lead compound is fairly stable, shows modest intestinal permeability, and demonstrates 12.7% oral bioavailability (Tables 8 and 9, and Figure 13). Investigations were performed on **27** to determine the stability in buffer, intestinal washings (also termed perfusates), and intestinal homogenates that were prepared from rat intestines. In these assays, aliquots of the synthetic peptide solution (1 mg/ml) were added to 0.9 ml of MES buffer, pH 6.5, intestinal perfusate, or intestinal homogenate at 37^{o}C and sampled over a 90 minute time period and assayed by LC/MS/MS analysis. In simple MES buffer, at pH 6.5, the half life of the compounds in pH 6.5 buffer varied from approximately 2 hours to stable over the time frame tested. As shown in Table 8, peptide **27** is 2-19 fold more stable than TH146, and peptide **29** showed no measurable breakdown throughout the duration of the assay. From these data, it is clear that those compounds with fewer natural peptide bonds were

the most stable in the intestinal setting, and are therefore more likely to be absorbed intact from the intestinal segment.

TABLE 8

Estimated half lives ($t_{½}$) for selected Thrombostatin analogs in buffer (pH 6.5), intestinal homogenates, and intestinal perfusate

Compounds	**MES Buffer (pH 6.5)**	**Intestinal Perfusate**	**Intestinal Homogenate**
	$t_{1/2}$ (min)		
TH146	178.70	110.55	40.32
27	363.01	313.99	756.95
29	stable	stable	ND

Stable refers to no observed breakdown over the time course of the experiment. ND: not determined.

Since compounds **27** and **29** displayed considerable stability in both buffer and in the intestinal setting, they are likely to be absorbed intact from the gastrointestinal tract. The *in situ* single pass perfusion experiments (data not shown) confirmed our assumption by showing that compound **27** displayed modest intestinal permeability, suggesting that this stable peptide could have the potential to be delivered orally. In order to test this hypothesis, the bioavailabilty of compounds **27** and **29** was determined by direct instillation of compounds into the duodenum, and the systemic levels of each peptide were monitored through blood collection. Figure 13 shows that substantial levels of both analogs are observed in the plasma over the course of 4 hours while no TH146 is detected.

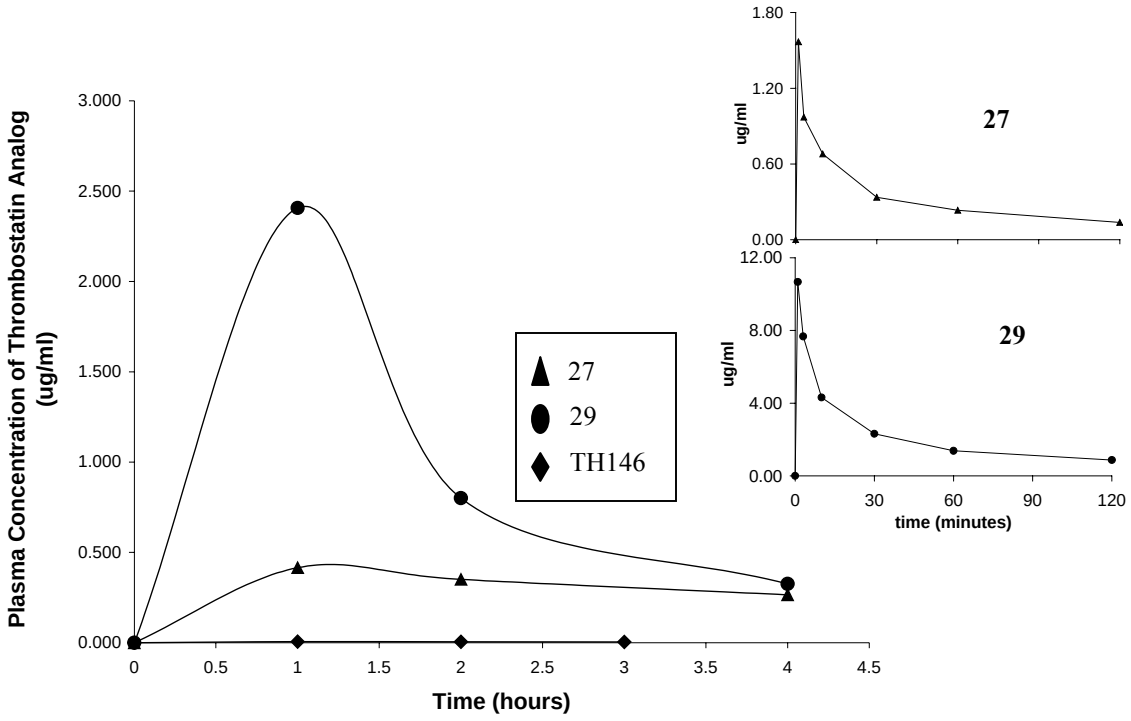

Figure 13: Systemic plasma levels of compound **27**after direct instillation into duodenum. 3 mg of TH146, **27**, or **29** were injected into the duodenum and blood was collected from the jugular vein at 0, 1, 2, 3, and 4 hours. The plasma levels were determined using LC/MS/MS analysis. The insets contain C_p vs. time profiles after IV dosing of **27** (top) and **29** (bottom). The assay was performed as described in *Materials and Methods*.

In order to determine the oral bioavailability of the analogs, the area under the curve (AUC_{0-t}) was calculated using the C_p (plasma concentration) versus time data (Figure 13). To derive the AUC directly from the C_p, a numerical approximation method known as trapezoidal rule was employed. In this technique the area under the curve is divided into segments assumed to be trapezoidal in shape then the sum of the segments gives an approximation for the definite integral[99, 100]. The calculated values for AUC_{0-t} are displayed in Table 9 along with the octanol:water partition coefficient at pH 7, Log $D_{pH7,}$ used to determine the lipophilicity of the analogs. Since both analogs are significantly more lipophilic than TH146, we expected that they would display higher oral bioavailability. Compound **27** was 12.7% bioavailable, which was in accordance

with the lipohilicity data. However, analog **29** was not as successful (5.2%), which was surprising due to its stability, lipophilicity profile, and plasma concentration over time. The oral bioavailability results for **29** are currently being re-evaluated by our collaborator along with compounds **33** and **36** to elaborate on the features required for improved bioavailabilty for our analogs.

TABLE 9

Compounds **27** and **29** show increased systemic exposure compared to TH146

Compounds	**Sequence**	**AUC_{0-t} (μg/mL*hr)**	**logD (pH 7)**
TH146	D-Arg-Oic-Pro-Gly-Phe-NH_2	0.016	0.21 ± 0.01
27	D-Arg-Oic-Pro-D-Ala-Phe(*p*-Me)-NH_2	1.208 (12.7%)	0.52 ± 0.02
29	D-Arg-Oic-Pro-D-Ser-Phe(*p*-Me)-NH_2	3.933 (5.2%)	0.52 ± 0.01

The AUC for the analogs was determined from the C_p x time data in Figure 13 using the trapezoidal rule. Oral bioavailability for the compounds (in parenthesis) were calculated from the ratio of the oral AUC divided by the compounds IV AUC data and a factor to account for the differences in the oral and IV dose (3 mg oral vs 0.2 mg IV). The Log $D_{pH\ 7}$ value for TH146, **27** and **29** are presented in the final column.

Compound **27** thus shows promise as a potent, orally available compound, and a patent has been applied for and accepted for this group of analogs as a new class of anticoagulant compounds (U.S. Patent Application #20060276402). In addition, as preparation for an Investigative New Drug application (IND), compound **27** underwent toxicology studies at independent research facilities to determine its safety profile. Toxicology studies on rats and dogs were performed to establish the therapeutic window for **27**. These experiments determined that the concentration of agent necessary to prevent arterial thrombosis *in vivo* was over an order of magnitude higher than the no-observable-adverse-effect-level (NOAEL) indicating that the compound has an acceptable therapeutic window. In addition, genotoxicity assays were performed and compound **27** was negative for mutagenic activity in selected bacteria, for induction of

structural or numerical chromosome aberrations in human lymphocytes, and for mouse bone marrow micronucleus frequency. In summary, the data collected indicate that **27** is well positioned for submission of its IND to the FDA for use in a human Phase I clinical trial to measure its pharmacokinetics and pharmacodynamics with a single intravenous infusion for the treatment of myocardial infarction and high-risk active angina.

CRYSTAL STRUCTURE SUPPPORTS THE BIOLOGICAL DATA. The biological data gathered thus far suggest that our lead compound acts as an antiplatelet and anticoagulant agent through the interaction with the active site of thrombin. This is contrary to our original hypothesis in which we sought to design a compound that would interact with the extracellular domain of PAR1. However, we were aware that bradykinin and RPPGF also interacted with the active site of thrombin at high concentrations (K_i = 1.7 mM)[81]. Through our design efforts we have made a low micromolar inhibitor of thrombin (K_i = 6.2 μM). Dr. Enrico Di Cera from Washington University recently elucidated the crystal structure of compound **27** bound to the active site of thrombin (Figure 14 represents the unpublished structure). This structure provides the definitive confirmation that our lead compound is indeed interacting with thrombin.

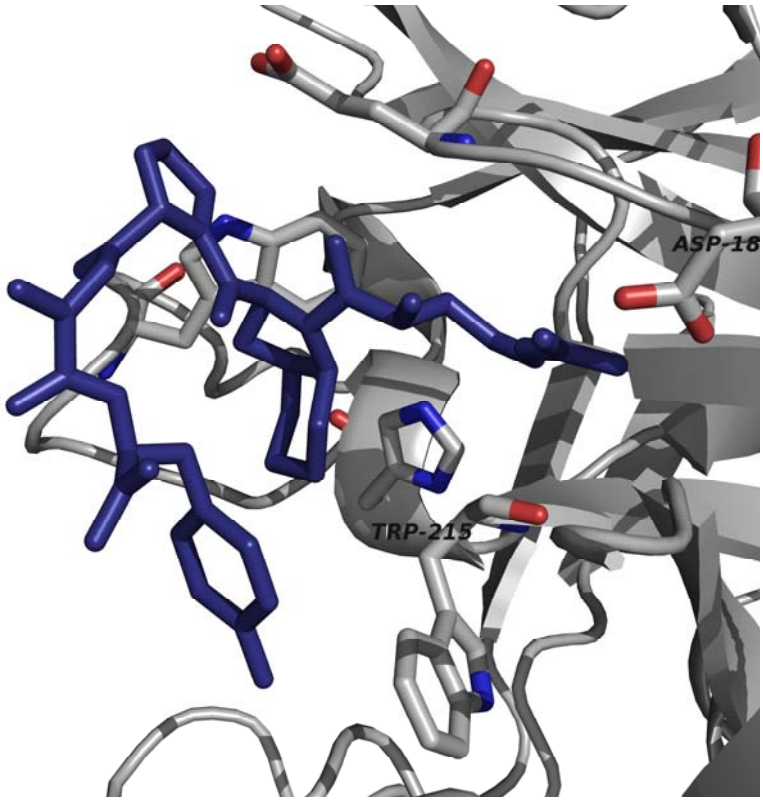

Figure 14: Crystal structure of **27** bound to the active site of thrombin.
Katrina Lexa created the image with the peptide in blue and thrombin in gray.

The design of a direct thrombin inhibitor was not the original goal of our research efforts, but there is great potential in developing an agent that displays favorable stability and oral bioavailability with minimal toxicological effects as eluded to in Chapter I. With the crystal structure in hand we were able to study the interaction of our compound with thrombin and determine the class of compounds that would best classify compound **27**. Katrina Lexa, a rotation student in the Mosberg lab, was able to overlay the structure of **27** bound to thrombin with other crystal structures of direct thrombin inhibitors available in the Protein Data Bank. Figure 15 displays the resulting overlay and shows that our compound has the distinct features of hirudin-like analogs with the sequence D-Phe-Pro-Arg. However, **27** acts as a retrobinder at the active site of the enzyme since its N-

terminus fits into the S1 pocket and the main chain runs parallel in respect to the Ser^{141}-Gly^{216} of the active site, hence the D-Arg-Oic-Pro-D-Ala-Phe(*p*Me)-NH_2 sequence[81, 101, 102]. In normal substrate binding to thrombin, the backbone of the peptide spans from C-terminus to N-terminus. The $D\text{-}Arg^1$ of **27** occupies the S1 pocket that corresponds to the C-terminus arginine of the hirudin-like inhibitors. The guanidino moiety is in prefect alignment with the carboxyl group of Asp^{189} of the active site. The presence of Oic at position 2 followed by Pro^3 creates a sterically restricted backbone that forces the *p*-methylphenylalanine side chain to be in close proximity with Trp^{215}, another important site of interaction in the active site. This location is consistent with the position of the N-teminus D-Phe residue of the hirudin analogs.

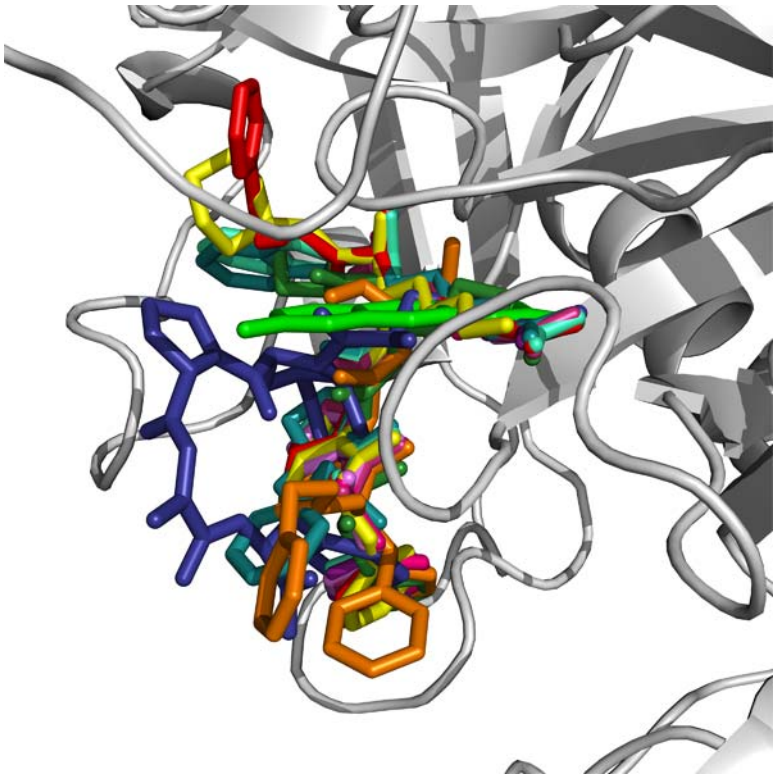

Figure 15: Overlay of compound **27** (in blue) with other direct thrombin inhibitors bound to the active site of the enzyme. The inhibitors used in the overlay are hirudin (3HAT-teal), hirugen (1AIX-orange, 1B5G-aqua, 1A5G-red, 1A46-yellow), hirugen residues 54-65 of hirudin (1BCU-green), hirulog (1ABI-dark green), thiazole containing hirugen (1TBZ-cyan), and D-Phe-Pro-Arg-chloromethylketone (1ABJ-lavender, 1B7X-magenta, and 1HAI-purple).

The next step in understanding the interaction of the lead peptide with thrombin was to look at the structure activity relationship data and apply it to the computational model. Our approach was to simply model the binding of our analogs by homology to the structure of compound **27** bound to thrombin. This approach ignores the possible conformational differences in the analogs so it is only a crude representation of the possible interactions with the active site residues. Numerous substitutions have been made at positions 4 and 5 of the peptide, and the resulting effect on activity was described in detail in Chapter II. Katrina Lexa has developed a computational model for several analogs of **27** based on its structure and position of the lead compound in the crystal structure, as shown in Figure 16.

The analogs selected have varying activities and were placed in the active site of thrombin as shown in Figure 16. This approach will allow us to generate structures for new analogs with improved activity and more favorable pharmacokinetic characteristics. Figure 16 illustrates the differences in position 5 substituents as compared to compound **27**. When the correlation between the platelet aggregation data and the computational studies was drawn, it suggested that the modifications leading to a change in positioning of the phenylalanine side chain translated into a change in activity. The compounds selected for analysis were compounds **40** (D-Arg-Oic-Pro-D-Ala-Phg-NH_2), **31** (D-Arg-Oic-Pro-D-Ala-Hfe-NH_2), **44** (D-Arg-Oic-Pro-D-Ala-D-Phe(2,4-DiMe)-NH_2) and the lead compound **27** (D-Arg-Oic-Pro-D-Ala-Phe(*p*-Me)-NH_2).

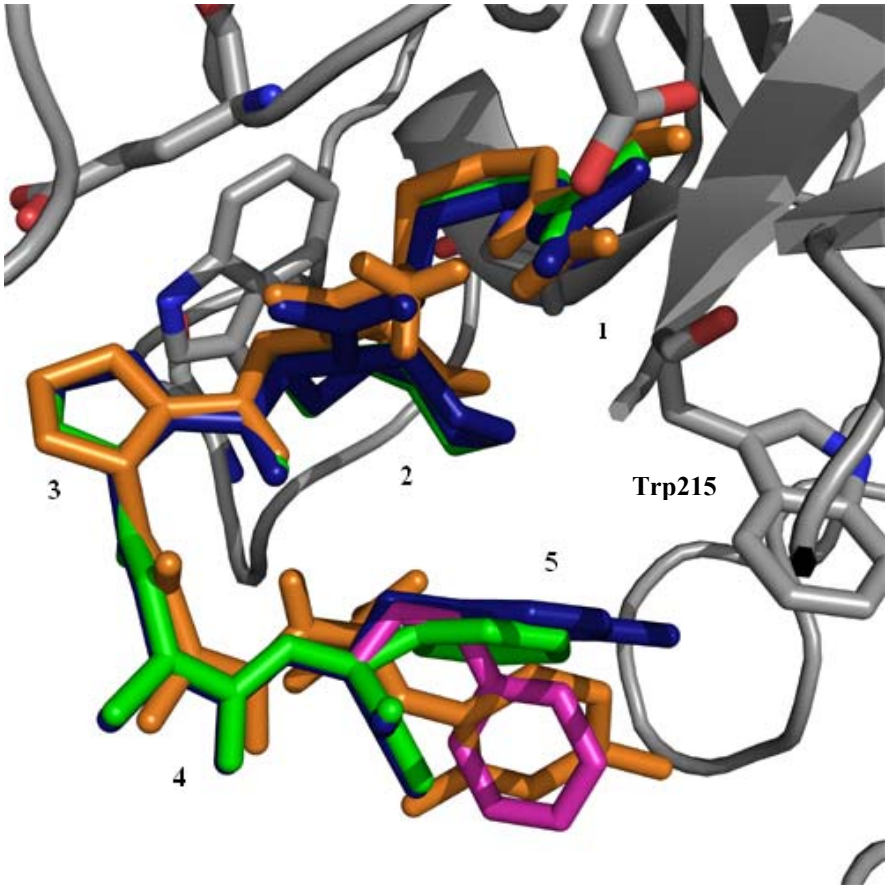

Figure 16: Overlay of structure activity relationship using the crystal structure of **27** bound to active site of thrombin for docking the peptides. **27** is represented in blue, **40** in green, **44** in orange and **31** in magenta.

Compound **40** (green) has phenylglycine (Phg) in position 5, which possesses one less methylene group since the aromatic ring is attached directly to the alpha carbon. In addition, phenylglycine does not have the methyl group at the *para* position on the ring. This analog was 2-fold less potent than compound **27** in the functional assay as shown in Table 5 (Chapter II). The resulting slight decrease in activity could be explained by the approximately 1.4 Å gap created between the aromatic ring and the Trp^{215} residue of the active site of thrombin. A 2-fold change in potency is not particularly relevant as it is within the experimental error for this assay. However, this particular analog was

analysized here since it fits into the trend we observed for the possible importance of the relative position of the aromatic ring of the fifth residue to Trp^{215}.

The spatial differences are even more accentuated in compound **31** (magenta) with homophenylalanine (Hfe) at the fifth position. The unusual residue possesses an additional methylene between the alpha carbon and the aromatic ring. In this case, the addition of the alkyl moiety changes not only the distance, but also the orientation of the ring due to the torsion angle introduced by the additional carbon-carbon bond. As illustrated in Figure 16, the aromatic ring faces away from the Trp^{215} residue, perhaps accounting for the 8-fold decrease in activity in the platelet aggregation assay. When observing the final compound, **44** (orange), docked to the active site, the D-stereochemistry of the amino acid residue (D-Phe(2,4-DiMe)^5) appears to position the ring somewhere between Phg and Hfe. Since the potency of **44** is 6-fold lower than that of **27** (in between 2 and 8 fold), this is consistent with the binding interaction trend between the Trp^{215} side chain and the fifth residue side chain of the inhibitor.

We can thus conclude that the orientation of the residues at position 5 plays a role in the activity of the analogs suggesting that the interaction between the residue and Trp^{215} is important for activity. The ability to correlate the functional activity with the docking studies solidifies the potential of employing the computational model for future development of novel analogs with optimized interactions with the important residues of the active site of thrombin. More extensive analysis of the docking results are ongoing in our lab and will be used to design future analogs.

CHAPTER IV

SYNTHESIS OF LIPOPHILIC ANALOGS OF COMPOUND 27 WITH IMPROVED STABILITY AND ORAL BIOAVAILABILITY.

As previously stated in Chapter I, the long-term objective of the project is to develop an orally bioavailable drug for treatment of individuals with acute coronary syndromes. Suitable progress has been made towards designing an inhibitor with favorable pharmacokinetic characteristics as shown in Chapter III with the results from the intestinal stability and absorption studies carried out by our collaborator, Dr. John Hilfinger (TSRL, Inc.). Since our lead compound is composed of unnatural amino acid residues, it is relatively stable in the intestinal setting and is more likely to be absorbed intact from the intestinal segment than are unmodified peptides. Many of the agents routinely used for anticoagulant and/or antiplatelet activity, such as heparin, are administered intravenously. Other oral agents attack specific platelet targets like the ADP receptor (clopidogrel) or platelet cyclooxygenase (aspirin).

Compound **27**, which displays modest oral bioavailability with 12.7% availability after simulated oral dosing as measured by LC/MS/MS, represents an excellent lead for the development of orally available thrombin inhibitors. Our aim is to improve the oral bioavailability of peptide **27** by incorporating other chemical modifications in order to make the compound less charged and more lipophilic. There are several sites on our lead pentapeptide that could be modified including both the N- and C-termini, the guanidino

moiety of the D-arginine in position 1, and the aromatic ring in position 5. For instance, di-substituted phenyalanine would increase the lipophilicity of the analog and acetylation of the N-terminus would decrease the net charge of the peptide. The targeted sites on the lead compound that could be modified are depicted in Figure 17.

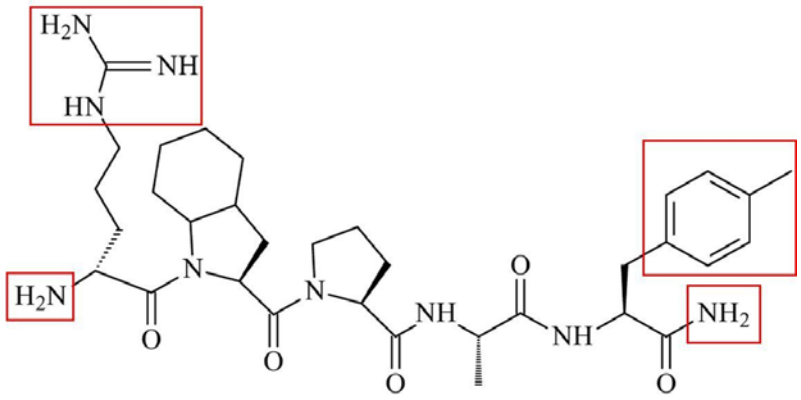

D-Arg-Oic-Pro-*D*-Ala-pMePheNH$_2$ [rOicPaF(p-Me)-NH$_2$]

Figure 17: Structure of **27** with the sites of modification marked with red rectangles.

The first modifications involved reducing the positive charge of the peptide by acetylating the N-terminus in one analog (**58**) and replacing the D-Arg with D-citrulline (guanidino group is substituted by a carbamoyl group) in another (this peptide was synthesized by Anjanette Turbiak). Both analogs were inactive in the platelet aggregation assay indicating that these are key features necessary for activity. Consequently, we decided to decrease the polarity of the guanidino group at position 1 by synthesizing N^{ω}-methyl-D-arginine (**1b** in Scheme 1) and incorporating the residue into the peptide[103-105]. The synthesis of protected N^{α}-Z,N^{ω}-(Me, Mtr)-D-arginine (**1**) for incorporation into analog **51** (Table 10) is shown in Scheme 2[106, 107].

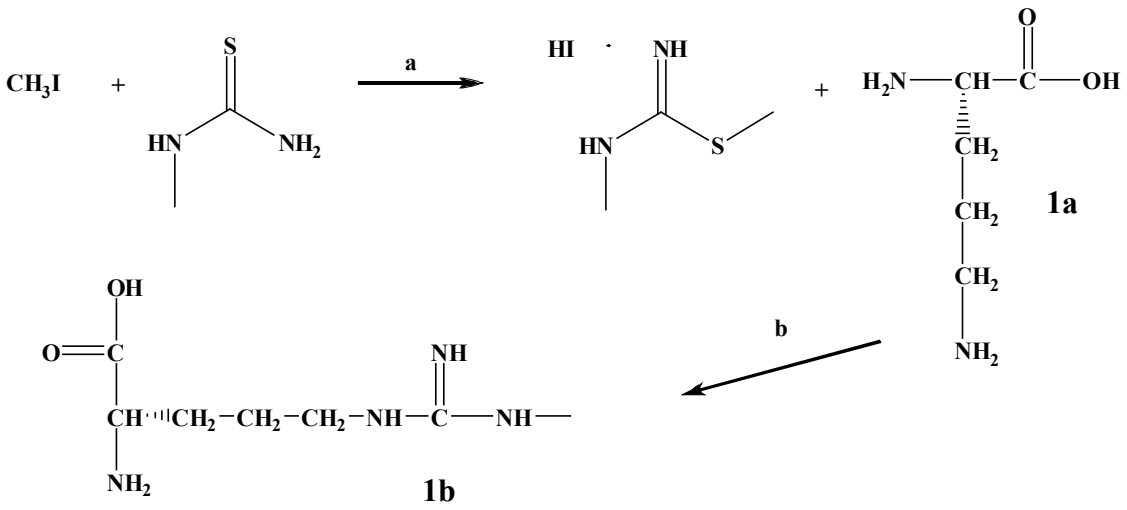

Scheme 1: Synthesis of N^{ω}-alkyl-D-arginine residues.
a: acetone, reflux; **b**: copper (II) acetate, 1:1 ammonium and water.

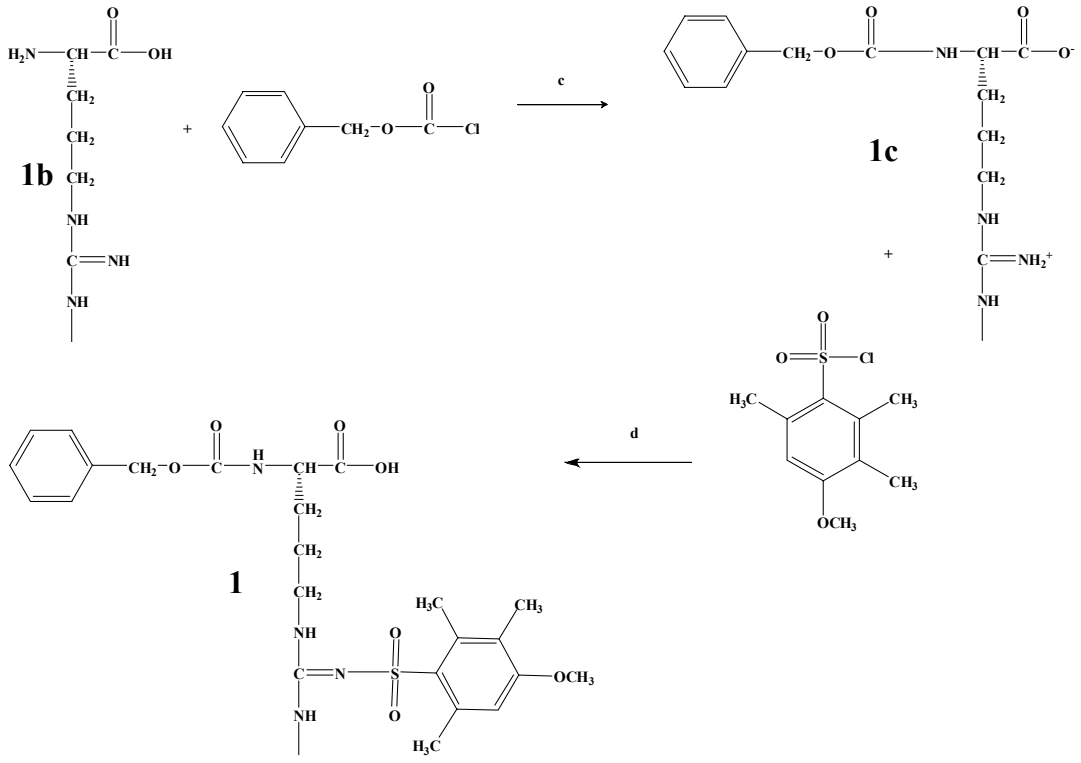

Scheme 2: Protection of N-terminus and side chain group.
c: 0.05 N sodium hydroxide,0˚C; **d**: 4 N sodium hydroxide in acetone, room temperature.

In parallel with the position 1 modifications, di-substituted phenylalanine analogs were synthesized and incorporated into the fifth position of the pentapeptide. These analogs have an additional methyl group at either *ortho* or *meta* positions on the aromatic ring. The synthesis of the di-substituted phenylalanine analogs is displayed in Scheme 3[108]. The position 5 analogs were designed to serve two purposes: increase the lipophilicity due to the additional alkyl group and potentially enhance the activity since large, aromatic groups were found to be favored at this position (see Chapter II).

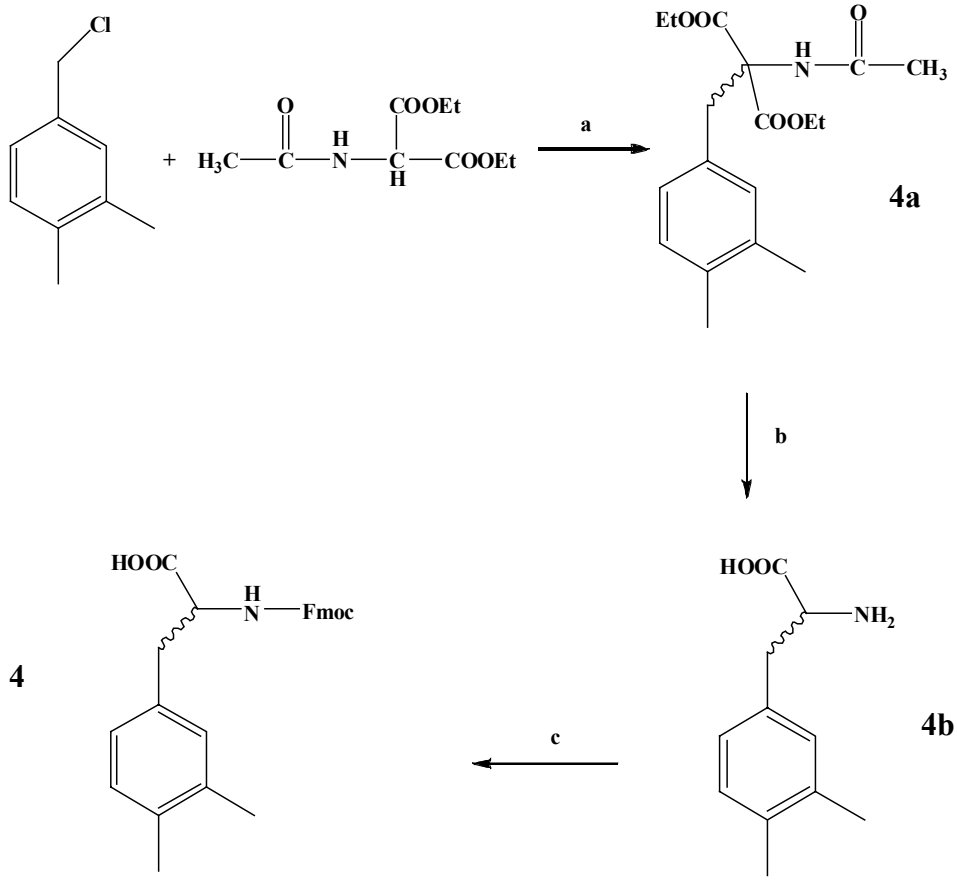

Scheme 3: Synthesis of Fmoc-3,4-dimethylphenylalanine.
a: sodium in absolute alcohol saturated with N_2,, reflux; **b**: 6 N HCl, reflux under N_2; **c**: Fmoc-OSu in DMF, acetone and 10% sodium bicarbonate, vigorous stirring, room temperature. Synthesis of 2,4-dimethylphenylalanine followed the same protocol starting with 2,4-dimethylbenzyl chloride.

The final site selected for modification was the amide group at the C-terminus of compound **27**. Unlike the N-terminus, the C-terminus of our lead peptide could be extended as was shown with the synthesis of labeled peptides, which required the addition of a C-terminal lysine residue in order to link the labeling agent. The labeled analogs were just as active as the unlabeled peptide in the platelet aggregation assay (19-28 μM). Two analogs were synthesized that contained N-alkyl modifications, compound **43** (N-methyl) and compound **48** (N-ethyl). These analogs were synthesized through the use of alkylated indole resins that give N-alkylated amides after cleavage with TFA (Scheme 4).

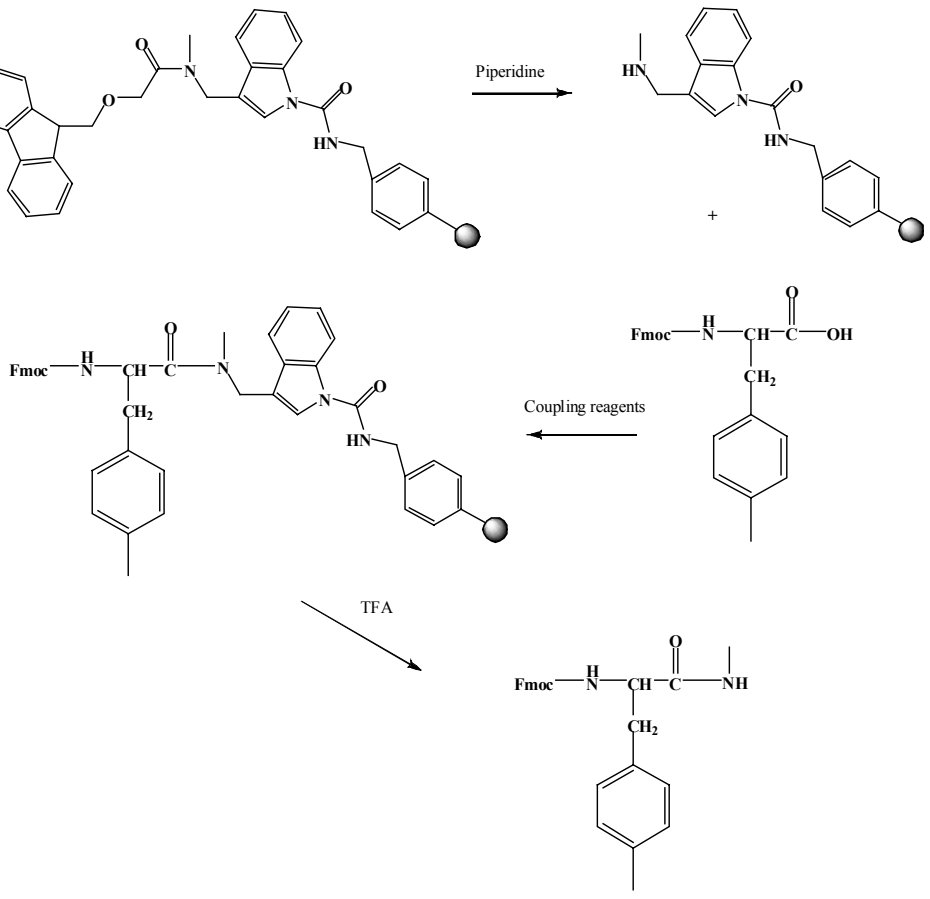

Scheme 4: Synthesis of N-methyl substituted carboxamide using [3-({methyl-Fmoc-amino}-methyl)-indol-1-yl] acetyl AM resin.

The proposed peptide analogs are displayed in Table 10 along with the corresponding results from the platelet aggregation assay. For clarification, compounds **44**/**45** and **46**/**47** were synthesized as a mixture of diasteriomeric peptides due to the use of racemic amino acid residues as starting materials (4b in Scheme 3). The diasteriomers were separated by RP-HPLC and the tentative assignment of **45** and **47** as L-stereochemistry for residue 5 was based solely on the activity in the platelet aggregation assay.

TABLE 10

Modifications at position 1 and 5 for increased lipophilicity

Compounds	**Sequence**	**Inhibition of Threshold Platelet Aggregation**
		μM ± S.E.M
27 (FM19)	D-Arg-Oic-Pro-D-Ala-Phe(*p*-Me)-NH_2	16 ± 4
43	D-Arg-Oic-Pro-D-Ala-Phe(*p*-Me)-NH-Me	21 ± 9
44	D-Arg-Oic-Pro-D-Ala-D-Phe(2,4-Me)-NH_2	100 ± 11
45	D-Arg-Oic-Pro-D-Ala-Phe(2,4-Me)-NH_2	28 ± 10
46	D-Arg-Oic-Pro-D-Ala-D-Phe(3,4-Me)-NH_2	750*
47	D-Arg-Oic-Pro-D-Ala-Phe(3,4-Me)-NH_2	62 ± 19
48	D-Arg-Oic-Pro-D-Ala-Phe(*p*-Me)-NH-Et	5 ± 0.4
49	Arg(Me)-Oic-Pro-D-Ala-Phe(*p*-Me)-NH_2	833 ± 167
50	Arg(Me)-Pro-Oic-D-Ala-Phe(*p*-Me)-NH_2	NE*
51	D-Arg(Me)-Oic-Pro-D-Ala-Phe(*p*-Me)-NH_2	1,000*

Data presented are the mean ± S.E.M. of $n > 3$ independent experiments. The values given represent the minimal concentration of peptide necessary to inhibit 100 % of threshold γ -thrombin-induced platelet aggregation (IC_{100}). * These data are presented as 1 experiment not as the mean of multiple experiments.

The data suggest that the addition of alkyl moieties to either the aromatic ring in position 5 or the amide of the C-terminus are well tolerated. Compounds **43** and **45** showed negligible changes in activity when compared to **27** (1.3 and 1.8-fold decrease, respectively), and both possessed an additional methyl group. However, the most promising compound in this series was peptide **48** (D-Arg-Oic-Pro-D-Ala-Phe(*p*-Me)-NH-Et), which was 3.2-fold more potent than the previous lead, compound **27**. The

alkylation of the amide group of the C-terminus with the ethyl moiety produced a 5 μM inhibitor of platelet aggregation and has provided a site at which longer aliphatic and aromatic groups can be added to modulate the lipophilicity and possibly improve the intestinal absorbance of the analogs.

This series has also provided information on requirements for position 1. Compounds **49** thru **51** were designed to explore whether any modifications to the guanidino group could be tolerated. Previously synthesized analogs with complete removal of the guanidino moiety (D-citrulline and D-lysine at position 1) produced inactive analogs. By alkylating the N^{ω} of the arginine residue, we were aiming to maintain activity due to the small size of the substituent. Unfortunately, all peptides with this modification were inactive in the platelet aggregation assay as shown in Table 10. The results were not surprising since the crystal structure of compound **27** bound to the active site of thrombin clearly showed that the alignment between the D-arginine residue and Asp^{189} (Figure 14) was ideal. Compound **51** was inserted into the active site and the interaction of N^{ω}-Methyl-D-arginine with Asp^{189} is highlighted in the computational model in Figure 18.

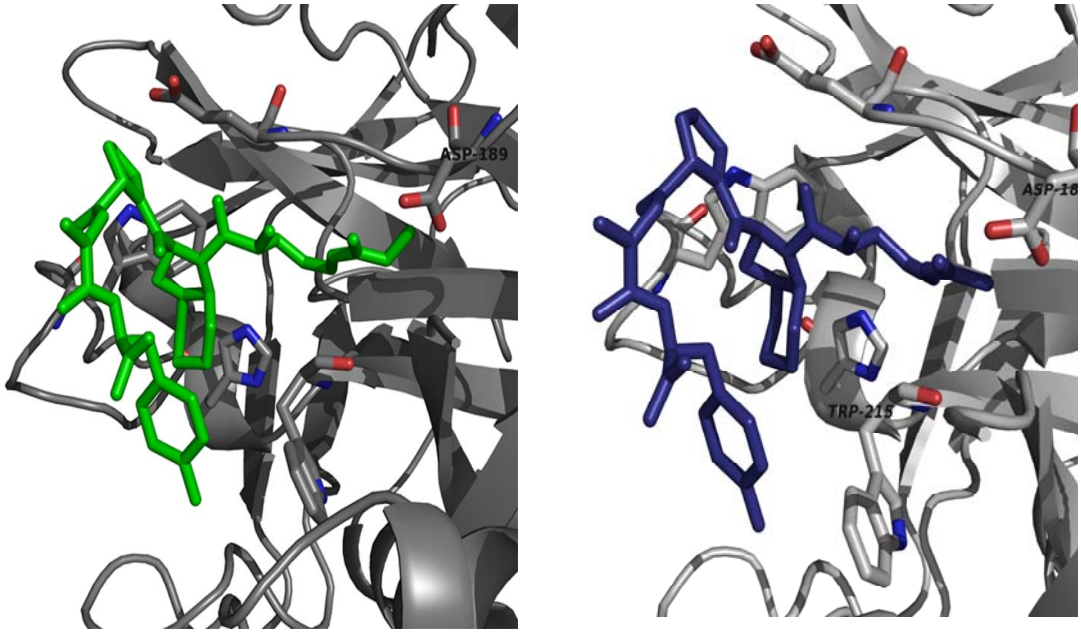

Figure 18: Compound **51** docked to the active site of thrombin highlighting the interaction of N^{ω}-Methyl-D-arginine (left side in green) and Asp^{189}. On the right, **27** is displayed in blue for comparison.

In order to experimentally examine whether the changes in the platelet aggregation results are due to variations in the interaction with the active site of thrombin, the inhibition constant (K_i) for several of the new analogs was determined as previously described in Chapter III. The K_i values of the peptide analogs correlated with the results of the platelet aggregation assay as shown in Table 11. For instance, compound **51**, which was inactive in the physiological assay, had significantly larger K_i value (409.5 ± 144 μM) than the new lead (compound **48**, K_i = 2.1 ± 0.4 μM). This suggests that the peptides are modulating platelet aggregation through their ability to interact with thrombin. Furthermore, compound **48** is 3-fold better inhibitor of thrombin than **27**, which precisely corresponds to the result for the platelet aggregation assay (3.2-

fold improvement over **27**). This series has provided further confirmation that our analogs are acting as direct thrombin inhibitors.

TABLE 11

Effect of peptide analogs on enzymatic activity of thrombin.

Compounds	**Sequence**	K_i ***(μM ± S.D.)***	**Platelet Aggregation *(μM ± S.E.M)***
TH146	D-Arg-Oic-Pro-Gly-Phe-NH_2	91.9 ± 7	140 ± 20
27	D-Arg-Oic-Pro-D-Ala-Phe(*p*-Me)-NH_2	5.9 ± 1	16 ± 4
29	D-Arg-Oic-Pro-D-Ser-Phe(*p*-Me)-NH_2	6.9 ± 0.9	13 ± 6
43	D-Arg-Oic-Pro-D-Ala-Phe(*p*-Me)-NH-Me	5.2 ± 0.7	21 ± 9
44	D-Arg-Oic-Pro-D-Ala-D-Phe(2,4-DiMe)-NH_2	25*	100 ± 11
45	D-Arg-Oic-Pro-D-Ala-Phe(2,4-DiMe)-NH_2	5 ± 0.8	28 ± 10
48	D-Arg-Oic-Pro-D-Ala-Phe(*p*-Me)-NH-Et	2.1 ± 0.4	5 ± 0.4
51	D-Arg(Me)-Oic-Pro-D-Ala-Phe(*p*-Me)-NH_2	409.5 ± 144	1,000*

The enzymatic activity assay was performed as described under *Materials and Methods*. The data presented are mean ± standard deviation of at least three independent experiments. *The result reported was based on a single experiment due to small amount of pure material available for testing.

We are currently awaiting the stability and bioavailability results that will determine if we have enhanced the lipophilicity and absorbance profile of our lead compound by introducing these small changes to its structure. Dr. John Hilfinger is examining the stability, LogD values, and oral bioavailability of a number of analogs including **48**, which has the potential of maintaining the stability and bioavailability of **27** since it has the same amino acid composition. We are hopeful that the additional ethyl group at the C-terminus may lead to improved absorption due to the possible increase in lipophilicity.

The absorption experiments are underway and the preliminary results suggest that the small modifications made to the sequence of our lead compound can modulate absorption in animal models. As postulated above, compound **48** displayed similar

absorption to analog **27**. This data is particularly interesting since compound **48** maintained the absorption profile of the previous lead while improving the activity by 3-fold.

CHAPTER V

CONCLUSIONS

The aims set forth for this research project were accomplished through the use of a variety of approaches including several series of peptide analogs, biochemical and molecular biology techniques, *in vivo* and *in situ* pharmacokinetic studies, and crystal structure driven computational models. This dissertation emphasizes the benefits of using unnatural and/or modified amino acid residues substituted into the sequence of a naturally occurring peptide as a means of modulating activity against platelet aggregation. Particular analogs were identified that are both potent inhibitors of the physiological action as well as direct inhibitors of thrombin with desirable pharmacokinetic profiles. In addition, this dissertation describes the key structural features required for potency and suggests modifications that may lead to improved oral absorption in the gastrointestinal tract. Peptides **27** and **48** show promise to become the first orally administered anticoagulant with action through the direct inhibition of thrombin.

Several trends were observed in the structure activity relationship studies described in Chapter II. These series of peptides were synthesized with the aim of inhibiting thrombin mediated platelet aggregation. The fourth position of the peptide analogs of D-Arg-Oic-Pro-Gly-Phe has a preference for D-amino acids, but is relatively

indiscriminant in regards to the actual amino acid residue and its side chain properties. The presence of an aromatic ring on the side chain of the amino acid in position 5 was preferred over all other amino acid side chains, with Phe(*p*-Me) displaying the best activity thus far. In compound **27**, (D-Arg-Oic-Pro-D-Ala-Phe(*p*-Me)-NH_2), we have developed a 16 μM inhibitor of thrombin-induced platelet aggregation, which represents an order of magnitude improvement over previous RPPGF-related inhibitors.

Further studies were then performed to elucidate the mechanism of action of the lead peptide and its analogs. Like RPPGF and TH146, compound **27** also displays direct inhibition of thrombin as evident by the results of the coagulation assays reported in Chapter II. The fact that this lead compound was a 10-20 fold better inhibitor of the clotting abilities of thrombin than TH146 indicates that this peptide acts as a direct thrombin inhibitor by interacting with the active site of the enzyme. Furthermore, **27** was approximately 16-fold more potent at inhibiting the catalytic activity of thrombin as determined by the lower K_i value (5.9 μM). The same outcome was observed in cells, since **27** was a potent inhibitor of calcium mobilization in normal human cells. Calcium influx in platelets is a downstream signal of thrombin induced platelet activation and aggregation.

The data thus far suggests that compound **27** is a potent direct thrombin inhibitor *in vitro* and in cells. However, previously reported work by Hasan et al.[80, 81, 92] suggested that RPPGF and TH146 inhibited platelet aggregation by both interacting with the active site of thrombin and by binding directly to the extracellular domain of PAR1. In order to address this hypothesis, a competition-binding experiment to measure whether compound **27** interferes with the binding of 15 μM RPPGFK-biotin to the exodomains of

PAR1 and PAR4 was performed. The results did not completely support the hypothesis proposed by Hasan et al. Since compound **27** was 2-fold less potent than TH146 at inhibiting the binding of the labeled compound to the receptor, the results were suggestive of an interaction with the receptor, but the IC_{50} observed did not correlate with the physiological assay results. In the platelet aggregation assay, **27** was 7-fold more potent than TH146 suggesting that a different mechanism of action was modulating the anticoagulant activity of the peptide.

The recent elucidation of the crystal structure of analog **27** bound to the active site of thrombin by Dr. Enrico Di Cera provides complimentary data to confirm that the lead compound is a direct thrombin inhibitor (Chapter III). In the overlay computational studies performed by Katrina Lexa, compound **27** appears to align with hirudin-like analogs containing the sequence D-Phe-Pro-Arg. These compounds are characterized as potent inhibitors of the active site of thrombin, which is consistent with the biological data described in Chapter III. Many direct thrombin inhibitors have been developed, but they do not possess the pharmacokinetic characteristics for oral delivery. Therefore, in collaboration with TSRL, Inc. the pharmacokinetic profile of compound **27** was studied including its intestinal stability and oral bioavailability in rats. Since the peptide contains mostly unnatural peptide bonds, it was very stable and was 12.7% available following *in situ* administration.

The promising results from the stability and bioavailability studies led to the design of a series of analogs with features aimed at improving the oral absorption of compound **27**. The modifications made to the sequence of the lead compound were relatively small and conservative so as not to adversely affect the activity of peptide.

Initially the focus was to change the net charge of the peptide by acetylating the free N-teminus and eliminating the guanidino moiety at position 1. Both modifications produced inactive analogs in the platelet aggregation assay suggesting that both are required for interaction with thrombin. Consequently, the focus shifted to the opposite end of the peptide and substituents were added to the aromatic ring of phenylalanine at position 5 and to the amide group at the C-terminus. These modifications were well tolerated and a new lead compound was discovered. Compound **48** (D-Arg-Oic-Pro-D-Ala-Phe(*p*-Me)-NH-Et) has the same amino acid sequence as analog **27**, but possesses an ethyl group at the amide of the C-terminus. This compound is a 3-fold more potent inhibitor of thrombin and platelet aggregation (K_i = 2.1 μM, IC_{100} = 5 μM) than is **27**.

Since the sequence of the new lead peptide is the same as that of compound **27**, it can be expected that the stability will remain constant. However, the additional ethyl group at the C-terminus has the potential to increase the lipophilicity of the molecule and possibly improve the intestinal absorption.

CHAPTER VI

MATERIALS AND METHODS

PEPTIDES AND REAGENTS. Peptides were prepared by standard solid-phase peptide synthesis methods[109, 110]. Syntheses were done using Fast-Moc chemistry (activation with HBTU/HOBt) on a Applied Biosystems, Inc. Model 431A peptide synthesizer (Foster City, CA)[111]. The peptides were assembled on peptide amide linker polyethylene glycol polystyrene resin (PAL-PEG-PS resin) (Applied Biosystems, Foster City, CA), Rink amide resin (Advanced ChemTech, Louisville, KY), [3-({methyl-Fmoc-amino}-methyl)-indol-1-yl] acetyl AM resin or [3-({ethyl-Fmoc-amino}-methyl)-indol-1-yl] acetyl AM resin (Novabiochem, San Diego, CA). The protected amino acids were obtained from Advanced ChemTech with side chain protecting groups including Pbf and Mtr for Arg, D-Arg and alkylated arginine derivatives, *t*Bu for D-Ser and Tyr, Boc, for Lys, and Trt for Cys. Dde and biotin protected Lys along with 5-carboxyfluorescein (5-FAM) labeling agent were purchased from Novabiochem.

The following solvents used were HPLC grade: water, acetonitrile (CH_3CN), methanol, iso-propanol and dichloromethane (DCM) (Fisher Scientific, Fair Lawn, NJ). Trifluoroacetic acid (TFA) used was Biograde (Pierce, Rockford, IL), DMF (anhydrous) (Sigma Aldrich, Milwaukee, WI) was saturated with N_2, and pyridine (Sigma Aldrich) was distilled over ninhydrin. All other reagents and solvents were purchased from Sigma

Aldrich and were used without further purification. Reverse phase high performance liquid chromatography (RP-HPLC) solvents, prepared with HPLC grade TFA, were filtered and degassed prior to use. ^{1}H-NMR spectra were recorded on a Bruker™ DRX-500 spectrometer. NMR samples were dissolved in D_2O (Sigma Aldrich) and spectra were taken at room temperature. Ion exchange chromatography was performed with Dowex™ 50W x 8 resin (200-400 mesh, Sigma Aldrich) on a 32 x 2 cm column. TLC was performed with pre-coated TLC plates (2.5 x 7.5 cm, 250 μm silica gel thickness, Fluka). The following solvent systems were used: 3:1 Phenol-water (A) and 9:1 MeOH-chloroform (B). Products were visualized with iodine vapor and/or 1% (w/v) ninhydrin in ethanol.

RP-HPLC was accomplished with C_{18} Vydac™ columns: 0.46 x 25 cm for analytical RP-HPLC on Waters Alliance system, flow rate of 1.0 mL/min; 1.0 x 25 cm for semi-preparative RP-HPLC, flow rate of 4.7 mL/min; 2.5 x 22 cm for preparative RP-HPLC, flow rate of 10 mL/min on Waters system. The solvent system consisted of 0.1% (w/v) TFA in acetonitrile (solvent B) and 0.1% (w/v) TFA in water (solvent A). Silica gel purification was performed on pre-packaged cartridges (KP-Sil™, 32-63 μM, 60Å silica) on a Biotage™ system. The pure peptides were freeze dried on a bench top SLC VirTis™ freeze dryer (VirTis, Gardiner, NY). Molecular weights were determined using ESI-MS (electron spray ionization) positive mode (ThermoFinnigan, San Jose, CA).

GENERAL PROTOCOL FOR SOLID PHASE PEPTIDE SYNTHESIS. The syntheses were carried out with 0.25 mmol scale with 4-fold excess of amino acid residue and coupling reagents, unless otherwise specified. The synthesis cycle was initiated by

swelling the resin (0.25 mmol) in NMP followed by removal of the Fmoc group from the empty resin with neat piperidine, followed by extensive NMP washes and, subsequently, by coupling of Fmoc-protected amino acid (1 mmole) dissolved in HBTU in 0.5 M solution of HOBt in DMF along with additional NMP. The reaction was carried out in the presence of 2 M DIEA in NMP (Applied Biosystems)[111]. The activated amino acid reacted with the deprotected amino-terminus of the growing peptide chain. After 10 min of coupling, the resin was washed repeatedly with NMP and unreacted amino groups were acetylated using 10-fold excess of the capping solution (0.5 M acetic anhydride, 0.125 M DIEA, and 0.015 M HOBt in NMP). This sequence of steps was repeated until the full-length, resin-bound, protected peptide was obtained. The resin was filtered, washed with DCM and ethyl alcohol and dried *in vacuo*.

GENERAL METHOD FOR LOADING RINK AMIDE RESIN (FM55 and FM59). The first amino acid residue was loaded manually on to the resin for FM55 and FM59. The reactions were carried out in a fritted reaction vessel (Peptide International, Louisville, KY) and agitated on a WS-180˚ Glas-Col shaker. The resin (0.25 mmol, 0.33 g) was swelled with DCM and washed with NMP. The resin was deprotected with 20% (v/v) piperidine in NMP, washed with NMP, and tested for free amino groups with ninhydrin test.

For FM55, 1 mmol (4-fold excess) of Fmoc-(3,4-Dimethylphenylalanine) was dissolved in 2.5 mL NMP and activated with 2.1 mL of 0.45 M HBTU/HOBt in DMF. The activated amino acid was transferred to the reaction vessel along with 0.34 mL 2M DIEA, and the reaction was allowed to proceed for 7 hrs. The coupling reaction was

monitored hourly by ninhydrin test. After completion of the coupling, the free amino groups of the resin were acetylated with capping solution composed of 19 mL acetic anhydride, 9 mL DIEA, and 6 mL 1M HOBt/DMF in total volume of 400 mL NMP. The resin was rinsed with NMP and DCM then dried *in vacuo*. FM59 was synthesized under the same protocol, but only 0.25 mmol of N^{α}-Z, N^{ω}-Me, Mtr-D-Arg-OH (1-fold) was available for coupling to the resin.

GENERAL PROTOCOL FOR CLEAVAGE AND DEPROTECTION. TFA/H_2O /thioanisole/ethylenedithiol solution (9:0.5:0.25:0.25, v/v/v/v) was used to cleave the peptide from the resin and simultaneously remove the side chain protecting groups. The mixture was stirred for 2 hrs at room temperature then the peptide solution was filtered from the resin. The solvent was removed by rotary evaporation and the peptide was precipitated with cold anhydrous ethyl ether. Crude material was filtered, dried, analyzed by analytical RP-HPLC and purified by semi preparative reverse-phase high-performance liquid chromatography (RP-HPLC) to afford the target peptide. Purity was determined by analytical RP-HPLC and molecular weight confirmation was confirmed by ESI-MS.

GENERAL METHOD FOR DISULFIDE CYCLIZATION OF PEPTIDES (FM13-FM15). Linear disulfhydryl-containing peptide was dissolved in a 1% (v/v) AcOH in H_2O solution (saturated with N_2) at 5˚C (1 mg linear peptide/ mL aqueous AcOH solution). The pH of the peptide solution was raised to 8.5 with NH_4OH, followed by the addition of 4 equivalents of potassium ferricyanide ($K_3Fe(CN)_6$). The reaction mixture was stirred for 1 min then the reaction was quenched by lowering the pH to 3.5 with

glacial acetic acid. The mixture was purified using semi preparative RP-HPLC to afford the disulfide cyclized peptide.

GENERAL METHOD FOR DITHIOETHER CYCLIZATION OF PEPTIDES (FM13-FM15). Linear disulfhydryl peptide was added to DMF and maintained at 5˚ C under N_2 atmosphere (0.1 mg linear peptide/mL DMF). Ten equivalents of potassium *tert*-butoxide (KO*t*Bu) were added to the peptide solution, followed by 10 equivalents of Br-$(CH_2)_2$-Br. The reaction was quenched with 5 mL AcOH after 2 hrs and the solvent was removed *in vacuo*. The residue was dissolved in water, filtered and subjected to semi preparative RP-HPLC to afford the dithioether cyclized peptide.

PEPTIDE CHARACTERIZATION. The purity of all final peptides was determined by analytical RP-HPLC with elution gradient of 0% to 70% solvent B in 70 min monitored at 230 nm. The purity of all peptides was ≥ 98% as analyzed by HPLC. Final product molecular weight was confirmed by ESI-MS.

SYNTHESIS OF UNNATURAL AMINO ACIDS.

N^{α}-Z,N^{ω}-(Me, Mtr)-D-Arginine (Scheme 1)[103-105] **(1)**

***N,S-dimethylpseudouronium iodide salt* (1a)**

3.1 mL of iodomethane (50 mmol) was added drop wise to a slurry of 4.5 g 1-methyl-2-thiourea (50 mmol) in 30 mL acetone. After the initial reaction subsided, the mixture was refluxed for 10 min and 10 mL absolute ethanol was added. The solution was saturated

with hexane while hot. After cooling, the formed crystals were collected by filtration and dried to give 11.2 g of white powder (97% yield).

N^{ω}-Methyl-D-arginine **(1b)**

1.7 g of D-ornithine (10 mmol) and 0.9 g of copper (II) acetate (5 mmol) were dissolved in 20 mL of 1:1 NH_4OH-H_2O then 2.3 g of N,S-dimethylpseudouronium salt (**1a**) (10 mmol) was added to the mixture. The solution was stoppered and stirred for 24 hrs at room temperature. The copper mercaptide was filtered and washed with 1:2 NH_4OH-H_2O. The blue filtrate was concentrated to 20 mL and loaded on a Dowex 50Wx8 column (200-400 mesh, H^+ form, 50x2 cm). The column was washed with 200 mL of water followed by 200 mL 0.2 N NH_4OH. The product was eluted with 300 mL 1 M NH_4OH and its presence was determined by TLC (solvent system A, developed with 1% ninhydrin). The fractions were dried to give 1 g of pure material (49.5% yield) with structure confirmed by NMR[103].

N^{α}-benzyloxycarbonyl-N^{ω}-D-methylarginine **(Scheme 2)**[106] **(1c)**

0.96 g N^{ω}-methyl-D-arginine (**1b**) (5.1 mmol) was dissolved in 0.05 N NaOH (9 mL) with stirring at 0˚C. Stirring was continued on ice as 0.93 mL of benzyl chloroformate (6.6 mmol) was added along with 2 mL of 0.05 N NaOH in alternating portions. The pH of the mixture was maintained at 9 to 10. The reaction was allowed to proceed for 2 hrs (the pH will dropped to 7-7.5 during this time) then the solution was acidified to pH 3 with 0.5 N HCl. The solution was filtered and extracted with ethyl acetate. The product was detected in the aqueous layer by TLC (solvent system B) and the solution was concentrated to 4 mL. The solution was loaded onto a silica gel column (KP-Sil™). The Product was purified using a 9:1 methanol-chloroform solvent system. The fractions

containing the product were combined, evaporated, and dried to give 1.2 g of desired product with molecular weight confirmed with ESI-MS. ESI-MS $[M+H]^+$ = 323.5.

N^{α}-Z- N^{ω}-(Me, Mtr)-* D-*arginine **(Scheme 2)**[107] **(1)**

0.8 g of N^{α}-benzyloxycarbonyl-N^{ω}-D-methylarginine (**1c**) (2.8 mmol) was dissolved in 4 N NaOH-acetone (4 mL-14 mL) and the solution was cooled on ice prior to the addition of 1.1 g 4-methoxy-2,3,6-trimethylbenzenesulfonyl chloride (Mtr-Cl) (5 mmol) in 4 mL acetone. The solution was stoppered and stirred for 25 hrs at room temperature then acidified to pH 3 with 10% citric acid. The solvent was evaporated and extracted with ethyl acetate, the organic layer washed with saturated NaCl and dried over anhydrous magnesium sulfate. The filtrate was concentrated to an oily residue then reconstituted in MeOH and purified by semi-preparative RP-HPLC with gradient 30-50% solvent B in 60 min. The fractions containing pure product were freeze dried to give 200 mg of white solid (13.3% yield). ESI-MS $[M+H]^+$ = 535.4.

N^{ω}-Ethyl-D-arginine (Scheme 1)[103-105] **(2)**

N-ethyl-S-methylpseudouronium iodide salt **(2a)**

3.1 mL of iodomethane (50 mmol) was added drop-wise to a slurry of 5.2 g 1-ethyl-2-thiourea (50 mmol) in 30 mL acetone. After initial reaction subsided, the mixture was refluxed for 10 min and 10 mL absolute ethanol was added. The solution was saturated with hexane while hot. Since no crystals formed after cooling, the solvent was evaporated to give 11.8 g of yellowish material (96.7% yield). The obtained solid was dissolved in 30 mL of hot water in the presence of activated charcoal. After filtration, evaporation of

solvent and repeated treatment with ethyl ether, 4 g of pure material was recovered (32.8% yield).

***N$^{\omega}$-ethyl*-D-*arginine* (2)**

1.7 g of D-ornithine (10 mmol) and 0.9 g of copper (II) acetate (5 mmol) were dissolved in 20 mL of 1:1 NH_4OH-H_2O, then 2.6 g of N-ethyl-S-methylpseudouronium salt (**2a**) (10 mmol) was added to the mixture. The solution was stoppered and stirred for 24 hrs at room temperature. The copper mercaptide was filtered and washed with 1:2 NH_4OH-H_2O. The blue filtrate was concentrated to 20 mL and loaded on a Dowex 50Wx8 column (200-400 mesh, H^+ form, 50x2 cm). The column was washed with 200 mL of water followed by 200 mL 0.2 N NH_4OH. The product was eluted with 300 mL 1 M NH_4OH and its presence was determined by TLC (solvent system A) and developed with 1% ninhydrin. The fractions were dried to give 1 g of pure material (49.5% yield) with structure of product confirmed by NMR[111].

N$^{\omega}$-2,4,5,6-tetrahydropyrimidyl-D-Arginine (Scheme 5)[103-105] (3)

***2-(methylthio)-1,4,5,6-tetrahydropyrimidine iodide* (3a)**

3.1 mL of iodomethane (50 mmol) was added drop-wise to a slurry of 5.8 g 3,4,5,6-tetrahydropyrimidine thiol (50 mmol) in 30 mL acetone. After initial reaction subsided, the mixture was refluxed for 10 min and 10 mL absolute ethanol was added. The solution was saturated with hexane while hot. After cooling, the formed crystals were collected by filtration and dried to give 12 g of white powder (96.3% yield).

N^{ω}-2,4,5,6-tetrahydropyrimidyl-D-arginine **(3)**

1.7 g of D-ornithine (10 mmol) and 2.6 g of 2-(methylthio)-1,4,5,6-tetrahydropyrimidine iodide (**3a**) (10 mmol) were dissolved in 10 mL 2 N NaOH. The solution was stoppered and stirred for 9 days at room temperature. The solution was brought to neutral pH by addition of 6 N HCl and loaded on a Dowex 50Wx8 column (200-400 mesh, H^+ form, 50x2 cm). The column was washed with 200 mL of water followed by 200 mL 0.2 N NH_4OH. The product was eluted with 300 mL 1 M NH_4OH and its presence was determined by TLC (solvent system A) and developed with 1% ninhydrin. The fractions containing the product were dried to give 600 mg of pure material (28.6% yield) with structure of product confirmed by NMR[103].

Fmoc-DL-2,4-Dimethylphenylalanine (Scheme 3)[112] (4)

diethyl acetamido-(2,4-dimethylbenzyl) malonate **(4a)**

200 mL of absolute ethanol was transferred to a 500-mL round bottom flask and saturated with N_2 for 30 min prior to the addition of 1.74 g of sodium (60 mmol). After all the sodium had reacted, 13 g of diethyl acetamidomalonate (60 mmol) was added and the mixture was stirred for 10 min. 8.8 mL of 2,4-dimethylbenzyl chloride (60 mmol) was added and reaction mixture was refluxed at 90˚ C for 2 hrs. The solution was cooled and filtered. The filtrate was evaporated *in vacuo* to obtain a white powder. The crude material was crystallized by triturating with 120 mL of warm 20% acetone in water. The crystals were filtered and dried overnight *in vacuo* to render 14.3 g of white powder (71.1% yield). The crude material was re-crystallized from 30 mL of warm benzene, then

filtered. The filtrate was cooled at 4˚ C for 2 hrs to promote crystal formation. The pure material was collected by filtration and dried to give 8.1 g (40.3% yield).

DL-*2,4-dimethylphenylalanine* (4b)

7.8 g of diethyl acetamido-(2,4-dimethylbenzyl) malonate (**4a**) (23.3 mmol) was dissolved in 35 mL of 6 N HCl and refluxed under N_2 for 15 hrs. The solution was cooled at 4˚ C for 2 hrs then filtered and dried to render 4.9 g crude material. The white powder was dissolved in 60 mL of water and the solution was neutralized with 1 M Na_2CO_3 to pH 6.5. Precipitated material was collected by filtration to give 3 g of product. An additional 2.1 g of product was collected from the mother liquid after cooling overnight (93% yield).

***Fmoc*-DL-*2,4-dimethylphenylalanine*[108] (4)**

1.2 g of 2,4-dimethylphenylalanine (**4b**) (3.3 mmol) was added to a solution of 14 mL DMF and 20 mL acetone. The suspension was cooled in an ice bath for 10 min before the drop-wise addition of 14 mL of 10% $NaHCO_3$ solution. Fmoc-OSu (2.6 g, 3.9 mmol) was added along with an additional 50 mL of DMF. The mixture was stirred vigorously overnight at room temperature. The solvent was evaporated followed by extraction with ethyl acetate, the organic layer was washed with saturated NaCl, and the ethyl acetate layer was dried over anhydrous magnesium sulfate. The filtrate was concentrated to a yellowish oil and dried *in vacuo* overnight to give a hard yellow solid. The product was suspended in 100 mL of chloroform then filtered to render 0.52 g of white powder (36.1% yield), 93.4% purity as determined through analytical RP-HPLC. Molecular weight was confirmed by ESI-MS ($[M+1]^+ = 438.2$).

Fmoc-DL-2,3-Dimethylphenylalanine (Scheme 3) (5)

Following the protocol described above, a colleague, Ping He, prepared this amino acid residue. Final product was a brownish oil weighing 1.2 g, which was used for the synthesis of **FM55** without further purification.

SYNTHESIS, PURIFICATION AND CHARACTERIZATION OF PEPTIDES.

H-D-Arg-Oic-Pro-D-Gln-Phe-NH_2 (#10, FM21)

0.61 g of PAL-PEG-PS amide resin (0.41 mmol/g) was used to synthesize the pentapeptide according to the general protocol. 0.72 g of peptide-resin was obtained from the solid phase peptide synthesis from which the peptide was cleaved according to the general cleavage and deprotection protocol to yield 150 mg of crude peptide. A 40 mg portion of crude peptide was purified by semi-preparative RP-HPLC with gradient 0-30% solvent B in 60 min to afford 29.2 mg pure peptide with elution time of 22.3 min (0-70% solvent B in 70 min) on analytical RP-HPLC. ESI-MS $[M+H]^+ = 697.5$.

H-D-Arg-Oic-Pro-D-Abu-Phe-NH_2 (#11, FM24)

0.61 g of PAL-PEG-PS amide resin (0.41 mmol/g) was used to synthesize the pentapeptide according to the general protocol. 0.74 g of peptide-resin was obtained from the solid phase peptide synthesis from which the peptide was cleaved according to the general cleavage and deprotection protocol to yield 140 mg of crude peptide. A 39 mg portion of crude peptide was purified by semi-preparative RP-HPLC with gradient 10-

40% solvent B in 60 min to afford 29.4 mg pure peptide with elution time of 27.2 min (0-70% solvent B in 70 min) on analytical RP-HPLC. ESI-MS $[M+H]^+$ = 654.5.

H-D-Arg-Oic-Pro-D-Orn-Phe-NH_2 (#12, FM25)

0.61 g of PAL-PEG-PS amide resin (0.41 mmol/g) was used to synthesize the pentapeptide according to the general protocol. 0.79 g of peptide-resin was obtained from the solid phase peptide synthesis from which the peptide was cleaved according to the general cleavage and deprotection protocol to yield 140 mg of crude peptide. A 38.2 mg portion of crude peptide was purified by semi-preparative RP-HPLC with gradient 0-30% solvent B in 60 min to afford 31.8 mg pure peptide with elution time of 21.4 min (0-70% solvent B in 70 min) on analytical RP-HPLC. ESI-MS $[M+H]^+$ = 683.5.

H-D-Arg-Oic-Pro-D-Nle-Phe-NH_2 (#13, FM26)

0.61 g of PAL-PEG-PS amide resin (0.41 mmol/g) was used to synthesize the pentapeptide according to the general protocol. 0.78 g of peptide-resin was obtained from the solid phase peptide synthesis from which the peptide was cleaved according to the general cleavage and deprotection protocol to yield 130 mg of crude peptide. A 39.7 mg portion of crude peptide was purified by semi-preparative RP-HPLC with gradient 10-40% solvent B in 60 min to afford 28.6 mg pure peptide with elution time of 32.1 min (0-70% solvent B in 70 min) on analytical RP-HPLC. ESI-MS $[M+H]^+$ = 682.5.

H-D-Arg-Oic-Pro-D-Ala-Phe(*p*-F)-NH_2 (#17, FM28)

0.61 g of PAL-PEG-PS amide resin (0.41 mmol/g) was used to synthesize the pentapeptide according to the general protocol. 0.77 g of peptide-resin was obtained from the solid phase peptide synthesis from which the peptide was cleaved according to the general cleavage and deprotection protocol to yield 90 mg of crude peptide. A 30.5 mg portion of crude peptide was purified by semi-preparative RP-HPLC with gradient 10-40% solvent B in 60 min to afford 23.9 mg pure peptide with elution time of 26.3 min (0-70% solvent B in 70 min) on analytical RP-HPLC. ESI-MS $[M+H]^+ = 658.5$.

H-D-Arg-Oic-Pro-Gly-Arg-NH_2 (#22, FM3)

0.31 g of Rink amide resin (0.8 mmol/g substitution) was used to synthesize the pentapeptide according to the general protocol. 0.5 g of peptide-resin was obtained from the solid phase peptide synthesis from which the peptide was cleaved according to the general cleavage and deprotection protocol to yield 127 mg of crude peptide. A 50.3 mg portion of crude peptide was purified by semi-preparative RP-HPLC with gradient 0-40% solvent B in 80 min to afford 22.4 mg pure peptide with elution time of 13.6 min (0-70% solvent B in 70 min) on analytical RP-HPLC. ESI-MS $[M+H]^+ = 635.4$.

H-D-Arg-Oic-Pro-Gly-Tyr-NH_2 (#23, FM4)

0.31 g of Rink amide resin (0.8 mmol/g) was used to synthesize the pentapeptide according to the general protocol. 0.45 g of peptide-resin was obtained from the solid phase peptide synthesis from which the peptide was cleaved according to the general cleavage and deprotection protocol to yield 140 mg of crude peptide. A 50 mg portion of

crude peptide was purified by semi-preparative RP-HPLC with gradient 0-30% solvent B in 60 min to afford 28.2 mg pure peptide with elution time of 18.2 min (0-70% solvent B in 70 min) on analytical RP-HPLC. ESI-MS $[M+H]^+$ = 642.4.

H-D-Arg-Oic-Pro-Gly-Phe(*p*-Me)-NH_2 (#24, FM27)

0.61 g of PAL-PEG-PS amide resin (0.41 mmol/g) was used to synthesize the pentapeptide according to the general protocol. 0.78 g of peptide-resin was obtained from the solid phase peptide synthesis from which the peptide was cleaved according to the general cleavage and deprotection protocol to yield 160 mg of crude peptide. A 45.3 mg portion of crude peptide was purified by semi-preparative RP-HPLC with gradient 10-40% solvent B in 60 min to afford 35.4 mg pure peptide with elution time of 26.0 min (0-70% solvent B in 70 min) on analytical RP-HPLC. ESI-MS $[M+H]^+$ = 640.5.

H-D-Arg-Oic-Pro-D-Ala-2-Nal-NH_2 (#25, FM16)

0.61 g of PAL-PEG-PS amide resin (0.41 mmol/g) was used to synthesize the pentapeptide according to the general protocol. 0.70 g of peptide-resin was obtained from the solid phase peptide synthesis from which the peptide was cleaved according to the general cleavage and deprotection protocol to yield 160 mg of crude peptide. A 40 mg portion of crude peptide was purified by semi-preparative RP-HPLC with gradient 10-40% solvent B in 60 min to afford 22.6 mg pure peptide with elution time of 30.6 min (0-70% solvent B in 70 min) on analytical RP-HPLC. ESI-MS $[M+H]^+$ = 690.4.

H-D-Arg-Oic-Pro-D-Ala-Bip-NH_2 (#26, FM18)

0.61 g of PAL-PEG-PS amide resin (0.41 mmol/g) was used to synthesize the pentapeptide according to the general protocol. 0.74 g of peptide-resin was obtained from the solid phase peptide synthesis from which the peptide was cleaved according to the general cleavage and deprotection protocol to yield 180 mg of crude peptide. A 38 mg portion of crude peptide was purified by semi-preparative RP-HPLC with gradient 0-45% solvent B in 90 min to afford 32.4 mg pure peptide with elution time of 33.9 min (0-70% solvent B in 70 min) on analytical RP-HPLC. ESI-MS $[M+H]^+ = 716.5$.

H-D-Arg-Oic-Pro-D-Ala-Phe(*p*-Me)-NH_2 (#27, FM19)

0.61 g of PAL-PEG-PS amide resin (0.41 mmol/g) was used to synthesize the pentapeptide according to the general protocol. 0.74 g of peptide-resin was obtained from the solid phase peptide synthesis from which the peptide was cleaved according to the general cleavage and deprotection protocol to yield 170 mg of crude peptide. A 40 mg portion of crude peptide was purified by semi-preparative RP-HPLC with gradient 0-40% solvent B in 80 min to afford 39 mg pure peptide with elution time of 27.7 min (0-70% solvent B in 70 min) on analytical RP-HPLC. ESI-MS $[M+H]^+ = 654.5$.

H-D-Arg-Oic-Pro-D-Ala-Phe(*p*-Cl)-NH_2 (#28, FM20)

0.61 g of PAL-PEG-PS amide resin (0.41 mmol/g) was used to synthesize the pentapeptide according to the general protocol. 0.75 g of peptide-resin was obtained from the solid phase peptide synthesis from which the peptide was cleaved according to the general cleavage and deprotection protocol to yield 130 mg of crude peptide. A 40 mg

portion of crude peptide was purified by semi-preparative RP-HPLC with gradient 0-35% solvent B in 70 min to afford 21.2 mg pure peptide with elution time of 29.2 min (0-70% solvent B in 70 min) on analytical RP-HPLC. ESI-MS $[M+H]^+ = 674.5$.

H-D-Arg-Oic-Pro-D-Ser-Phe(*p*-Me)-NH_2 (#29, FM29)

0.61 g of PAL-PEG-PS amide resin (0.41 mmol/g) was used to synthesize the pentapeptide according to the general protocol. 0.79 g of peptide-resin was obtained from the solid phase peptide synthesis from which the peptide was cleaved according to the general cleavage and deprotection protocol to yield 170 mg of crude peptide. A 42 mg portion of crude peptide was purified by semi-preparative RP-HPLC with gradient 10-40% solvent B in 60 min to afford 32 mg pure peptide with elution time of 26.1 min (0-70% solvent B in 70 min) on analytical RP-HPLC. ESI-MS $[M+H]^+ = 670.5$.

H-D-Arg-Oic-Pro-D-Asn-Phe(*p*-Me)-NH_2 (#30, FM30)

0.61 g of PAL-PEG-PS amide resin (0.41 mmol/g) was used to synthesize the pentapeptide according to the general protocol. 0.86 g of peptide-resin was obtained from the solid phase peptide synthesis from which the peptide was cleaved according to the general cleavage and deprotection protocol to yield 210 mg of crude peptide. A 41.1 mg portion of crude peptide was purified by semi-preparative RP-HPLC with gradient 10-40% solvent B in 60 min to afford 27.3 mg pure peptide with elution time of 28.8 min (0-70% solvent B in 70 min) on analytical RP-HPLC. ESI-MS $[M+H]^+ = 697.6$.

H-D-Arg-Oic-Pro-D-Ala-Hfe-NH_2 (#31, FM31)

0.61 g of PAL-PEG-PS amide resin (0.41 mmol/g) was used to synthesize the pentapeptide according to the general protocol. 0.71 g of peptide-resin was obtained from the solid phase peptide synthesis from which the peptide was cleaved according to the general cleavage and deprotection protocol to yield 120 mg of crude peptide. A 40.8 mg portion of crude peptide was purified by semi-preparative RP-HPLC with gradient 10-40% solvent B in 60 min to afford 25.6 mg pure peptide with elution time of 30.2 min (0-70% solvent B in 70 min) on analytical RP-HPLC. ESI-MS $[M+H]^+ = 654.5$.

H-D-Arg-Oic-Pro-D-Ala-Phe(*p*-NH_2)-NH_2 (#32, FM32)

0.61 g of PAL-PEG-PS amide resin (0.41 mmol/g) was used to synthesize the pentapeptide according to the general protocol. 0.77 g of peptide-resin was obtained from the solid phase peptide synthesis from which the peptide was cleaved according to the general cleavage and deprotection protocol to yield 170 mg of crude peptide. A 39.6 mg portion of crude peptide was purified by semi-preparative RP-HPLC with gradient 0-30% solvent B in 60 min to afford 32 mg pure peptide with elution time of 14.5 min (0-70% solvent B in 70 min) on analytical RP-HPLC. ESI-MS $[M+H]^+ = 655.5$.

H-D-Arg-Oic-Pro-D-Ala-Phe(*p*-Br)-NH_2 (#33, FM33)

0.61 g of PAL-PEG-PS amide resin (0.41 mmol/g) was used to synthesize the pentapeptide according to the general protocol. 0.74 g of peptide-resin was obtained from the solid phase peptide synthesis from which the peptide was cleaved according to the general cleavage and deprotection protocol to yield 130 mg of crude peptide. A 39.9 mg

portion of crude peptide was purified by semi-preparative RP-HPLC with gradient 10-40% solvent B in 60 min to afford 31.8 mg pure peptide with elution time of 32.6 min (0-70% solvent B in 70 min) on analytical RP-HPLC. ESI-MS $[M+H]^+$ = 718.5.

H-D-Arg-Oic-Pro-D-Ala-Phe(*p*-*t*Bu)-NH_2 (#34, FM34)

0.61 g of PAL-PEG-PS amide resin (0.41 mmol/g) was used to synthesize the pentapeptide according to the general protocol. 0.77 g of peptide-resin was obtained from the solid phase peptide synthesis from which the peptide was cleaved according to the general cleavage and deprotection protocol to yield 150 mg of crude peptide. A 39.8 mg portion of crude peptide was purified by semi-preparative RP-HPLC with gradient 15-50% solvent B in 70 min to afford 18.6 mg pure peptide with elution time of 37.6 min (0-70% solvent B in 70 min) on analytical RP-HPLC. ESI-MS $[M+H]^+$ = 696.6.

H-D-Arg-Oic-Pro-D-Ala-Phe(*p*-CN)-NH_2 (#35, FM35)

0.61 g of PAL-PEG-PS amide resin (0.41 mmol/g) was used to synthesize the pentapeptide according to the general protocol. 0.74 g of peptide-resin was obtained from the solid phase peptide synthesis from which the peptide was cleaved according to the general cleavage and deprotection protocol to yield 150 mg of crude peptide. A 40.2 mg portion of crude peptide was purified by semi-preparative RP-HPLC with gradient 10-40% solvent B in 60 min to afford 33.7 mg pure peptide with elution time of 26.9 min (0-70% solvent B in 70 min) on analytical RP-HPLC. ESI-MS $[M+H]^+$ = 665.5.

H-D-Arg-Oic-Pro-D-Ala-Phe(*p*-I)-NH_2 (#36, FM36)

0.61 g of PAL-PEG-PS amide resin (0.41 mmol/g) was used to synthesize the pentapeptide according to the general protocol. 0.8 g of peptide-resin was obtained from the solid phase peptide synthesis from which the peptide was cleaved according to the general cleavage and deprotection protocol to yield 150 mg of crude peptide. A 42.8 mg portion of crude peptide was purified by semi-preparative RP-HPLC with gradient 10-40% solvent B in 60 min to afford 35 mg pure peptide with elution time of 30.9 min (0-70% solvent B in 70 min) on analytical RP-HPLC. ESI-MS $[M+H]^+$ = 766.4.

H-D-Arg-Oic-Pro-D-Ala-Phe(2-Me)-NH_2 (#37, FM37)

0.61 g of PAL-PEG-PS amide resin (0.41 mmol/g) was used to synthesize the pentapeptide according to the general protocol. 0.77 g of peptide-resin was obtained from the solid phase peptide synthesis from which the peptide was cleaved according to the general cleavage and deprotection protocol to yield 170 mg of crude peptide. A 44.3 mg portion of crude peptide was purified by semi-preparative RP-HPLC with gradient 10-40% solvent B in 60 min to afford 20.9 mg pure peptide with elution time of 30.0 min (0-70% solvent B in 70 min) on analytical RP-HPLC. ESI-MS $[M+H]^+$ = 654.5.

H-D-Arg-Oic-Pro-D-Ala-Phe(3-Me)-NH_2 (#38, FM38)

0.61 g of PAL-PEG-PS amide resin (0.41 mmol/g) was used to synthesize the pentapeptide according to the general protocol. 0.76 g of peptide-resin was obtained from the solid phase peptide synthesis from which the peptide was cleaved according to the general cleavage and deprotection protocol to yield 130 mg of crude peptide. A 42 mg

portion of crude peptide was purified by semi-preparative RP-HPLC with gradient 10-40% solvent B in 60 min to afford 27 mg pure peptide with elution time of 27.8 min (0-70% solvent B in 70 min) on analytical RP-HPLC. ESI-MS $[M+H]^+ = 654.5$.

H-D-Arg-Oic-Pro-D-Ala-Phe(*p*-NO_2)-NH_2 (#39, FM39)

0.61 g of PAL-PEG-PS amide resin (0.41 mmol/g) was used to synthesize the pentapeptide according to the general protocol. 0.77 g of peptide-resin was obtained from the solid phase peptide synthesis from which the peptide was cleaved according to the general cleavage and deprotection protocol to yield 150 mg of crude peptide. A 41.2 mg portion of crude peptide was purified by semi-preparative RP-HPLC with gradient 10-40% solvent B in 60 min to afford 31.7 mg pure peptide with elution time of 25.1 min (0-70% solvent B in 70 min) on analytical RP-HPLC. ESI-MS $[M+H]^+ = 685.5$.

H-D-Arg-Oic-Pro-D-Ala-Phg-NH_2 (#40, FM40)

0.61 g of PAL-PEG-PS amide resin (0.41 mmol/g) was used to synthesize the pentapeptide according to the general protocol. 0.77 g of peptide-resin was obtained from the solid phase peptide synthesis from which the peptide was cleaved according to the general cleavage and deprotection protocol to yield 170 mg of crude peptide. A 36.6 mg portion of crude peptide was purified by semi-preparative RP-HPLC with gradient 5-35% solvent B in 60 min to afford 16.7 mg pure peptide with elution time of 23.3 min (0-70% solvent B in 70 min) on analytical RP-HPLC. ESI-MS $[M+H]^+ = 626.5$.

H-D-Arg-Oic-Pro-D-Ala-Phe(*p*-COOH)-NH_2 (#41, FM52)

0.34 g of Rink amide resin (0.75 mmol/g) was used to synthesize the pentapeptide according to the general protocol. 0.46 g of peptide-resin was obtained from the solid phase peptide synthesis from which the peptide was cleaved according to the general cleavage and deprotection protocol to yield 130 mg of crude peptide. A 80 mg portion of the crude peptide was purified by semi-preparative RP-HPLC with gradient 10-40% solvent B in 60 min to afford 55.8 mg pure peptide with elution time of 23.9 min (0-70% solvent B in 70 min) on analytical RP-HPLC. ESI-MS $[M+H]^+ = 684.4$.

H-D-Arg-Oic-Pro-D-Ala-Phe(*p*-Me)-NH-Me (#43, FM53)

0.4 g of [3-({methyl-Fmoc-amino}-methyl)-indol-1-yl] acetyl AM resin (0.63 mmol/g) was used to synthesize the N-methyl amide pentapeptide according to the general protocol. 0.57 g of peptide-resin was obtained from the solid phase peptide synthesis from which the peptide was cleaved according to the general cleavage and deprotection protocol to yield 150 mg of crude peptide. A 90 mg portion of the crude peptide was purified by semi-preparative RP-HPLC with gradient 15-45% solvent B in 60 min to afford 49.6 mg pure peptide with elution time of 31.6 min (0-70% solvent B in 70 min) on analytical RP-HPLC. ESI-MS $[M+H]^+ = 668.5$.

H-D-Arg-Oic-Pro-D-Ala-DL-Phe(2,4-DiMe)-NH_2 (#44/#45, FM54)

0.33 g of Rink amide resin (0.75 mmol/g) was used to synthesize the pentapeptide according to the general protocol. 0.39 g of peptide-resin was obtained from the solid phase peptide synthesis from which the peptide was cleaved according to the general

cleavage and deprotection protocol to yield 130 mg of crude peptide. A 80 mg portion of the crude peptide was purified by semi-preparative RP-HPLC with gradient 15-50% solvent B in 70 min to afford two major products, **#44/FM54a** (10.8 mg) and **#45/FM54b** (28.1 mg), with elution times of 30.2 min and 33.2 min (0-70% solvent B in 70 min), respectively, on analytical RP-HPLC. ESI-MS $[M+H]^+ = 668.5$.

H-D-Arg-Oic-Pro-D-Ala-DL-Phe(2,3-DiMe)-NH_2 (#46/#47, FM55)

0.34 g of Rink amide resin (0.75 mmol/g) was used to synthesize the pentapeptide according to the general protocol. The first amino acid residue was pre-loaded on to the resin manually due to solubility issues of the residue. 0.46 g of peptide-resin was obtained from the solid phase peptide synthesis from which the peptide was cleaved according to the general cleavage and deprotection protocol to yield 175 mg of crude peptide. A 80 mg portion of the crude peptide was purified by semi-preparative RP-HPLC with gradient 10-40% solvent B in 60 min to afford two major products, **#46/FM55a** (24.3 mg) and **#47/FM55b** (31.2 mg), with elution times of 26.8 min and 29.8 min (0-70% solvent B in 70 min), respectively, on analytical RP-HPLC. ESI-MS $[M+H]^+ = 668.5$.

H-D-Arg-Oic-Pro-D-Ala-Phe(*p*-Me)-NH-Et (#48, FM56)

0.33 g of [3-({ethyl-Fmoc-amino}-methyl)-indol-1-yl] acetyl AM resin (0.83 mmol/g) was used to synthesize the N-ethyl amide pentapeptide according to the general protocol. 0.4 g of peptide-resin was obtained from the solid phase peptide synthesis from which the peptide was cleaved according to the general cleavage and deprotection protocol to yield

170 mg of crude peptide. A 100 mg portion of the crude peptide was purified by semi-preparative RP-HPLC with gradient 15-45% solvent B in 60 min to afford 78.3 mg pure peptide with elution time of 29.4 min (0-70% solvent B in 70 min) on analytical RP-HPLC. ESI-MS $[M+H]^+ = 682.4$.

H-N$^{\omega}$-methyl-Arg-Oic-Pro-D-Ala-Phe(*p*-Me)-NH$_2$ (#49, FM57)

0.34 g of Rink amide resin (0.75 mmol/g) was used to synthesize the pentapeptide according to the general protocol. 0.45 g of peptide-resin was obtained from the solid phase peptide synthesis from which the peptide was cleaved according to the general cleavage and deprotection protocol to yield 40 mg of crude peptide. All of the crude peptide was purified by semi-preparative RP-HPLC with gradient 10-40% solvent B in 60 min to afford 10.8 mg pure peptide with elution time of 27.8 min (0-70% solvent B in 70 min) on analytical RP-HPLC. ESI-MS $[M+H]^+ = 668.4$.

H-N$^{\omega}$-methyl-Arg-Pro-Oic-D-Ala-Phe(*p*-Me)-NH$_2$ (#50, FM58)

0.34 g of Rink amide resin (0.75 mmol/g) was used to synthesize the pentapeptide according to the general protocol. 0.40 g of peptide-resin was obtained from the solid phase peptide synthesis from which the peptide was cleaved according to the general cleavage and deprotection protocol to yield 50 mg of crude peptide. All of the crude peptide was purified by semi-preparative RP-HPLC with gradient 10-40% solvent B in 60 min to afford 11.3 mg pure peptide with elution time of 30.9 min (0-70% solvent B in 70 min) on analytical RP-HPLC. ESI-MS $[M+H]^+ = 668.4$.

H-N$^{\omega}$-methyl-D-Arg-Pro-Oic-D-Ala-Phe(*p*-Me)-NH$_2$ (#51, FM59)

0.34 g of Rink amide resin (0.75 mmol/g) was used to synthesize the pentapeptide according to the general protocol. The first amino acid residue was pre-loaded on to the resin manually due to small amount of amino acid used for the coupling reaction. 0.48 g of peptide-resin was obtained from the solid phase peptide synthesis from which the peptide was cleaved according to the general cleavage and deprotection protocol to yield 200 mg of crude peptide. Since the last amino acid in the sequence was protected with the Cbz group, the crude material was treated for 30 min with 33% HBr in acetic acid (2 mL HBr and 4 mL acetic acid) in order to remove the protecting group. A 150 mg portion of the crude peptide was purified by semi-preparative RP-HPLC with gradient 10-50% solvent B in 80 min to afford 81.3 mg of pure peptide with elution time of 31.6 min (0-70% solvent B in 70 min) on analytical RP-HPLC. ESI-MS $[M+H]^+ = 668.5$.

H-D-Arg-Oic-Pro-D-Phe-2-Nal-NH$_2$ (#52, FM7)

0.5 g of Rink amide resin (0.5 mmol/g) was used to synthesize the pentapeptide according to the general protocol. 0.56 g of peptide-resin was obtained from the solid phase peptide synthesis from which the peptide was cleaved according to the general cleavage and deprotection protocol to yield 100 mg of crude peptide. A 50 mg portion of crude peptide was purified by semi-preparative RP-HPLC with gradient 0-50% solvent B in 100 min to afford 27.4 mg pure peptide with elution time of 38.2 min (0-70% solvent B in 70 min) on analytical RP-HPLC. ESI-MS $[M+H]^+ = 766.5$.

H-D-Arg-Oic-Pro-D-Ser-2-Nal-NH_2 (#53, FM8)

0.5 g of Rink amide resin (0.5 mmol/g) was used to synthesize the pentapeptide according to the general protocol. 0.61 g of peptide-resin was obtained from the solid phase peptide synthesis from which the peptide was cleaved according to the general cleavage and deprotection protocol to yield 86 mg of crude peptide. A 32.1 mg portion of crude peptide was purified by semi-preparative RP-HPLC with gradient 0-40% solvent B in 120 min to afford 15.8 mg pure peptide with elution time of 29.6 min (0-70% solvent B in 70 min) on analytical RP-HPLC. ESI-MS $[M+H]^+ = 706.5$.

H-D-Arg-Oic-Pro-D-Thr-2-Nal-NH_2 (#54, FM9)

0.5 g of Rink amide resin (0.5 mmol/g) was used to synthesize the pentapeptide according to the general protocol. 0.60 g of peptide-resin was obtained from the solid phase peptide synthesis from which the peptide was cleaved according to the general cleavage and deprotection protocol to yield 80 mg of crude peptide. A 33.6 mg portion of crude peptide was purified by semi-preparative RP-HPLC with gradient 10-40% solvent B in 120 min to afford 22.0 mg pure peptide with elution time of 30.8 min (0-70% solvent B in 70 min) on analytical RP-HPLC. ESI-MS $[M+H]^+ = 720.4$

H-D-Arg-Oic-Pro-D-His-2-Nal-NH_2 (#55, FM10)

0.5 g of Rink amide resin (0.5 mmol/g) was used to synthesize the pentapeptide according to the general protocol. 0.63 g of peptide-resin was obtained from the solid phase peptide synthesis from which the peptide was cleaved according to the general cleavage and deprotection protocol to yield 110 mg of crude peptide. A 30.6 mg portion

of crude peptide was purified by semi-preparative RP-HPLC with a gradient of 10-40% solvent B in 120 min to afford a mixture of the two major peaks since they overlapped due to larger quantity used in the purification. Consequent, I decided to purify a second batch of 15.8 mg with the same gradient that afforded only trace amounts of pure material. Another 3 runs were performed in order to produce 11.4 mg pure peptide with elution time of 27.2 min (0-70% solvent B in 70 min) on analytical RP-HPLC. ESI-MS $[M+H]^+ = 757.5$.

H-D-Arg-Oic-Pro-β-Ala-2-Nal-NH_2 (#56, FM11)

0.5 g of Rink amide resin (0.5 mmol/g) was used to synthesize the pentapeptide according to the general protocol. 0.61 g of peptide-resin was obtained from the solid phase peptide synthesis from which the peptide was cleaved according to the general cleavage and deprotection protocol to yield 100 mg of crude peptide. A 34.9 mg portion of crude peptide was purified by semi-preparative RP-HPLC with gradient 10-40% solvent B in 120 min to afford 18.2 mg pure peptide with elution time of 29.5 min (0-70% solvent B in 70 min) on analytical RP-HPLC. ESI-MS $[M+H]^+ = 690.5$.

H-D-Arg-Oic-Pro-D-Gln-2-Nal-NH_2 (#57, FM6)

0.5 g of Rink amide resin (0.5 mmol/g) was used to synthesize the pentapeptide according to the general protocol. 0.69 g of peptide-resin was obtained from the solid phase peptide synthesis from which the peptide was cleaved according to the general cleavage and deprotection protocol to yield 100 mg of crude peptide. A 30.7 mg portion of crude peptide was purified by semi-preparative RP-HPLC with gradient 0-40% solvent

B in 120 min to afford 9.7 mg pure peptide with elution time of 28.1 min (0-70% solvent B in 70 min) on analytical RP-HPLC. ESI-MS $[M+H]^+$ = 747.5.

Ac-D-Arg-Oic-Pro-Gly-Phe-NH_2 (#58, FM5)

0.31 g of Rink amide resin (0.8 mmol/g) was used to synthesize the pentapeptide according to the general protocol with additional final capping step using solution composed of 19 mL acetic anhydride, 9 mL DIEA, and 6 mL 1M HOBt/DMF in total volume of 400 mL NMP in order to acetylate the amino terminus of the peptide. 0.45 g of peptide-resin was obtained from the solid phase peptide synthesis from which the peptide was cleaved according to the general cleavage and deprotection protocol to yield 145 mg of crude peptide. A 52.5 mg portion of crude peptide was purified by semi-preparative RP-HPLC with gradient 0-35% solvent B in 70 min to afford 29.0 mg pure peptide with elution time of 25.9 min (0-70% solvent B in 70 min) on analytical RP-HPLC. ESI-MS $[M+H]^+$ = 668.4.

H-D-Arg-Oic-Cys-Gly-Phe-Cys-NH_2 (FM13(SH_2))

0.5 g of Rink amide resin (0.5 mmol/g) was used to synthesize the peptide according to the general protocol. 0.66 g of peptide-resin was obtained from the solid phase peptide synthesis from which the peptide was cleaved according to the general cleavage and deprotection protocol to yield 79.1 mg of crude peptide. All of the crude material was purified by semi-preparative RP-HPLC with gradient 0-40% solvent B in 120 min to afford 9.8 mg pure peptide with elution time of 28.6 min (0-70% solvent B in 70 min) on analytical RP-HPLC. ESI-MS $[M+H]^+$ = 735.3. Unfortunately the amount of pure

material was not sufficient to carry out the subsequent cyclization reaction and a new synthesis was attempted with a double couple, double deprotection protocol to improve the yield.

H-D-Arg-Oic-Cys-Gly-Phe-Cys-NH_2 (FM13(SH_2)DC)

0.5 g of Rink amide resin (0.5 mmol/g) was used to synthesize the peptide according to the general protocol. 0.70 g of peptide-resin was obtained from the solid phase peptide synthesis incorporating the double couple, double deprotection protocol. This protocol consists two individual rounds of deprotection of the resin/peptide-resin and coupling with each amino acid residue to maximize the yield. The peptide was cleaved from the resin according to the general cleavage and deprotection protocol to yield 95 mg of crude peptide. All of the crude material was purified by semi-preparative RP-HPLC with gradient 10-40% solvent B in 90 min to afford 16.2 mg pure peptide with elution time of 28.6 min (0-70% solvent B in 70 min) on analytical RP-HPLC. ESI-MS $[M+H]^+$ = 735.3.

H-D-Arg-Oic-c[Cys-Gly-Phe-Cys]-NH_2 (#59, FM13(SS))

The linear peptide (22.6 mg) produced from the single and double couple syntheses (**FM13(SH_2)** and **FM13(SH_2)DC**) was subjected to cyclization with $K_3Fe(CN)_6$ according to the general disulfide cyclization protocol. The cyclic peptide was purified by semi-preparative RP-HPLC to afford 14.1 mg (62.4%) of **FM13(SS)**, 99% pure as determined by analytical RP-HPLC with elution time of 24 min (0-70% solvent B in 70 min). ESI-MS $[M+H]^+$ = 733.4.

H-D-Arg-Oic-Cys-Gly-Phe-Cys-NH_2 (FM13(SH_2)DC/PEG)

In order to generate enough material to run the dithioether cyclization reaction, the synthesis of **FM13(SH_2)** was repeated for a third time. A new resin was used with an extended linker, PAL-PEG-PS amide resin (0.41 mmol/g). 0.61 mg of resin was used to synthesize the peptide according to the double couple, double deprotection protocol. 0.76 g of peptide-resin was obtained from the solid phase peptide synthesis from which the peptide was cleaved according to the general cleavage and deprotection protocol to yield 80 mg of crude peptide. All of the crude material was purified by semi-preparative RP-HPLC with gradient 0-40% solvent B in 120 min to afford 39.8 mg pure peptide with elution time of 28.6 min (0-70% solvent B in 70 min) on analytical RP-HPLC. ESI-MS $[M+H]^+ = 735.3$.

H-D-Arg-Oic-c[Cys-Gly-Phe-Cys]-NH_2 (#60, FM13(S-Et-S))

FM13(SH_2)DC/PEG (25 mg) was reacted with 1,2-dibromomethane in the presence of KO*t*Bu as described in the general protocol for dithioether cyclization. The cyclic peptide was purified by semi-preparative RP-HPLC to afford 9 mg (35%) of **FM13(S-Et-S)**, 97% pure as determined by analytical RP-HPLC with elution time of 31 min (0-70% solvent B in 70 min). ESI-MS $[M+H]^+ = 761.4$.

H-D-Arg-Cys-Pro-Gly-Phe-Cys-NH_2 (FM14(SH_2))

0.5 g of Rink amide resin (0.5 mmol/g) was used to synthesize the peptide according to the general protocol. 0.66 g of peptide-resin was obtained from the solid phase peptide synthesis from which the peptide was cleaved according to the general cleavage and

deprotection protocol to yield 70 mg of crude peptide. All of the crude material was purified by semi-preparative RP-HPLC with gradient 0-30% solvent B in 90 min to afford 26.1 mg pure peptide with elution time of 20.4 min (0-70% solvent B in 70 min) on analytical RP-HPLC. ESI-MS $[M+H]^+$ = 681.4. Unfortunately the amount of pure material was not enough to carry out the both cyclization reaction and a new synthesis was attempted with the new resin and double couple, double deprotection protocol to improve the yield.

H-D-Arg-Cys-Pro-Gly-Phe-Cys-NH_2 (FM14(SH_2)DC/PEG)

In order to generate enough material to run the dithioether cyclization reaction, the synthesis of **FM14(SH_2)** was repeated for a third time. A new resin was used with an extended linker, PAL-PEG-PS amide resin (0.41 mmol/g). 0.61 mg of resin was used to synthesize the peptide according to the double couple, double deprotection protocol. 0.65 g of peptide-resin was obtained from the solid phase peptide synthesis from which the peptide was cleaved according to the general cleavage and deprotection protocol to yield 85 mg of crude peptide. All of the crude material was semi-purified by preparative RP-HPLC with gradient 0-30% solvent B in 90 min to afford 20.8 mg pure peptide with elution time of 20.4 min (0-70% solvent B in 70 min) on analytical RP-HPLC. ESI-MS $[M+H]^+$ = 681.4.

H-D-Arg-c[Cys-Pro-Gly-Phe-Cys]-NH_2 (#61, FM14(SS))

The linear peptide (21 mg) was subjected to cyclization with $K_3Fe(CN)_6$ according to the general disulfide cyclization protocol. The cyclic peptide was purified by semi-

preparative RP-HPLC to afford 7.3 mg (34.8%) of **FM14(SS)**, 99% pure as determined by analytical RP-HPLC with elution time of 17.6 min (0-70% solvent B in 70 min). ESI-MS $[M+H]^+$ = 679.3.

H-D-Arg-c[Cys-Pro-Gly-Phe-Cys]-NH_2 (#62, FM14(S-Et-S))

FM14(SH_2)DC/PEG (27.8 mg) was reacted with 1,2-dibromomethane in the presence of KO*t*Bu as described in the general protocol for dithioether cyclization. The cyclic peptide was purified by semi-preparative RP-HPLC to afford 9.2 mg (32%) of **FM14(S-Et-S)**, 99% pure as determined by analytical RP-HPLC with elution time of 26.7 min (0-70% solvent B in 70 min). ESI-MS $[M+H]^+$ = 707.4.

H-Cys-D-Arg-Oic-Pro-Gly-Phe-Cys-NH_2 (FM15(SH_2))

0.5 g of Rink amide resin (0.5 mmol/g) was used to synthesize the peptide according to the general protocol. 0.72 g of peptide-resin was obtained from the solid phase peptide synthesis from which the peptide was cleaved according to the general cleavage and deprotection protocol to yield 110 mg of crude peptide. All of the crude material was purified by semi-preparative RP-HPLC with gradient 0-30% solvent B in 90 min to afford 48.6 mg pure peptide with elution time of 25.9 min (0-70% solvent B in 70 min) on analytical RP-HPLC. ESI-MS $[M+H]^+$ = 832.5.

H-c[Cys-D-Arg-Oic-Pro-Gly-Phe-Cys]-NH_2 (#63, FM15(SS))

The linear peptide (22.2 mg) was subjected to cyclization with $K_3Fe(CN)_6$ according to the general disulfide cyclization protocol. The cyclic peptide was purified by semi-

preparative RP-HPLC to afford 12.3 mg (55.4%) of **FM15(SS)**, 100% pure as determined by analytical RP-HPLC with elution time of 24.3 min (0-70% solvent B in 70 min). ESI-MS $[M+H]^+$ = 830.4.

H-c[Cys-D-Arg-Oic-Pro-Gly-Phe-Cys]-NH_2 (#64, FM15(S-Et-S))

The linear peptide (20.8 mg) was reacted with 1,2-dibromomethane in the presence of KO*t*Bu as described in the general dithioether cyclization protocol. The cyclic peptide was purified by semi-preparative RP-HPLC to afford 8.3 mg (49.4%) of **FM15(S-Et-S)**, 98% pure as determined by analytical RP-HPLC with elution time of 26.1 min (0-70% solvent B in 70 min). ESI-MS $[M+H]^+$ = 857.4.

H-D-Arg-Oic-Pro-D-Ala-Phe(*p*-Me)-N^{ε}-biotinyl-Lys-NH_2 (27K-biotin, FM42)

0.67 g of PAL-PEG-PS amide resin (0.38 mmol/g) was used to synthesize the peptide according to the general protocol. 0.86 g of peptide-resin was obtained from the solid phase peptide synthesis from which the peptide was cleaved according to the general cleavage and deprotection protocol to yield 190 mg of crude peptide. All of crude peptide was purified by semi-preparative RP-HPLC with gradient 10-40% solvent B in 60 min to afford 111.8 mg pure peptide with elution time of 29.4 min (0-70% solvent B in 70 min) on analytical RP-HPLC. ESI-MS $[M+H]^+$ = 1008.6.

H-D-Arg-Pro-Oic-D-Ala-Phe(*p*-Me)-N^{ε}-5-FAM-Lys-NH_2 (27K-FAM, FM61)

0.34 g of Rink amide resin (0.75 mmol/g) was used to synthesize the pentapeptide according to the general protocol. 0.44 g of peptide-resin was obtained from the solid

phase peptide synthesis. In order to introduce the lysine with the fluorophore, 5-carboxyfluorescein (5-FAM), the Dde protecting group on the lysine was removed by treating the resin with 2% hydrazine in DMF for 30 min. Excess 5-FAM (310 mg, 8-fold excess) was dissolved in 1.3 mL of DMF then activated by DIC (137 μL, 0.88 mmol) and HOBt (135 mg, 0.88 mmol). The activated fluorophore was added to the resin and the reaction allowed to proceed for 2 hrs. The resin was washed with 20% piperidine in DMF (v/v) until the solution was free of excess fluorophore (approximately 45 min). The labeled peptide was cleaved according to the general cleavage and deprotection protocol to yield 170 mg of crude peptide. All of the crude peptide was dissolved in MeOH and purified by semi-preparative RP-HPLC with gradient 25-55% solvent B in 60 min to afford 67.4 mg pure peptide with elution time of 38.5 min (0-70% solvent B in 70 min) on analytical RP-HPLC. ESI-MS $[M+H]^+$ = 1140.5. All of the above reactions were carried out in complete darkness due to the light sensitivity of the fluorophore.

H-D-Arg-Oic-Pro-D-Asn-Dpa-NH_2 (FM12)

0.5 g of Rink amide resin (0.5 mmol/g) was used to synthesize the pentapeptide according to the general protocol. 0.67 g of peptide-resin was obtained from the solid phase peptide synthesis from which the peptide was cleaved according to the general cleavage and deprotection protocol to yield 90 mg of crude peptide. A 30.3 mg portion of crude peptide was purified by semi-preparative RP-HPLC with gradient 0-40% solvent B in 80 min to afford 18.0 mg pure peptide with elution time of 29.6 min (0-70% solvent B in 70 min) on analytical RP-HPLC. ESI-MS $[M+H]^+$ = 759.4.

H-D-Arg-Oic-Pro-D-Ala-Thi-NH_2 (FM17)

0.61 g of PAL-PEG-PS amide resin (0.41 mmol/g) was used to synthesize the pentapeptide according to the general protocol. 0.71 g of peptide-resin was obtained from the solid phase peptide synthesis from which the peptide was cleaved according to the general cleavage and deprotection protocol to yield 150 mg of crude peptide. A 41 mg portion of crude peptide was purified by semi-preparative RP-HPLC with gradient 10-40% solvent B in 60 min to afford 29.4 mg pure peptide with elution time of 23.9 min (0-70% solvent B in 70 min) on analytical RP-HPLC. ESI-MS $[M+H]^+ = 646.4$.

H-D-Arg-Oic-Pro-D-Dab-Phe-NH_2 (FM22)

0.61 g of PAL-PEG-PS amide resin (0.41 mmol/g) was used to synthesize the pentapeptide according to the general protocol. 0.78 g of peptide-resin was obtained from the solid phase peptide synthesis from which the peptide was cleaved according to the general cleavage and deprotection protocol to yield 100 mg of crude peptide. A 44 mg portion of crude peptide was purified by semi-preparative RP-HPLC with gradient 0-30% solvent B in 60 min to afford 29.6 mg pure peptide with elution time of 21.9 min (0-70% solvent B in 70 min) on analytical RP-HPLC. ESI-MS $[M+H]^+ = 655.5$.

H-D-Arg-Oic-Pro-D-Dap-Phe-NH_2 (FM23)

0.61 g of PAL-PEG-PS amide resin (0.41 mmol/g) was used to synthesize the pentapeptide according to the general protocol. 0.75 g of peptide-resin was obtained from the solid phase peptide synthesis from which the peptide was cleaved according to the general cleavage and deprotection protocol to yield 130 mg of crude peptide. A 35.9 mg

portion of crude peptide was purified by semi-preparative RP-HPLC with gradient 0-30% solvent B in 60 min to afford 28.6 mg pure peptide with elution time of 21.3 min (0-70% solvent B in 70 min) on analytical RP-HPLC. ESI-MS $[M+H]^+$ = 669.5.

H-D-Arg-Oic-Pro-D-Ala-Phe(*p*-Me)-Lys-NH_2 (FM41)

0.67 g of PAL-PEG-PS amide resin (0.38 mmol/g) was used to synthesize the peptide according to the general protocol. 0.76 g of peptide-resin was obtained from the solid phase peptide synthesis from which the peptide was cleaved according to the general cleavage and deprotection protocol to yield 230 mg of crude peptide. A 100 mg portion of crude peptide was purified by semi-preparative RP-HPLC with gradient 10-40% solvent B in 60 min to afford 86 mg pure peptide with elution time of 24.8 min (0-70% solvent B in 70 min) on analytical RP-HPLC. ESI-MS $[M+H]^+$ = 782.6.

H-Trp-Oic-Pro-D-Ala-Phe(*p*-Me)-NH_2 (FM49)

0.67 g of PAL-PEG-PS amide resin (0.38 mmol/g) was used to synthesize the peptide according to the general protocol. 0.74 g of peptide-resin was obtained from the solid phase peptide synthesis from which the peptide was cleaved according to the general cleavage and deprotection protocol to yield 110 mg of crude peptide. A 30 mg of the crude peptide was purified by semi-preparative RP-HPLC with gradient 15-50% solvent B in 70 min to afford 22.6 mg pure peptide with elution time of 40.1 min (0-70% solvent B in 70 min) on analytical RP-HPLC. ESI-MS $[M+H]^+$ = 684.5.

H-Trp-Pro-Pro-Gly-Phe-NH_2 (FM50)

0.67 g of PAL-PEG-PS amide resin (0.38 mmol/g) was used to synthesize the peptide according to the general protocol. 0.78 g of peptide-resin was obtained from the solid phase peptide synthesis from which the peptide was cleaved according to the general cleavage and deprotection protocol to yield 90 mg of crude peptide. This peptide was not purified or characterized due to difficulties with solubility of the crude material.

H-D-Glu-Oic-Pro-D-Ala-Phe(*p*-Me)-NH_2 (FM51)

1.0 g of PAL-PEG-PS amide resin (0.20 mmol/g) was used to synthesize the peptide according to the general protocol. 0.98 g of peptide-resin was obtained from the solid phase peptide synthesis from which the peptide was cleaved according to the general cleavage and deprotection protocol to yield 13.6 mg of crude peptide. All of the crude peptide was purified by semi-preparative RP-HPLC with gradient 10-40% solvent B in 60 min to afford 8.4 mg pure peptide with elution time of 30.0 min (0-70% solvent B in 70 min) on analytical RP-HPLC. ESI-MS $[M+H]^+ = 627.3$.

"SCRAMBLED" ANALOGS OF 27

H-Phe(*p*-Me)-Oic-D-Arg-Pro-D-Ala-NH_2 (FM43)

0.67 g of PAL-PEG-PS amide resin (0.38 mmol/g) was used to synthesize the pentapeptide according to the general protocol. 0.77 g of peptide-resin was obtained from the solid phase peptide synthesis from which the peptide was cleaved according to the general cleavage and deprotection protocol to yield 150 mg of crude peptide. A 100 mg portion of crude peptide was purified by semi-preparative RP-HPLC with gradient 10-

40% solvent B in 60 min to afford 87.8 mg pure peptide with elution time of 25.9 min (0-70% solvent B in 70 min) on analytical RP-HPLC. ESI-MS $[M+H]^+$ = 654.4.

H-D-Ala-Pro-D-Arg-Oic-Phe(*p*-Me)-NH_2 (FM44)

0.67 g of PAL-PEG-PS amide resin (0.38 mmol/g) was used to synthesize the pentapeptide according to the general protocol. 0.77 g of peptide-resin was obtained from the solid phase peptide synthesis from which the peptide was cleaved according to the general cleavage and deprotection protocol to yield 160 mg of crude peptide. A 100 mg portion of crude peptide was purified by semi-preparative RP-HPLC with gradient 10-40% solvent B in 60 min to afford 40.4 mg pure peptide with elution time of 32.1 min (0-70% solvent B in 70 min) on analytical RP-HPLC. ESI-MS $[M+H]^+$ = 654.5.

H-Pro-D-Ala-Phe(*p*-Me)-D-Arg-Oic-NH_2 (FM45)

0.67 g of PAL-PEG-PS amide resin (0.38 mmol/g) was used to synthesize the pentapeptide according to the general protocol. 0.75 g of peptide-resin was obtained from the solid phase peptide synthesis from which the peptide was cleaved according to the general cleavage and deprotection protocol to yield 170 mg of crude peptide. A 56.8 mg portion of crude peptide was purified by semi-preparative RP-HPLC with gradient 10-40% solvent B in 60 min to afford 49 mg pure peptide with elution time of 28.6 min (0-70% solvent B in 70 min) on analytical RP-HPLC. ESI-MS $[M+H]^+$ = 654.5.

H-Pro-Phe(*p*-Me)-Oic-D-Arg-D-Ala-NH_2 (FM46)

0.67 g of PAL-PEG-PS amide resin (0.38 mmol/g) was used to synthesize the pentapeptide according to the general protocol. 0.81 g of peptide-resin was obtained from the solid phase peptide synthesis from which the peptide was cleaved according to the general cleavage and deprotection protocol to yield 170 mg of crude peptide. A 55.5 mg portion of crude peptide was purified by semi-preparative RP-HPLC with gradient 10-40% solvent B in 60 min to afford 43.7 mg pure peptide with elution time of 27.3 min (0-70% solvent B in 70 min) on analytical RP-HPLC. ESI-MS $[M+H]^+ = 654.5$.

H-Pro-D-Arg-D-Ala-Phe(*p*-Me)-Oic-NH_2 (FM47)

0.67 g of PAL-PEG-PS amide resin (0.38 mmol/g) was used to synthesize the pentapeptide according to the general protocol. 0.75 g of peptide-resin was obtained from the solid phase peptide synthesis from which the peptide was cleaved according to the general cleavage and deprotection protocol to yield 170 mg of crude peptide. A 57.5 mg portion of crude peptide was purified by semi-preparative RP-HPLC with gradient 10-40% solvent B in 60 min to afford 44.7 mg pure peptide with elution time of 29.8 min (0-70% solvent B in 70 min) on analytical RP-HPLC. ESI-MS $[M+H]^+ = 654.5$.

H-Pro-D-Arg-Oic-Phe(*p*-Me)-D-Ala-NH_2 (FM48)

0.67 g of PAL-PEG-PS amide resin (0.38 mmol/g) was used to synthesize the pentapeptide according to the general protocol. 0.77 g of peptide-resin was obtained from the solid phase peptide synthesis from which the peptide was cleaved according to the general cleavage and deprotection protocol to yield 180 mg of crude peptide. A 54.6 mg

portion of crude peptide was purified by semi-preparative RP-HPLC with gradient 10-40% solvent B in 60 min to afford 47.3 mg pure peptide with elution time of 31.5 min (0-70% solvent B in 70 min) on analytical RP-HPLC. ESI-MS $[M+H]^+ = 654.5$.

PLATELET AGGREGATION ASSAY. Each peptide was examined for its ability to inhibit γ-thrombin-induced platelet aggregation of human platelet-rich plasma as described by Hasan et al. [81, 92]. Fresh whole blood from healthy human donors was collected into a syringe containing 3.8 % sodium citrate (1:9 citrate/blood). Whole blood was centrifuged at 180x*g* (Beckman GRP Centrifuge, Schaumburg, IL) for 10 min at room temperature to prepare platelet-rich plasma (PRP). Platelet-poor plasma (PPP) was prepared by centrifugation of PRP at 1,000×*g* for 20 min at room temperature or by centrifugation at 10,000×*g* for 2 min (Microcentrifuge E, Beckman Instruments, Palo Alto, CA). The platelets were counted on a Coulter counter (Model Z, Coulter Electronics, Hialeah, FL), and PRP was adjusted to a platelet count of 2.5×10^8 platelets/mL, using PPP for dilution prior to all platelet aggregation studies. A Chronolog dual-channel aggregometer (Havertown, PA) was used to assess platelet aggregation by recording the increase in light transmittance through a stirred suspension of PRP maintained at 37°C in the cuvette. Variable concentrations of γ-thrombin (Haematologic Technologies, Essex Junction VT) were added to the PRP to determine the threshold concentration for maximal percent aggregation, i.e., the minimal concentration of the agonist to induce full aggregation and secretion. γ-Thrombin (Haematologic Technologies, Essex Junction, VT, ~3000 U/mg specific activity) was used for these studies because this form of the enzyme is unable to bind and proteolyze plasma

fibrinogen in plasma to produce a clot. Peptides were dissolved in fresh HEPES-Tyrodes buffer (pH = 7.40) and added at concentrations ranging from 5 μM to 1 mM to the PRP in the cuvette, allowing the baseline to stabilize. Platelet aggregation was initiated by the addition of threshold amounts of γ-thrombin (usually 30 to 70 nM for human platelets) determined for each donor on the day of assay. The aggregation was allowed to proceed for 5 minutes and the minimal concentration of each peptide to achieve 100 % inhibition of platelet aggregation (IC_{100}) was determined.

CALCIUM MOBILIZATION ASSAY. Each peptide was studied to determine its potential to inhibit α-thrombin-induced calcium mobilization in human fibroblast cells as previously described by Nieman et al.[92]. Normal human fibroblast cells were purchased from Clonetics (San Diego, CA) and were cultured according to the supplier's instructions. The cytoplasmic concentration of free calcium was measured with Fura-2 (Molecular Probes, Eugene, OR), a Ca^{2+} indicator. Cell suspensions in HEPES-Tyrodes buffer supplemented with 100 mM Ca^{2+} and 100 mM Mg^{2+} were incubated with 5 μM Fura for 60 minutes at room temperature. The excess indicator was removed by washing and centrifuging the cells three times with buffer. Aliquots of the cell suspensions were placed in a quartz cuvette that was positioned in a thermostatically controlled chamber at 37°C in a fluorescence spectrophotometer (LS50B spectrofluorometer from PerkinElmer Life and Analytical Sciences. Boston, MA). Cells were treated with 0.5 to 2 nM of α-thrombin to determine minimal amount required to achieve the maximum response. A variety of concentrations of the peptides were added to the cells suspension followed by the addition of threshold amounts of α-thrombin. The degree of inhibition by each

peptide was determined by calculating the change in the area under the curve produced by threshold α-thrombin using Winlab software (PerkinElmer Life and Analytical Sciences). The calcium mobilization data was expressed as percentage of inhibition as related to samples with α-thrombin alone.

CLOTTING ASSAYS. The effect of each peptide on the activated partial thromboplastin time (APTT), prothrombin time (PT), and thrombin clotting time (TCT) was examined. The protocols used for the APTT, PT and TCT assays were previously described by Hasan et al.[80]. The APTT test was carried out by incubating 50 μL of normal human plasma (George King, Overland Park, KS) with 0-1mM of each peptide and 50 μL 1:2 APTT reagent (kaolin)-Tris buffer (Organon Teknika, Durham, NC) for 5 min at 37˚ C. After incubation period, 50 μL of 30 mM $CaCl_2$ was added and the time to clot formation was measured.

The PT test was performed by incubating 50 μL of normal human plasma with 0-1mM of each peptide for 5 min at 37˚ C. Then 100 μL of PT reagent (thromboplastin) (Simplastin, Organon Teknika) and 100 μL of 30 mM $CaCl_2$ were added and the time to clot formation was measured. The TCT experiment was carried out in a similar fashion with incubation followed by addition of 8 nM of human α-thrombin (1 U/mL) and the time to clot formation was then measured. All coagulant assays were performed in an Amelung KC4 coagulant analyzer (Sigma Aldrich). Values were considered significantly prolonged when the mean result at each concentration of peptide was $p < 0.05$ from the control on a nonpaired *t* test.

ENZYMATIC ACTIVITY EXPERIMENTS. An assay of enzymatic activity inhibition was employed to explore the interactions of our peptides with the active site of thrombin. The rate of cleavage of a chromogenic compound, Sar-Pro-Arg- *p*-nitroanilide, by both α- and γ-thrombin was monitored in the presence of 0, 20, 40, and 80 μM peptide. The experiment was carried out in triplactes with 2 nM α- and γ-thrombin (Haematologic Technologies), 1 mM Sar-Pro-Arg-*p*-nitroanilide (Sigma-Aldrich) (K_m = 138 μM), and 10 mM Tris-HCl, 0.15 M NaCl, pH 7.6 (Hasan et al., 2003). The same studies were carried out for several clotting factors to probe the ability of each peptide to inhibit other enzymes of the coagulation system as described by Nieman et al.[92]. To determine the inhibition of factor Xa (FXa) (Enzyme Research Laboratories Inc., South Bend, IN), 2 nM of enzyme was used to cleave 0.4 mM *N*-(*p*-Tosyl)-Gly-Pro-Arg-*p*-nitroanilide. Inhibition of 3 nM factor XIa (FXIa) (Hematologic Technologies) cleavage of 0.6 mM L-pyro-Glu-Pro-Arg-*p*-nitroanilide (Diaphram, Franklin, OH) was also studied in presence and absence of each peptide. Additional experiments were carried out with 50 nM factor VIIa (FVIIa) with preformed complex of enzyme and 70 nM soluble recombinant tissue factor, $sTF_{1\text{-}219}$, provided by Tom Girard (Monsanto, St. Louis, MO). The chromogenic substrate used in the FVIIa assay was 1.25 mM Spectrozyme fXa (methoxycarbonyl-D-cyclohexylglycyl-glycyl-arginine-*p*-nitroanilide)[113]. The same experiment was performed without the formation of the enzyme-tissue factor complex by incubation of the peptide with FVIIa prior to the addition of tissue factor. The K_i values were calculated from the K_{iapp} as described previously described by Bieth[114].

EXPRESSION OF RECOMBINANT PROTEINS. The protocol for the cloning and expression of the recombinant exodomain of PAR1 was previously described by Hasan

et al.[81]. Purified recombinant exodomain of PAR1 and PAR4 was prepared from 1 liter cultures of *Escherichia coli* BLR(DE3) with the plasmid pET31b containing the corresponding cDNA that were grown to mid-log phase at 37 °C in Luria broth containing 1 mL carbenicilllin. This was followed by induction with 10 mL of 1 mM IPTG for 4 h. After induction, the bacteria were harvested by centrifugation (10 min, 5000 × *g*) and the pellet was re-suspended in binding buffer (40 mM Tris–HCl and 500 mM NaCl, pH 7.4) containing 8 mg/ml lysozyme and 5 μL of lysonase bioprocessing reagent. The bacterial extracts were then incubated for 15 min at room temperature. Bacterial lysates were centrifuged at 12000 × *g* for 10 min at 4˚ C and the pellet was re-suspended in 12.5 mL of binding buffer containing 6 M guanidine HCl and 5 mM imidazole and purified with nickel-chelate affinity chromatography. This was followed by treatment with CNBr to remove the KSI fusion protein and the His tag according to the manufacturer's protocol (Novagen, Madison, WI). The final recombinant proteins were further purified by HPLC. The integrity of the expressed PAR1 and PAR4 exodomains were verified by MALDI-TOF mass spectrometry and ESI-MS.

COMPETITION-BINDING EXPERIMENTS. Recombinant PAR1 and PAR4 exodomains ($rPAR4_{EC}$ and $rPAR4_{EC}$) were prepared as described above, and peptide binding was examined using the protocol previously described by Nieman et al.[92]. $rPAR1_{EC}$ (1 μg/well) in 0.1 M Na_2CO_3, pH 9.6, was bound to microtiter plate wells (F96 CERT.MAXISORP, #439454; Nunc-Immuno Plate, Fisher Scientific, Chicago, IL) by incubation at 4°C overnight. After incubation, wells were washed three times with 10 mM NaH_2PO_4, 150 mM NaCl, pH 7.4, containing 0.05% Tween 20. After blocking the wells with 1% gelatin, the bound $rPAR1_{EC}$ was incubated with 20 μM RPPGFK-biotin

(Multiple Peptide Systems, Inc., San Diego, CA) in the presence or absence of various peptides 1 h at 37°C. After incubation, the wells were washed three times with 10 mM NaH_2PO_4, 150 mM NaCl, pH 7.4, containing 0.05% Tween 20 and the bound RPPGFK-biotin was detected by using Immune-Pure streptavidin horseradish peroxidase conjugate (Pierce Chemical, Rockville, IL) and peroxidase-specific fast reacting substrate turbo-3,3'5,5'-tetramethylbenzidine (turbo-TMB; Pierce Chemical) as described previously[115]. The color reaction was quenched by the addition of 1 M phosphoric acid, and the reaction was quantitated by measuring the absorbance at 450 nm in a Microplate auto reader EL311 (Bio-Tek Instruments, Winooski, VT). The same experimental protocol was applied to $rPAR4_{EC}$ to determine the ability of the peptides to bind to PAR4.

DIRECT BINDING EXPERIMENT WITH D-Arg-Oic-Pro-D-Ala-Phe(*p*-Me)-Lys(biotin)-NH_2. Recombinant PAR1 exodomain ($rPAR1_{EC}$) was prepared as described above, and peptide binding was examined using the protocol previously described by Nieman et al.[92]. $rPAR1_{EC}$ was incubated overnight at 4°C in 0.1 M Na_2CO_3, pH 9.6, to link the receptor to the wells of a 96-well microtiter plate (F96 CERT.MAXISORP, #439454; Nunc-Immuno Plate, Fisher Scientific). After incubation, the wells were washed five times with 10 mM NaH_2PO_4, 150 mM NaCl, pH 7.4, containing 0.05% Tween 20. The wells were then blocked with 0.2% bovine serum albumin in PBS with 0.05% Tween 20 for one hour at 37° C. After blocking and washing of the wells, the bound $rPAR1_{EC}$ was incubated with 5-100 μM rOicPaF(*p*-Me)K-biotin in the presence and absence of 150-fold excess of unlabeled rOicPaF(*p*-Me) for 1 hr at 37° C. After incubation, the wells were washed three times with 10 mM NaH_2PO_4, 150 mM NaCl, pH

7.4, containing 0.05% Tween 20 and the bound rOicPaF(*p*-Me)K-biotin was detected by using Immune-Pure streptavidin horseradish peroxidase conjugate (Pierce Chemical) and peroxidase-specific fast reacting substrate turbo-3,3'5,5'-tetramethylbenzidine (turbo-TMB; Pierce Chemical) as described previously[115]. The color reaction was stopped by the addition of 1 M phosphoric acid, and the reaction was quantitated by measuring the absorbance at 450 nm in a Microplate auto reader EL311 (Bio-Tek Instruments).

PHARMACOKINETIC STUDIES. All animal studies were conducted by Mark Warnock in accordance with the Guide for the Care and Use of Laboratory Animals. Purpose-bred beagle dogs (8.8-12.5 kg) were anesthetized with intravenous administration of sodium pentobarbital (30 mg/kg), and anesthesia was maintained by intramuscular pentobarbital (90 mg) as needed. After tracheotomy, intubation, and positive pressure ventilation with room air using a Harvard respirator (Harvard Instruments, South Natick, MA), the right jugular vein and right femoral vein were cannulated for blood collection and drug administration, respectively. Arterial blood pressure was monitored from a cannulated right carotid artery with a blood pressure transducer (Gould Inc., Cardiovascular Product, Oxford, CA). Standard limb lead II of the electrocardiogram was recorded continuously and used to monitor heart rate. After a single intravenous administration of rOicPaF(*p*-Me) (4.4 mg/kg in 5 mL saline infused over 1 minute to each four dogs), blood samples were collected at 1, 5, 10, 15, 30, 25, 30, 40, 60, 90, and 120 minutes by withdrawing 5 mL of blood into a syringe containing 3.8 % sodium citrate (1:9, citrate/blood). The blood was centrifuged at 12,000*g* for 2 minutes at room temperature to prepare platelet-poor plasma that was stored in small aliquots at

-70°C until assay. The canine plasma samples in the pharmacokinetic studies were analyzed by HPLC chromatographic method using a C4 column as reported previously[80]. The pharmacokinetics were calculated using noncompartmental methods of Rowland and Tozer (1989).

STABILITY ASSAYS. *Simulated Intestinal Fluid Stability Assays*. The stability of the peptide analogs were tested by Dr. John Hilfinger from TSRL, Inc. in simulated gastric and simulated intestinal fluid to ensure their integrity under these conditions. For these assays, equal volumes of a stock solution of the analog to be tested (≥ 1 mg/mL in HPLC-grade water) and 2 x simulated gastric fluid [70 mM NaCl and 6.4 mg/ml porcine mucosal pepsin (800-2500 units/mg of protein) in water, final pH ~ 1.2] or 2x simulated intestinal fluid (100 mM KH_2PO_4 with 20 mg/ml pancreatin, final pH 6.8) was mixed and incubated at 37^o C in a shaking water bath. Aliquots of 0.25 ml were removed at time points: 0, 1, 2, 3 and 4 h and prepared for LC/MS/MS analysis.

Homogenate Stability Assays. The perfusion buffer used in stability testing was 10 mM MES (pH 6.5) containing 135 mM NaCl, and 5 mM KCl. To collect intestinal perfusate from rats, male Sprague Dawley rats, 8 to 10 weeks old, weighing 250 to 350 g were fasted 15 to 18 hours with water given ad libitum. Anesthesia was administered by intramuscular injection of pentobarbital/ketamine (40 mg/kg and 80 mg/kg, respectively). The rats were placed on a warming pad under a surgical lamp to maintain body temperature and jejunal intestinal segments were exposed through a midline, abdominal incision. An approximately 20 cm segment of the jejunum (2 to 4 cm distal to the ligament of Treitz) was cannulated and the intestinal segments were perfused with 10 mM MES (pH 6.5) containing 135 mM NaCl, and 5 mM KCl at a flow-rate of 0.5 ml/min

at 37°C using a constant infusion pump (Harvard Apparatus, South Natick, Mass.). The collected perfusate was stored at -80°C until used for *ex vivo* stability studies. After collection, the perfused intestinal segments were flushed with ice-cold 0.15 M KCl solution and the animal was euthanized and the jejunal intestinal segment detached. The inner intestinal tissue layers were scraped out and homogenized in MES buffer (pH 6.5) at a ratio of 1 part of intestinal tissue to 5 parts buffer. For liver homogenates, the liver was removed from the animals and prepared as described for the intestinal perfusates. Total protein content of the perfusate and the homogenates were determined using a BioRad protein assay kit. The tissue homogenate samples were used immediately or rapidly frozen at -80°C until stability analysis.

For the stability analysis, 0.7 mg of total protein (homogenates) was added to 0.6 ml of 100 mM phosphate buffer (pH 6.5). The reactions were initiated by adding the peptide analogs (~ 200 μM final) at 37°C. 0.2 ml aliquots were withdrawn at predetermined time intervals (e.g., 0, 5, 15, and 30 min). The reaction was quenched by adding 0.2 ml of ice cold 10% trifluoroacetic acid (TFA). The samples were centrifuged, filtered and analyzed for the intact peptide by LC/MS/MS.

ORAL ABSORPTION STUDIES IN RATS USING DUODENAL ADMINISTRATION. All of the experiments described below were conducted at TSRL, Inc. Compounds were administered by intraduodenal injection and blood samples were taken at timed intervals over the course of ~ 4 hours. For comparative purposes between the different drugs, the dosing was performed at 10 mg/kg. For the dosing, on the day of the study, 3 fasted, male Sprague-Dawley rats were anesthetized and the femoral artery

catheterized following standard procedures. A midline incision was made to open the abdominal cavity, and the duodenal section of the intestine was isolated. Compounds were directly injected into the duodenum and 0.5 ml plasma samples were taken at timed intervals over the course of about 4 hours.

Rat plasma samples containing test peptides were analyzed by LCMS/MS. A solid phase extraction cartridge (HLB, 30 mg/1 cc, Waters) was activated with 1 mL of methanol and equilibrated with 1 mL of water. A 200 µL aliquot of rat plasma was acidified and loaded onto the cartridge. After washing with 1 mL of 5% methanol, the compounds were eluted with 1 mL of methanol. The solvent was evaporated under vacuum and the residue was reconstituted in 200 µL of mobile phase. Samples were analyzed using ESI-LCMS/MS (Micromass Quattro II) (Micromass, Beverly, MA), employing a HP1100 HPLC system (Hewlett Packard, CA). 10 µL of sample was purified with a C18, 5 µm, 50 mm X 2.2 mm (Higgins Analytical Inc., Mountain View, CA) using a mobile phase of 50:50 acetonitrile and water containing 0.1 % formic acid. Calibration curves were constructed by weighted (1/x) least square regression of peak area versus concentrations of the calibration standards.

OCTANOL:WATER PARTITION COEFFICIENT. A 1 mg/ml aqueous solution of peptide analog in 50 mM phosphate buffer, pH = 7, was mixed with an equal volume of n-octanol and vigorously stirred for 4 hours at room temperature. At the end of the incubation time, aliquots of the phases were analyzed for the peptide analogs. The log $D_{pH\ 7}$ was calculated by calculating the log of $[drug]_{octanol}$ /$[drug]_{aq\ (pH\ 7)}$.

DOCKING STUDIES AND COMPUTATIONAL MODELS. The computational studies were carried out by Katrina Lexa as part of a rotation project in the Mosberg lab. Each peptide was initially built in MOE2006.08 to create analogs through sequence mutation of compound **27**. Structure development was performed through use of the Build feature, after which each analog's energy was calculated using PEOE charges. The crystal-structure derived analogs were docked into the binding pocket of thrombin using the active site defined by all receptor amino acids with the potential for electrostatic interaction with the ligand as determined by Dr. Enrico Di Cera and MOE2006.08. Ligand docking was performed to solvated thrombin through the Dock feature in MOE2006.08, using affinity ΔG as the scoring function and alpha triangle as the placement set.

STATISTICAL ANALYSIS. Statistical comparisons between treatment groups used unpaired Student's *t* test or the nonparametric Mann-Whitney signed rank test as needed (p values < 0.05 were considered significant).

APPENDICES

APPENDIX A

LIST OF AMINO ACIDS

Abu		aminobutyric acid
Ala	(A)	alanine
Arg	(R)	arginine
Asn	(N)	asparigine
Asp	(D)	aspartic acid
β-Ala		beta-alanine
Bip		4,4'-biphenylphenylalanine
Cys	(C)	cysteine
Dab		diaminobutyric acid
Dap		diaminopropionic acid
Dpa		diphenylalanine
Gln	(Q)	glutamine
Glu	(E)	glutamic acid
Gly	(G)	glycine
Hfe		homophenylalanine
His	(H)	histidine
Ile	(I)	isoleucine
Leu	(L)	leucine
Lys	(K)	lysine
1-Nal		3-(1-naphthyl)-L-alanine
2-Nal		3-(2-naphthyl)-L-alanine
Nle		norleucine
Oic		octahydroindole-2-carboxylic acid
Orn		ornithine

Pro	(P)	proline
Phe	(F)	phenylalanine
Phe(*p*-Br)		*p*-bromophenylalanine
Phe(*p*-*t*Bu)		*p*-*tert*-butylphenylalanine
Phe(*p*-Cl)		*p*-chlorophenylalanine
Phe(*p*-CN)		*p*-cyanophenylalanine
Phe(*p*-COOH)		*p*-carboxyphenylalanine
Phe(*p*-F)		*p*-fluorophenylalanine
Phe(*p*-I)		*p*-iodophenylalanine
Phe(2-Me)		2-methylphenylalanine
Phe(3Me)		3-methylphenylalanine
Phe(*p*-Me)		*p*-methylphenylalanine
Phe(*p*-NH_2)		*p*-nitrophenylalanine
Phg		phenylglycine
Sar		sarcosine, N-methylglycine
Ser	(S)	serine
Thi		thienylalanine
Thr	(T)	threonine
Trp	(W)	tryptophan
Tyr	(Y)	tyrosine

APPENDIX B

STRUCTURE OF AMINO ACIDS SUBSTITUTED AT POSITION 1, 2 AND 4

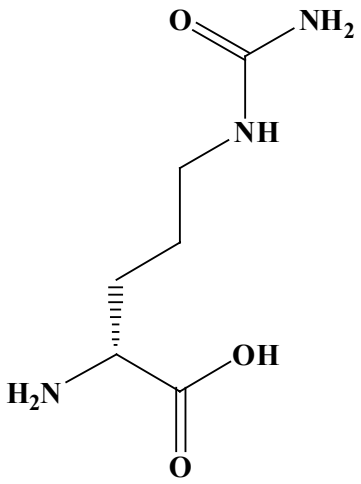

D-Citrulline (D-Cit)

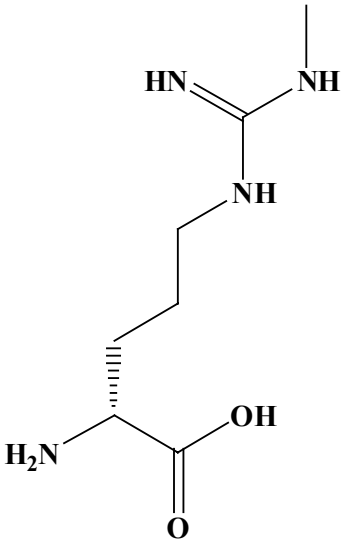

N$^{\omega}$-Methyl-D-arginine (D-Arg(Me))

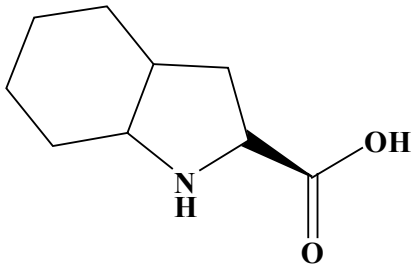

L-Octahydroindole-2-carboxylic acid (Oic)

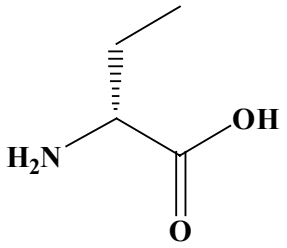

D-Aminobutyric acid (D-Abu)

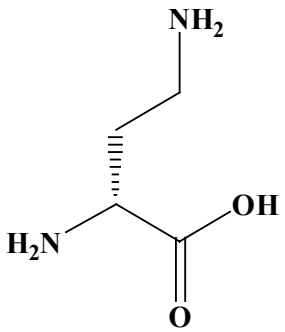

D-2,4-Diaminobutyric acid (D-Dab)

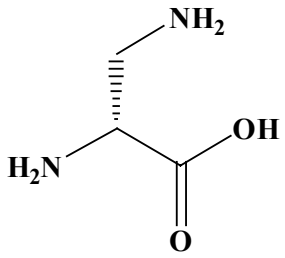

D-2,3-Diaminopropionic acid (D-Dap)

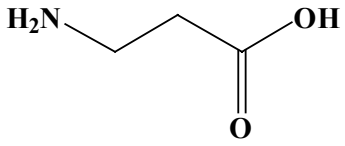

β-Alanine
(β-Ala)

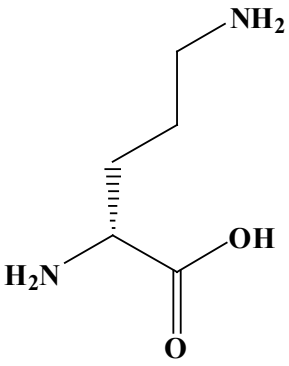

D-Ornithine
(D-Orn)

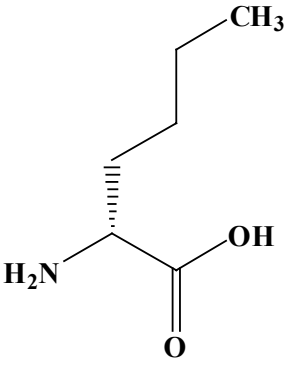

D-Norleucine
(D-Nle)

APPENDIX C

STRUCTURE OF AMINO ACIDS SUBSTITUTED AT POSITION 5

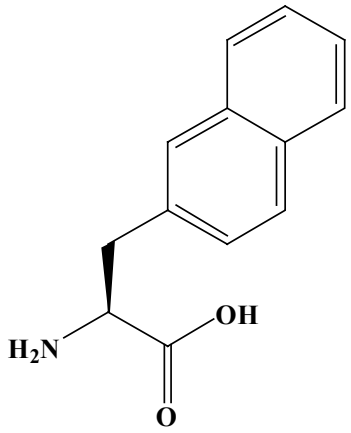

3-(2-Naphthyl)-L-alanine
(2-Nal)

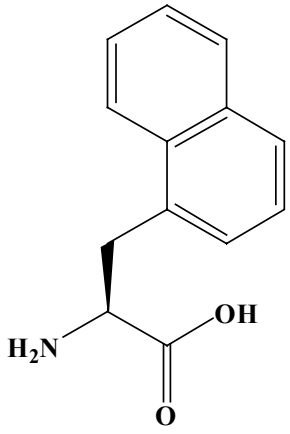

3-(1-Naphthyl)-L-alanine
(1-Nal)

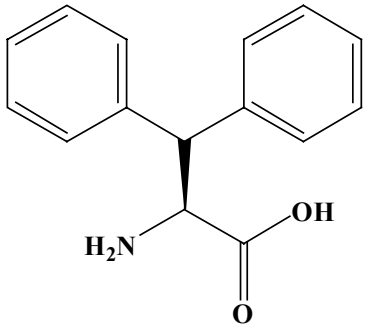

3,3-Diphenyl-L-alanine
(Dpa)

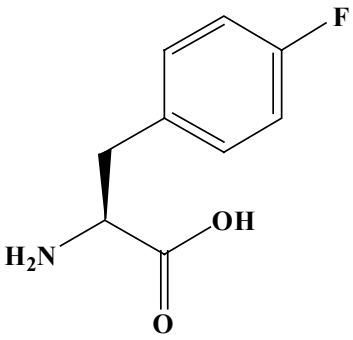

***p*-Fluorophenylalanine**
Phe(*p*-F)

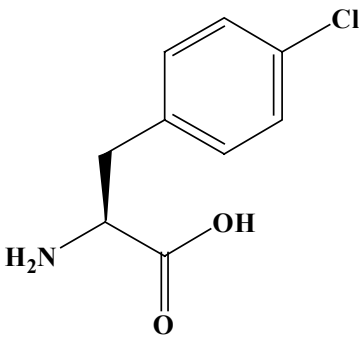

***p*-Chlorophenylalanine**
Phe(*p*-Cl)

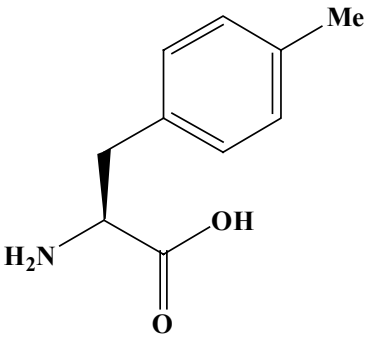

***p*-Methylphenylalanine**
Phe(*p*-Me)

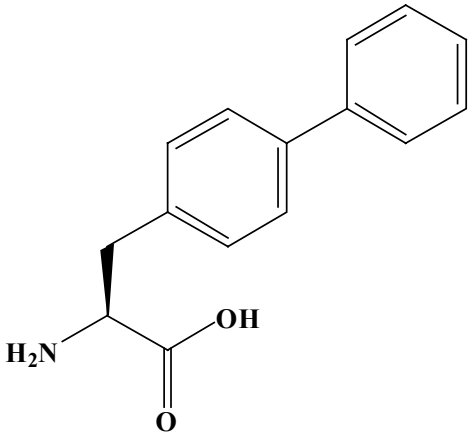

4.4'-Biphenyl-L-alanine
(Bip)

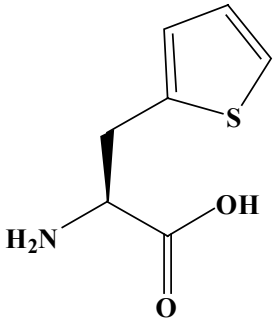

β-(2-Thienyl)-L-alanine
(Thi)

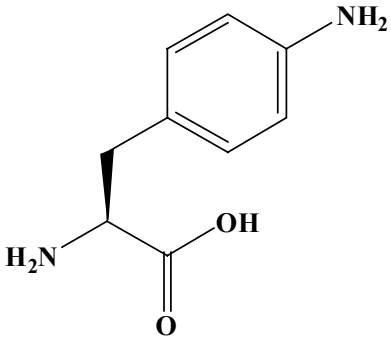

***p*-Aminophenylalanine**
Phe(*p*-NH2)

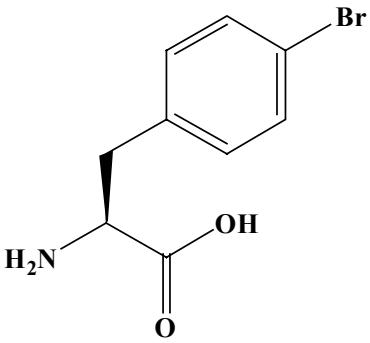

***p*-Bromophenylalanine**
Phe(*p*-Br)

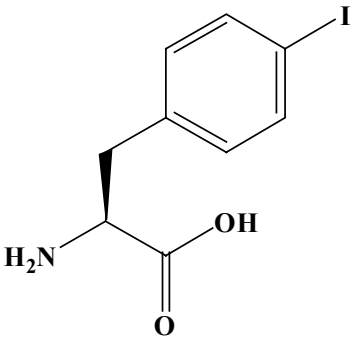

***p*-Iodophenylalanine**
Phe(*p*-I)

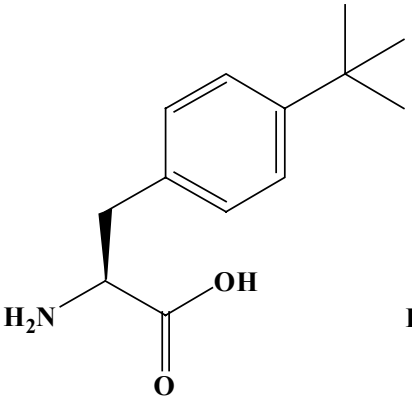

***p*-*t*-Butylphenylalanine**
Phe(*p*-*t*-Bu)

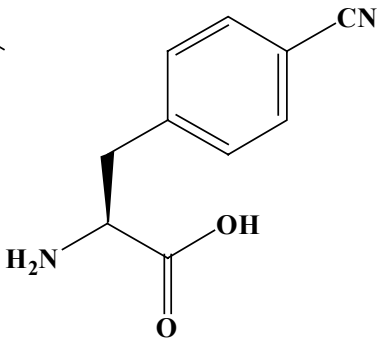

***p*-Cyanophenylalanine**
Phe(*p*-CN)

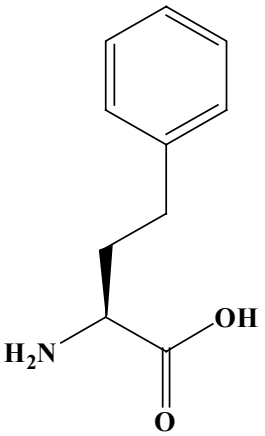

L-Homophenylalanine
(Hfe)

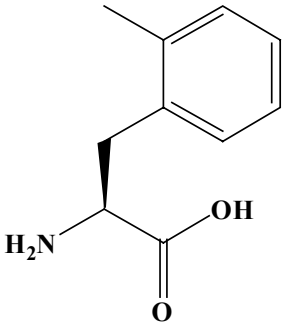

2-Methylphenylalanine
Phe(2-Me)

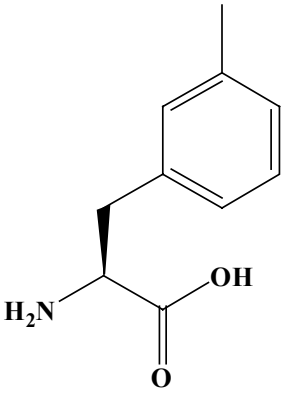

3-Methylphenylalanine
Phe(3-Me)

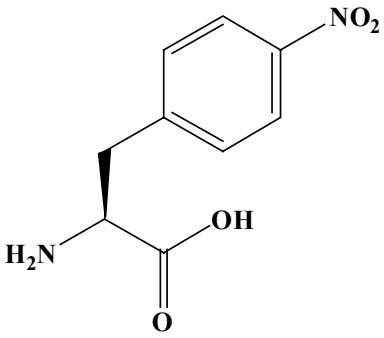

***p*-Nitrophenylalanine**
Phe(*p*-NO_2)

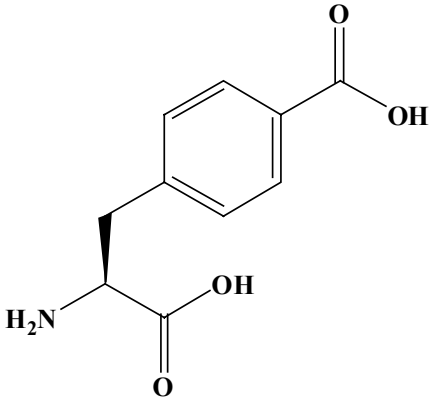

***p*-Carboxyphenylalanine**
Phe(*p*-COOH)

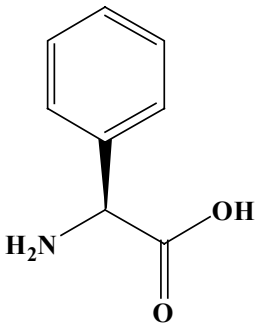

L-Phenylglycine
(Phg)

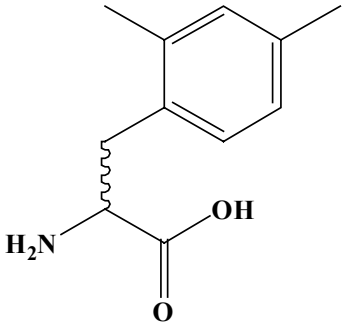

2,4-Dimethyl-LD-phenylalanine
Phe(2,4-DiMe)

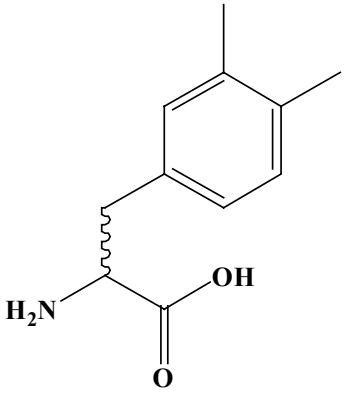

3,4-Dimethyl-LD-phenylalanine
Phe(3,4-DiMe)

Appendix D. Physicochemical Data for FM Analogs.

NAME	SEQUENCE	Cyclization	RP-HPLC Elution Time (min)	ESI-MS [M+H]+	Purity %
FM3	H-D-Arg-Oic-Pro-D-Ala-Arg-NH2	linear	13.6	635	99
FM4	H-D-Arg-Oic-Pro-D-Ala-Tyr-NH2	linear	18.2	642	99
FM5	Ac-D-Arg-Oic-Pro-D-Ala-Phe-NH2	linear	25.9	668	99
FM6	H-D-Arg-Oic-Pro-D-Gln-2-Nal-NH2	linear	28.1	748	99
FM7	H-D-Arg-Oic-Pro-D-Phe-2-Nal-NH2	linear	38.2	767	99
FM8	H-D-Arg-Oic-Pro-D-Ser-2-Nal-NH2	linear	29.6	707	99
FM9	H-D-Arg-Oic-Pro-D-Thr-2-Nal-NH2	linear	30.8	720	99
FM10	H-D-Arg-Oic-Pro-D-His-2-Nal-NH2	linear	27.2	758	100
FM11	H-D-Arg-Oic-Pro-β-Ala-2-Nal-NH2	linear	29.5	691	99
FM12	H-D-Arg-Oic-Pro-D-Asn-Dpa-NH2	linear	29.6	759	99
FM13	H-D-Arg-Oic-Cys-Gly-Phe-Cys-NH2	linear	28.6	735	97
FM13DC	H-D-Arg-Oic-Cys-Gly-Phe-Cys-NH2	linear	28.6	735	98
FM13DC/PEG	H-D-Arg-Oic-Cys-Gly-Phe-Cys-NH2	linear	28.6	735	100
FM13(SS)	H-D-Arg-Oic-c[Cys-Gly-Phe-Cys]-NH2	SS	24	733	99
FM13(S-Et-S)	H-D-Arg-Oic-c[Cys-Gly-Phe-Cys]-NH2	S-Et-S	31	761	97
FM14	H-D-Arg-Cys-Pro-Gly-Phe-Cys-NH2	linear	20.4	681	97
FM14DC/PEG	H-D-Arg-Cys-Pro-Gly-Phe-Cys-NH2	linear	20.4	681	99
FM14(SS)	H-D-Arg-c[Cys-Pro-Gly-Phe-Cys]-NH2	SS	17.6	679	99
FM14(S-Et-S)	H-D-Arg-c[Cys-Pro-Gly-Phe-Cys]-NH2	S-Et-S	26.7	707	99
FM15	H-Cys-D-Arg-Oic-Pro-Gly-Phe-Cys-NH2	linear	25.9	832	99
FM15(SS)	H-c[Cys-D-Arg-Oic-Pro-Gly-Phe-Cys]-NH2	SS	24.3	830	100
FM15(S-Et-S)	H-c[Cys-D-Arg-Oic-Pro-Gly-Phe-Cys]-NH2	S-Et-S	26.1	857	98
FM16	H-D-Arg-Oic-Pro-D-Ala-2-Nal-NH2	linear	22.6	690	98
FM17	H-D-Arg-Oic-Pro-D-Ala-Thi-NH2	linear	23.9	646	97

NAME	SEQUENCE	Cyclization	RP-HPLC Elution Time (min)	ESI-MS [M+H]+	Purity %
FM18	H-D-Arg-Oic-Pro-D-Ala-Bip-NH2	linear	33.9	717	99
FM19	H-D-Arg-Oic-Pro-D-Ala-Phe(*p* -Me)-NH2	linear	27.7	655	99
FM20	H-D-Arg-Oic-Pro-D-Ala-Phe(*p* -Cl)-NH2	linear	29.2	675	97
FM21	H-D-Arg-Oic-Pro-D-Gln-Phe-NH2	linear	22.3	698	99
FM22	H-D-Arg-Oic-Pro-D-Dab-Phe-NH2	linear	21.9	656	98
FM23	H-D-Arg-Oic-Pro-D-Dap-Phe-NH2	linear	21.3	670	99
FM24	H-D-Arg-Oic-Pro-D-Abu-Phe-NH2	linear	27.2	655	99
FM25	H-D-Arg-Oic-Pro-D-Orn-Phe-NH2	linear	21.4	684	99
FM26	H-D-Arg-Oic-Pro-D-Nle-Phe-NH2	linear	32.1	683	100
FM27	H-D-Arg-Oic-Pro-Gly-Phe(*p* -Me)-NH2	linear	26	641	99
FM28	H-D-Arg-Oic-Pro-D-Ala-Phe(*p* -F)-NH2	linear	26.3	659	99
FM29	H-D-Arg-Oic-Pro-D-Ser-Phe(*p* -Me)-NH2	linear	26.1	671	96
FM30	H-D-Arg-Oic-Pro-D-Asn-Phe(*p* -Me)-NH2	linear	28.8	698	99
FM31	H-D-Arg-Oic-Pro-D-Ala-Hfe-NH2	linear	30.2	655	98
FM32	H-D-Arg-Oic-Pro-D-Ala-Phe(*p* -NH2)-NH2	linear	14.5	656	99
FM33	H-D-Arg-Oic-Pro-D-Ala-Phe(*p* -Br)-NH2	linear	32.6	719	99
FM34	H-D-Arg-Oic-Pro-D-Ala-Phe(*p* -*t* Bu)-NH2	linear	37.6	697	100
FM35	H-D-Arg-Oic-Pro-D-Ala-Phe(*p* -CN)-NH2	linear	26.9	666	99
FM36	H-D-Arg-Oic-Pro-D-Ala-Phe(*p* -I)-NH2	linear	30.9	766	100
FM37	H-D-Arg-Oic-Pro-D-Ala-Phe(2-Me)-NH2	linear	30	655	98
FM38	H-D-Arg-Oic-Pro-D-Ala-Phe(3-Me)-NH2	linear	27.8	655	97
FM39	H-D-Arg-Oic-Pro-D-Ala-Phe(*p* -NO2)-NH2	linear	25.1	686	99
FM40	H-D-Arg-Oic-Pro-D-Ala-Phg-NH2	linear	23.3	627	100
FM41	H-D-Arg-Oic-Pro-D-Ala-Phe(*p* -Me)-Lys-NH2	linear	24.8	783	99

NAME	SEQUENCE	Cyclization	RP-HPLC Elution Time (min)	ESI-MS [M+H]+	Purity %
FM42	H-D-Arg-Oic-Pro-D-Ala-Phe(*p*-Me)-Lys(biotin)-NH2	linear	29.4	1009	97
FM43	H-Phe(*p*-Me)-Oic-D-Arg-Pro-D-Ala-NH2	linear	25.9	655	96
FM44	H-D-Ala-Pro-D-Arg-Oic-Phe(*p*-Me)-NH2	linear	32.1	655	97
FM45	H-Pro-D-Ala-Phe(*p*-Me)-D-Arg-Oic-NH2	linear	28.6	655	98
FM46	H-Pro-Phe(*p*-Me)-Oic-D-Arg-D-Ala-NH2	linear	27.3	655	100
FM47	H-Pro-D-Arg-D-Ala-Phe(*p*-Me)-Oic-NH2	linear	29.8	655	99
FM48	H-Pro-D-Arg-Oic-Phe(*p*-Me)-D-Ala-NH2	linear	31.5	655	98
FM49	H-Trp-Oic-Pro-D-Ala-Phe(*p*-Me)-NH2	linear	40.1	685	99
FM50	H-Trp-Pro-Pro-Gly-Phe-NH2	linear	ND	ND	ND
FM51	H-D-Glu-Oic-Pro-D-Ala-Phe(*p*-Me)-NH2	linear	30	627	96
FM52	H-D-Arg-Oic-Pro-D-Ala-Phe(*p*-COOH)-NH2	linear	23.9	684	99
FM53	H-D-Arg-Oic-Pro-D-Ala-Phe(*p*-Me)-NH-Me	linear	31.6	669	99
FM54a	H-D-Arg-Oic-Pro-D-Ala-D-Phe(2,4-DiMe)-NH2	linear	30.2	669	98
FM54b	H-D-Arg-Oic-Pro-D-Ala-Phe(2,4-DiMe)-NH2	linear	33.2	669	99
FM55a	H-D-Arg-Oic-Pro-D-Ala-D-Phe(2,3-DiMe)-NH2	linear	26.8	669	97
FM55b	H-D-Arg-Oic-Pro-D-Ala-Phe(2,3-DiMe)-NH2	linear	29.8	669	98
FM56	H-D-Arg-Oic-Pro-D-Ala-Phe(*p*-Me)-NH-Et	linear	29.4	682	99
FM57	H-Arg(Me)-Oic-Pro-D-Ala-Phe(*p*-Me)-NH2	linear	27.8	668	99
FM58	H-Arg(Me)-Pro-Oic-D-Ala-Phe(*p*-Me)-NH2	linear	30.9	668	96
FM59	H-D-Arg(Me)-Oic-Pro-D-Ala-Phe(*p*-Me)-NH2	linear	31.6	669	96
FM61	H-D-Arg-Oic-Pro-D-Ala-Phe(*p*-Me)-Lys(5-FAM)-NH2	linear	38.5	1141	99

Appendix E. Platelet Aggregation Data for FM Analogs.

NAME	SEQUENCE	Cyclization	ESI-MS [M+H]+	100% Inhibition of Threshold γ-Thrombin-Induced Platelet Aggregation (μM)
FM3	H-D-Arg-Oic-Pro-D-Ala-Arg-NH2	linear	635	NE
FM4	H-D-Arg-Oic-Pro-D-Ala-Tyr-NH2	linear	642	300
FM5	Ac-D-Arg-Oic-Pro-D-Ala-Phe-NH2	linear	668	NE
FM6	H-D-Arg-Oic-Pro-D-Gln-2-Nal-NH2	linear	748	83
FM7	H-D-Arg-Oic-Pro-D-Phe-2-Nal-NH2	linear	767	83
FM8	H-D-Arg-Oic-Pro-D-Ser-2-Nal-NH2	linear	707	56
FM9	H-D-Arg-Oic-Pro-D-Thr-2-Nal-NH2	linear	720	75
FM10	H-D-Arg-Oic-Pro-D-His-2-Nal-NH2	linear	758	75
FM11	H-D-Arg-Oic-Pro-β-Ala-2-Nal-NH2	linear	691	675
FM12	H-D-Arg-Oic-Pro-D-Asn-Dpa-NH2	linear	759	1,000
FM13	H-D-Arg-Oic-Cys-Gly-Phe-Cys-NH2	linear	735	ND
FM13DC	H-D-Arg-Oic-Cys-Gly-Phe-Cys-NH2	linear	735	ND
FM13DC/PEG	H-D-Arg-Oic-Cys-Gly-Phe-Cys-NH2	linear	735	ND
FM13(SS)	H-D-Arg-Oic-c[Cys-Gly-Phe-Cys]-NH2	SS	733	1,000
FM13(S-Et-S)	H-D-Arg-Oic-c[Cys-Gly-Phe-Cys]-NH2	S-Et-S	761	ND
FM14	H-D-Arg-Cys-Pro-Gly-Phe-Cys-NH2	linear	681	ND
FM14DC/PEG	H-D-Arg-Cys-Pro-Gly-Phe-Cys-NH2	linear	681	ND
FM14(SS)	H-D-Arg-c[Cys-Pro-Gly-Phe-Cys]-NH2	SS	679	733
FM14(S-Et-S)	H-D-Arg-c[Cys-Pro-Gly-Phe-Cys]-NH2	S-Et-S	707	ND
FM15	H-Cys-D-Arg-Oic-Pro-Gly-Phe-Cys-NH2	linear	832	ND
FM15(SS)	H-c[Cys-D-Arg-Oic-Pro-Gly-Phe-Cys]-NH2	SS	830	550
FM15(S-Et-S)	H-c[Cys-D-Arg-Oic-Pro-Gly-Phe-Cys]-NH2	S-Et-S	857	ND
FM16	H-D-Arg-Oic-Pro-D-Ala-2-Nal-NH2	linear	690	100
FM17	H-D-Arg-Oic-Pro-D-Ala-Thi-NH2	linear	646	250

NAME	SEQUENCE	Cyclization	ESI-MS [M+H]+	100% Inhibition of Threshold γ-Thrombin-Induced Platelet Aggregation (μM)
FM18	H-D-Arg-Oic-Pro-D-Ala-Bip-NH2	linear	717	200
FM19	H-D-Arg-Oic-Pro-D-Ala-Phe(*p* -Me)-NH2	linear	655	16
FM20	H-D-Arg-Oic-Pro-D-Ala-Phe(*p* -Cl)-NH2	linear	675	44
FM21	H-D-Arg-Oic-Pro-D-Gln-Phe-NH2	linear	698	400
FM22	H-D-Arg-Oic-Pro-D-Dab-Phe-NH2	linear	656	175
FM23	H-D-Arg-Oic-Pro-D-Dap-Phe-NH2	linear	670	175
FM24	H-D-Arg-Oic-Pro-D-Abu-Phe-NH2	linear	655	275
FM25	H-D-Arg-Oic-Pro-D-Orn-Phe-NH2	linear	684	250
FM26	H-D-Arg-Oic-Pro-D-Nle-Phe-NH2	linear	683	275
FM27	H-D-Arg-Oic-Pro-Gly-Phe(*p* -Me)-NH2	linear	641	120
FM28	H-D-Arg-Oic-Pro-D-Ala-Phe(*p* -F)-NH2	linear	659	200
FM29	H-D-Arg-Oic-Pro-D-Ser-Phe(*p* -Me)-NH2	linear	671	13
FM30	H-D-Arg-Oic-Pro-D-Asn-Phe(*p* -Me)-NH2	linear	698	64
FM31	H-D-Arg-Oic-Pro-D-Ala-Hfe-NH2	linear	655	128
FM32	H-D-Arg-Oic-Pro-D-Ala-Phe(*p* -NH2)-NH2	linear	656	128
FM33	H-D-Arg-Oic-Pro-D-Ala-Phe(*p* -Br)-NH2	linear	719	18
FM34	H-D-Arg-Oic-Pro-D-Ala-Phe(*p* -*t* Bu)-NH2	linear	697	32
FM35	H-D-Arg-Oic-Pro-D-Ala-Phe(*p* -CN)-NH2	linear	666	32
FM36	H-D-Arg-Oic-Pro-D-Ala-Phe(*p* -I)-NH2	linear	766	16
FM37	H-D-Arg-Oic-Pro-D-Ala-Phe(2-Me)-NH2	linear	655	32
FM38	H-D-Arg-Oic-Pro-D-Ala-Phe(3-Me)-NH2	linear	655	64
FM39	H-D-Arg-Oic-Pro-D-Ala-Phe(*p* -NO2)-NH2	linear	686	48
FM40	H-D-Arg-Oic-Pro-D-Ala-Phg-NH2	linear	627	32
FM41	H-D-Arg-Oic-Pro-D-Ala-Phe(*p* -Me)-Lys-NH2	linear	783	ND

NAME	SEQUENCE	Cyclization	ESI-MS [M+H]+	100% Inhibition of Threshold γ-Thrombin-Induced Platelet Aggregation (μM)
FM42	H-D-Arg-Oic-Pro-D-Ala-Phe(*p*-Me)-Lys(biotin)-NH2	linear	1009	24
FM43	H-Phe(*p*-Me)-Oic-D-Arg-Pro-D-Ala-NH2	linear	655	NE
FM44	H-D-Ala-Pro-D-Arg-Oic-Phe(*p*-Me)-NH2	linear	655	NE
FM45	H-Pro-D-Ala-Phe(*p*-Me)-D-Arg-Oic-NH2	linear	655	NE
FM46	H-Pro-Phe(*p*-Me)-Oic-D-Arg-D-Ala-NH2	linear	655	150
FM47	H-Pro-D-Arg-D-Ala-Phe(*p*-Me)-Oic-NH2	linear	655	NE
FM48	H-Pro-D-Arg-Oic-Phe(*p*-Me)-D-Ala-NH2	linear	655	NE
FM49	H-Trp-Oic-Pro-D-Ala-Phe(*p*-Me)-NH2	linear	685	ND
FM50	H-Trp-Pro-Pro-Gly-Phe-NH2	linear	ND	ND
FM51	H-D-Glu-Oic-Pro-D-Ala-Phe(*p*-Me)-NH2	linear	627	ND
FM52	H-D-Arg-Oic-Pro-D-Ala-Phe(*p*-COOH)-NH2	linear	684	560
FM53	H-D-Arg-Oic-Pro-D-Ala-Phe(*p*-Me)-NH-Me	linear	669	21
FM54a	H-D-Arg-Oic-Pro-D-Ala-D-Phe(2,4-DiMe)-NH2	linear	669	100
FM54b	H-D-Arg-Oic-Pro-D-Ala-Phe(2,4-DiMe)-NH2	linear	669	28
FM55a	H-D-Arg-Oic-Pro-D-Ala-D-Phe(2,3-DiMe)-NH2	linear	669	750
FM55b	H-D-Arg-Oic-Pro-D-Ala-Phe(2,3-DiMe)-NH2	linear	669	62
FM56	H-D-Arg-Oic-Pro-D-Ala-Phe(*p*-Me)-NH-Et	linear	682	5
FM57	H-Arg(Me)-Oic-Pro-D-Ala-Phe(*p*-Me)-NH2	linear	668	833
FM58	H-Arg(Me)-Pro-Oic-D-Ala-Phe(*p*-Me)-NH2	linear	668	NE
FM59	H-D-Arg(Me)-Oic-Pro-D-Ala-Phe(*p*-Me)-NH2	linear	669	1,000
FM61	H-D-Arg-Oic-Pro-D-Ala-Phe(*p*-Me)-Lys(5-FAM)-NH2	linear	1141	28

REFERENCES

REFERENCES

1. Paoli, G., Merlini, P.A., and Ardissino, D., *Direct thrombin inhibitors for the treatment of acute coronary syndromes and during percutaneous coronary interventions.* Current Pharmaceutical Design, 2005. **11**(30): p. 3919-29.

2. Rauch, U., Osende, J.I., Fuster, V., Badimon, J.J., Fayad, Z., and Chesebro, J.H., *Thrombus formation on atherosclerotic plaques: pathogenesis and clinical consequences.* Ann Intern Med, 2001. **134**(3): p. 224-38.

3. Rosamond, W., Flegal, K., Friday, G., Furie, K., Go, A., Greenlund, K., Haase, N., Ho, M., Howard, V., Kissela, B., Kittner, S., Lloyd-Jones, D., McDermott, M., Meigs, J., Moy, C., Nichol, G., O'Donnell, C.J., Roger, V., Rumsfeld, J., Sorlie, P., Steinberger, J., Thom, T., Wasserthiel-Smoller, S., and Hong, Y., *Heart disease and stroke statistics--2007 update: a report from the American Heart Association Statistics Committee and Stroke Statistics Subcommittee.* Circulation, 2007. **115**(5): p. e69-171.

4. Yang, E.H., Brilakis, E.S., Reeder, G.S., and Gersh, B.J., *Modern management of acute myocardial infarction.* Curr Probl Cardiol, 2006. **31**(12): p. 769-817.

5. Gustafsson, D., Bylund, R., Antonsson, T., Nilsson, I., Nystrom, J.E., Eriksson, U., Bredberg, U., and Teger-Nilsson, A.C., *A new oral anticoagulant: the 50-year challenge.* Nat Rev Drug Discov, 2004. **3**(8): p. 649-59.

6. Fang, J. and Alderman, M.H., *Dissociation of hospitalization and mortality trends for myocardial infarction in the United States from 1988 to 1997.* Am J Med, 2002. **113**(3): p. 208-14.

7. Nordstrom, M., Lindblad, B., Bergqvist, D., and Kjellstrom, T., *A prospective study of the incidence of deep-vein thrombosis within a defined urban population.* J Intern Med, 1992. **232**(2): p. 155-60.

8. Daly, E., Vessey, M.P., Hawkins, M.M., Carson, J.L., Gough, P., and Marsh, S., *Risk of venous thromboembolism in users of hormone replacement therapy.* Lancet, 1996. **348**(9033): p. 977-80.

9. Lefkovits, J. and Topol, E.J., *Direct thrombin inhibitors in cardiovascular medicine.* Circulation, 1994. **90**(3): p. 1522-36.

10. Kissela, B., Broderick, J., Woo, D., Kothari, R., Miller, R., Khoury, J., Brott, T., Pancioli, A., Jauch, E., Gebel, J., Shukla, R., Alwell, K., and Tomsick, T.,

Greater Cincinnati/Northern Kentucky Stroke Study: volume of first-ever ischemic stroke among blacks in a population-based study. Stroke, 2001. **32**(6): p. 1285-90.

11. Leary, M.C. and Saver, J.L., *Annual incidence of first silent stroke in the United States: a preliminary estimate.* Cerebrovasc Dis, 2003. **16**(3): p. 280-5.

12. Kelley, R.E. and Minagar, A., *Cardioembolic stroke: an update.* South Med J, 2003. **96**(4): p. 343-9.

13. Murtagh, B. and Smalling, R.W., *Cardioembolic stroke.* Curr Atheroscler Rep, 2006. **8**(4): p. 310-6.

14. Di Tullio, M.R. and Homma, S., *Mechanisms of cardioembolic stroke.* Curr Cardiol Rep, 2002. **4**(2): p. 141-8.

15. Ohira, T., Shahar, E., Chambless, L.E., Rosamond, W.D., Mosley, T.H., Jr., and Folsom, A.R., *Risk factors for ischemic stroke subtypes: the Atherosclerosis Risk in Communities study.* Stroke, 2006. **37**(10): p. 2493-8.

16. Schmaier, A.H. and Petruzzelli, L.M., *Hematology for medical students*. 2003, Philadelphia: Lippincott Williams & Wilkins. 71-125.

17. Walsh, P.N. and Ahmad, S.S., *Proteases in blood clotting.* Essays Biochem, 2002. **38**: p. 95-111.

18. Nylander, S. and Mattsson, C., *Thrombin-induced platelet activation and its inhibition by anticoagulants with different modes of action.* Blood Coagul Fibrinolysis, 2003. **14**(2): p. 159-67.

19. Huntington, J.A. and Baglin, T.P., *Targeting thrombin--rational drug design from natural mechanisms.* Trends Pharmacol Sci, 2003. **24**(11): p. 589-95.

20. De Cristofaro, R. and De Candia, E., *Thrombin domains: structure, function and interaction with platelet receptors.* J Thromb Thrombolysis, 2003. **15**(3): p. 151-63.

21. Roth, G.J., *A new "kid" on the platelet thrombin receptor "block": glycoprotein Ib-IX-V.* Proc Natl Acad Sci U S A, 2001. **98**(4): p. 1330-1.

22. Di Cera, E., Dang, Q.D., and Ayala, Y.M., *Molecular mechanisms of thrombin function.* Cell Mol Life Sci, 1997. **53**(9): p. 701-30.

23. Stubbs, M.T. and Bode, W., *The clot thickens: clues provided by thrombin structure.* Trends Biochem Sci, 1995. **20**(1): p. 23-8.

24. Spronk, H.M., Govers-Riemslag, J.W., and ten Cate, H., *The blood coagulation system as a molecular machine.* Bioessays, 2003. **25**(12): p. 1220-8.

25. Levi, M., Keller, T.T., van Gorp, E., and ten Cate, H., *Infection and inflammation and the coagulation system.* Cardiovasc Res, 2003. **60**(1): p. 26-39.

26. Fuentes-Prior, P., Iwanaga, Y., Huber, R., Pagila, R., Rumennik, G., Seto, M., Morser, J., Light, D.R., and Bode, W., *Structural basis for the anticoagulant activity of the thrombin-thrombomodulin complex.* Nature, 2000. **404**(6777): p. 518-25.

27. Chung, A.W., Jurasz, P., Hollenberg, M.D., and Radomski, M.W., *Mechanisms of action of proteinase-activated receptor agonists on human platelets.* Br J Pharmacol, 2002. **135**(5): p. 1123-32.

28. Sambrano, G.R., Weiss, E.J., Zheng, Y.W., Huang, W., and Coughlin, S.R., *Role of thrombin signalling in platelets in haemostasis and thrombosis.* Nature, 2001. **413**(6851): p. 74-8.

29. Dormann, D., Clemetson, K.J., and Kehrel, B.E., *The GPIb thrombin-binding site is essential for thrombin-induced platelet procoagulant activity.* Blood, 2000. **96**(7): p. 2469-78.

30. Callahan, K.P., Malinin, A.I., Gurbel, P.A., Alexander, J.H., Granger, C.B., and Serebruany, V.L., *Platelet function and fibrinolytic agents: two sides of a coin?* Cardiology, 2001. **95**(2): p. 55-60.

31. Coughlin, S.R., *Thrombin signalling and protease-activated receptors.* Nature, 2000. **407**(6801): p. 258-64.

32. Cottrell, G.S., Coelho, A.M., and Bunnett, N.W., *Protease-activated receptors: the role of cell-surface proteolysis in signalling.* Essays Biochem, 2002. **38**: p. 169-83.

33. Derian, C.K., Damiano, B.P., D'Andrea, M.R., and Andrade-Gordon, P., *Thrombin regulation of cell function through protease-activated receptors: implications for therapeutic intervention.* Biochemistry (Mosc), 2002. **67**(1): p. 56-64.

34. O'Brien, P.J., Molino, M., Kahn, M., and Brass, L.F., *Protease activated receptors: theme and variations.* Oncogene, 2001. **20**(13): p. 1570-81.

35. Mackie, E.J., Pagel, C.N., Smith, R., de Niese, M.R., Song, S.J., and Pike, R.N., *Protease-activated receptors: a means of converting extracellular proteolysis into intracellular signals.* IUBMB Life, 2002. **53**(6): p. 277-81.

36. Ossovskaya, V.S. and Bunnett, N.W., *Protease-activated receptors: contribution to physiology and disease.* Physiol Rev, 2004. **84**(2): p. 579-621.

37. Bretschneider, E., Spanbroek, R., Lotzer, K., Habenicht, A.J., and Schror, K., *Evidence for functionally active protease-activated receptor-3 (PAR-3) in human vascular smooth muscle cells.* Thromb Haemost, 2003. **90**(4): p. 704-9.

38. Kahn, M.L., Zheng, Y.W., Huang, W., Bigornia, V., Zeng, D., Moff, S., Farese, R.V., Jr., Tam, C., and Coughlin, S.R., *A dual thrombin receptor system for platelet activation.* Nature, 1998. **394**(6694): p. 690-4.

39. Covic, L., Gresser, A.L., and Kuliopulos, A., *Biphasic kinetics of activation and signaling for PAR1 and PAR4 thrombin receptors in platelets.* Biochemistry, 2000. **39**(18): p. 5458-67.

40. Henriksen, R.A. and Hanks, V.K., *PAR-4 agonist AYPGKF stimulates thromboxane production by human platelets.* Arterioscler Thromb Vasc Biol, 2002. **22**(5): p. 861-6.

41. Hou, L., Howells, G.L., Kapas, S., and Macey, M.G., *The protease-activated receptors and their cellular expression and function in blood-related cells.* Br J Haematol, 1998. **101**(1): p. 1-9.

42. Jacques, S.L. and Kuliopulos, A., *Protease-activated receptor-4 uses dual prolines and an anionic retention motif for thrombin recognition and cleavage.* Biochem J, 2003. **376**(Pt 3): p. 733-40.

43. Hollenberg, M.D., *Proteinase-mediated signaling: proteinase-activated receptors (PARs) and much more.* Life Sci, 2003. **74**(2-3): p. 237-46.

44. Cleary, D.B., Trumbo, T.A., and Maurer, M.C., *Protease-activated receptor 4-like peptides bind to thrombin through an optimized interaction with the enzyme active site surface.* Arch Biochem Biophys, 2002. **403**(2): p. 179-88.

45. Grand, R.J., Turnell, A.S., and Grabham, P.W., *Cellular consequences of thrombin-receptor activation.* Biochem J, 1996. **313 (Pt 2)**: p. 353-68.

46. Turner, J.S., Redpath, G.T., Humphries, J.E., Gonias, S.L., and Vandenberg, S.R., *Plasmin modulates the thrombin-evoked calcium response in C6 glioma cells.* Biochem J, 1994. **297 (Pt 1)**: p. 175-9.

47. Kuliopulos, A., Covic, L., Seeley, S.K., Sheridan, P.J., Helin, J., and Costello, C.E., *Plasmin desensitization of the PAR1 thrombin receptor: kinetics, sites of truncation, and implications for thrombolytic therapy.* Biochemistry, 1999. **38**(14): p. 4572-85.

48. Hirsh, J., *Current anticoagulant therapy--unmet clinical needs.* Thromb Res, 2003. **109 Suppl 1**: p. S1-8.

49. Fareed, J., Hoppensteadt, D.A., and Bick, R.L., *Management of thrombotic and cardiovascular disorders in the new millenium.* Clin Appl Thromb Hemost, 2003. **9**(2): p. 101-8.

50. Bjork, I. and Lindahl, U., *Mechanism of the anticoagulant action of heparin.* Mol Cell Biochem, 1982. **48**(3): p. 161-82.

51. Linhardt, R.J., *Heparin: an important drug enters its seventh decade.* Chemistry and Industry, 1991. **2**: p. 45-50.

52. Hull, R.D. and Pineo, G.F., *Heparin and low-molecular-weight heparin therapy for venous thromboembolism: will unfractionated heparin survive?* Semin Thromb Hemost, 2004. **30 Suppl 1**: p. 11-23.

53. Stone, S.R. and Hofsteenge, J., *Kinetics of the inhibition of thrombin by hirudin.* Biochemistry, 1986. **25**(16): p. 4622-8.

54. Markwardt, F., *Hirudin as alternative anticoagulant--a historical review.* Semin Thromb Hemost, 2002. **28**(5): p. 405-14.

55. Rydel, T.J., Ravichandran, K.G., Tulinsky, A., Bode, W., Huber, R., Roitsch, C., and Fenton, J.W., 2nd, *The structure of a complex of recombinant hirudin and human alpha-thrombin.* Science, 1990. **249**(4966): p. 277-80.

56. Bates, S.M. and Weitz, J.I., *Direct thrombin inhibitors for treatment of arterial thrombosis: potential differences between bivalirudin and hirudin.* Am J Cardiol, 1998. **82**(8B): p. 12P-18P.

57. Carswell, C.I. and Plosker, G.L., *Bivalirudin: a review of its potential place in the management of acute coronary syndromes.* Drugs, 2002. **62**(5): p. 841-70.

58. Hirsh, J., O'Donnell, M., and Weitz, J.I., *New anticoagulants.* Blood, 2005. **105**(2): p. 453-63.

59. Gustafsson, D. and Elg, M., *The pharmacodynamics and pharmacokinetics of the oral direct thrombin inhibitor ximelagatran and its active metabolite melagatran: a mini-review.* Thromb Res, 2003. **109 Suppl 1**: p. S9-15.

60. Mlinsek, G., Oblak, M., Hodoscek, M., and Solmajer, T., *Thrombin inhibitors with novel P1 binding pocket functionality: free energy of binding analysis.* J Mol Model, 2007. **13**(1): p. 247-54.

61. Gustafsson, D., Nystrom, J., Carlsson, S., Bredberg, U., Eriksson, U., Gyzander, E., Elg, M., Antonsson, T., Hoffmann, K., Ungell, A., Sorensen, H., Nagard, S., Abrahamsson, A., and Bylund, R., *The direct thrombin inhibitor melagatran and its oral prodrug H 376/95: intestinal absorption properties, biochemical and pharmacodynamic effects.* Thromb Res, 2001. **101**(3): p. 171-81.

62. Eriksson, U.G., Bredberg, U., Hoffmann, K.J., Thuresson, A., Gabrielsson, M., Ericsson, H., Ahnoff, M., Gislen, K., Fager, G., and Gustafsson, D., *Absorption, distribution, metabolism, and excretion of ximelagatran, an oral direct thrombin inhibitor, in rats, dogs, and humans.* Drug Metab Dispos, 2003. **31**(3): p. 294-305.

63. Choudhury, A., Goyal, D., and Lip, G.Y., *Ximelagatran.* Drugs Today (Barc), 2006. **42**(1): p. 3-19.

64. Hrebickova, L., Nawarskas, J.J., and Anderson, J.R., *Ximelagatran: a new oral anticoagulant.* Heart Dis, 2003. **5**(6): p. 397-408.

65. Gulseth, M.P., *Ximelagatran: an orally active direct thrombin inhibitor.* Am J Health Syst Pharm, 2005. **62**(14): p. 1451-67.

66. Ray, A., Hegde, L.G., and Gupta, J.B., *Thrombin receptor: a novel target for antiplatelet drug development.* Thromb Res, 1997. **87**(1): p. 37-50.

67. Chackalamannil, S., *G-protein coupled receptor antagonists-1: protease activated receptor-1 (PAR-1) antagonists as novel cardiovascular therapeutic agents.* Curr Top Med Chem, 2003. **3**(10): p. 1115-23.

68. Fujita, T., Nakajima, M., Inoue, Y., Nose, T., and Shimohigashi, Y., *A novel molecular design of thrombin receptor antagonist.* Bioorg Med Chem Lett, 1999. **9**(10): p. 1351-6.

69. Kato, Y., Kita, Y., Nishio, M., Hirasawa, Y., Ito, K., Yamanaka, T., Motoyama, Y., and Seki, J., *In vitro antiplatelet profile of FR171113, a novel non-peptide thrombin receptor antagonist.* Eur J Pharmacol, 1999. **384**(2-3): p. 197-202.

70. Ahn, H.S., Chackalamannil, S., Boykow, G., Graziano, M.P., and Foster, C., *Development of proteinase-activated receptor 1 antagonists as therapeutic agents for thrombosis, restenosis and inflammatory diseases.* Curr Pharm Des, 2003. **9**(28): p. 2349-65.

71. Clasby, M.C., Chackalamannil, S., Czarniecki, M., Doller, D., Eagen, K., Greenlee, W.J., Lin, Y., Tsai, H., Xia, Y., Ahn, H.S., Agans-Fantuzzi, J., Boykow, G., Chintala, M., Foster, C., Bryant, M., and Lau, J., *Discovery and synthesis of a novel series of quinoline-based thrombin receptor (PAR-1) antagonists.* Bioorg Med Chem Lett, 2006. **16**(6): p. 1544-8.

72. Chackalamannil, S., Xia, Y., Greenlee, W.J., Clasby, M., Doller, D., Tsai, H., Asberom, T., Czarniecki, M., Ahn, H.S., Boykow, G., Foster, C., Agans-Fantuzzi, J., Bryant, M., Lau, J., and Chintala, M., *Discovery of potent orally active thrombin receptor (protease activated receptor 1) antagonists as novel antithrombotic agents.* J Med Chem, 2005. **48**(19): p. 5884-7.

73. Derian, C.K., Maryanoff, B.E., Zhang, H.C., and Andrade-Gordon, P., *Therapeutic potential of protease-activated receptor-1 antagonists.* Expert Opin Investig Drugs, 2003. **12**(2): p. 209-21.

74. Derian, C.K., Damiano, B.P., Addo, M.F., Darrow, A.L., D'Andrea, M.R., Nedelman, M., Zhang, H.C., Maryanoff, B.E., and Andrade-Gordon, P., *Blockade of the thrombin receptor protease-activated receptor-1 with a small-molecule antagonist prevents thrombus formation and vascular occlusion in nonhuman primates.* J Pharmacol Exp Ther, 2003. **304**(2): p. 855-61.

75. Meloni, F.J. and Schmaier, A.H., *Low molecular weight kininogen binds to platelets to modulate thrombin-induced platelet activation.* J Biol Chem, 1991. **266**(11): p. 6786-94.

76. Colman, R.W., White, J.V., Scovell, S., Stadnicki, A., and Sartor, R.B., *Kininogens are antithrombotic proteins In vivo.* Arterioscler Thromb Vasc Biol, 1999. **19**(9): p. 2245-50.

77. Chavakis, T., Boeckel, N., Santoso, S., Voss, R., Isordia-Salas, I., Pixley, R.A., Morgenstern, E., Colman, R.W., and Preissner, K.T., *Inhibition of platelet adhesion and aggregation by a defined region (Gly-486-Lys-502) of high molecular weight kininogen.* J Biol Chem, 2002. **277**(26): p. 23157-64.

78. Puri, R.N., Zhou, F., Hu, C.J., Colman, R.F., and Colman, R.W., *High molecular weight kininogen inhibits thrombin-induced platelet aggregation and cleavage of aggregin by inhibiting binding of thrombin to platelets.* Blood, 1991. **77**(3): p. 500-7.

79. Hasan, A.A., Amenta, S., and Schmaier, A.H., *Bradykinin and its metabolite, Arg-Pro-Pro-Gly-Phe, are selective inhibitors of alpha-thrombin-induced platelet activation.* Circulation, 1996. **94**(3): p. 517-28.

80. Hasan, A.A., Warnock, M., Srikanth, S., and Schmaier, A.H., *Developing peptide inhibitors to thrombin activation of platelets from bradykinin analogs.* Thromb Res, 2001. **104**(6): p. 451-65.

81. Hasan, A.A., Warnock, M., Nieman, M., Srikanth, S., Mahdi, F., Krishnan, R., Tulinsky, A., and Schmaier, A.H., *Mechanisms of Arg-Pro-Pro-Gly-Phe inhibition of thrombin.* Am J Physiol Heart Circ Physiol, 2003. **285**(1): p. H183-93.

82. Quinn, M.J. and Fitzgerald, D.J., *Ticlopidine and clopidogrel.* Circulation, 1999. **100**(15): p. 1667-72.

83. Bhatt, D.L., Chew, D.P., Hirsch, A.T., Ringleb, P.A., Hacke, W., and Topol, E.J., *Superiority of clopidogrel versus aspirin in patients with prior cardiac surgery.* Circulation, 2001. **103**(3): p. 363-8.

84. Bhatt, D.L., Marso, S.P., Hirsch, A.T., Ringleb, P.A., Hacke, W., and Topol, E.J., *Amplified benefit of clopidogrel versus aspirin in patients with diabetes mellitus.* Am J Cardiol, 2002. **90**(6): p. 625-8.

85. Latham, P.W., *Therapeutic peptides revisited.* Nat Biotechnol, 1999. **17**(8): p. 755-7.

86. Yang, C.Y., Dantzig, A.H., and Pidgeon, C., *Intestinal peptide transport systems and oral drug availability.* Pharm Res, 1999. **16**(9): p. 1331-43.

87. Sadrzadeh, N., Glembourtt, M.J., and Stevenson, C.L., *Peptide drug delivery strategies for the treatment of diabetes.* J Pharm Sci, 2007.

88. Bjork, E., Isaksson, U., Edman, P., and Artursson, P., *Starch microspheres induce pulsatile delivery of drugs and peptides across the epithelial barrier by reversible separation of the tight junctions.* J Drug Target, 1995. **2**(6): p. 501-7.

89. *Recent patent applications relating to peptide therapeutics.* Nat Biotechnol, 2006. **24**(6): p. 656.

90. Marx, V., *Watching peptide drugs grow up.* chemistry & engineering news, 2005. **83**: p. 17-24.

91. Lalezari, J.P., Henry, K., O'Hearn, M., Montaner, J.S., Piliero, P.J., Trottier, B., Walmsley, S., Cohen, C., Kuritzkes, D.R., Eron, J.J., Jr., Chung, J., DeMasi, R., Donatacci, L., Drobnes, C., Delehanty, J., and Salgo, M., *Enfuvirtide, an HIV-1 fusion inhibitor, for drug-resistant HIV infection in North and South America.* N Engl J Med, 2003. **348**(22): p. 2175-85.

92. Nieman, M.T., Warnock, M., Hasan, A.A., Mahdi, F., Lucchesi, B.R., Brown, N.J., Murphey, L.J., and Schmaier, A.H., *The preparation and characterization of novel peptide antagonists to thrombin and factor VIIa and activation of protease-activated receptor 1.* J Pharmacol Exp Ther, 2004. **311**(2): p. 492-501.

93. Lembeck, F., Griesbacher, T., Eckhardt, M., Henke, S., Breipohl, G., and Knolle, J., *New, long-acting, potent bradykinin antagonists.* Br J Pharmacol, 1991. **102**(2): p. 297-304.

94. Stewart, J.M., *Bradykinin antagonists: discovery and development.* Peptides, 2004. **25**(3): p. 527-32.

95. Burke, F.M., Warnock, M., Schmaier, A.H., and Mosberg, H.I., *Synthesis of novel peptide inhibitors of thrombin-induced platelet activation.* Chem Biol Drug Des, 2006. **68**(5): p. 235-8.

96. Brass, S., *Cardiovascular biology. Platelets and proteases.* Nature, 2001. **413**(6851): p. 26-7.

97. Dubois, C., Panicot-Dubois, L., Gainor, J.F., Furie, B.C., and Furie, B., *Thrombin-initiated platelet activation in vivo is vWF independent during thrombus formation in a laser injury model.* J Clin Invest, 2007. **117**(4): p. 953-60.

98. Mazharian, A., Roger, S., Berrou, E., Adam, F., Kauskot, A., Nurden, P., Jandrot-Perrus, M., and Bryckaert, M., *Protease-activating receptor-4 induces full platelet spreading on a fibrinogen matrix: involvement of ERK2 and p38 and Ca2+ mobilization.* J Biol Chem, 2007. **282**(8): p. 5478-87.

99. Purves, R.D., *Optimum numerical integration methods for estimation of area-under-the-curve (AUC) and area-under-the-moment-curve (AUMC).* J Pharmacokinet Biopharm, 1992. **20**(3): p. 211-26.

100. Yeh, K.C. and Kwan, K.C., *A comparison of numerical integrating algorithms by trapezoidal, Lagrange, and spline approximation.* J Pharmacokinet Biopharm, 1978. **6**(1): p. 79-98.

101. Mochalkin, I. and Tulinsky, A., *Structures of thrombin retro-inhibited with SEL2711 and SEL2770 as they relate to factor Xa binding.* Acta Crystallogr D Biol Crystallogr, 1999. **55**(Pt 4): p. 785-93.

102. Matthews, J.H., Krishnan, R., Costanzo, M.J., Maryanoff, B.E., and Tulinsky, A., *Crystal structures of thrombin with thiazole-containing inhibitors: probes of the S1' binding site.* Biophys J, 1996. **71**(5): p. 2830-9.

103. Kennedy, K.J., Simandan, T.L. and Dix, T.A., *A facile route to cyclic and acyclic alkyl-arginines.* Synthetic Communications, 1998. **28**(4): p. 741-746.

104. Kennedy, K.J., Lundquist, J.T.t., Simandan, T.L., Kokko, K.P., Beeson, C.C., and Dix, T.A., *Design rationale, synthesis, and characterization of non-natural analogs of the cationic amino acids arginine and lysine.* J Pept Res, 2000. **55**(4): p. 348-58.

105. Corbin, J.L. and Reporter, M., *N-G-methylated arginines; a convenient preparation of N-G-methylarginine.* Anal Biochem, 1974. **57**(1): p. 310-2.

106. Bodanszky, M.a.B., A., *The practice of peptide synthesis*. 1984, Berlin: Springer-Verlag. 13.

107. Fujino, M., Wakimasu, M., and Kitada, C., *Further studies on the use of multi-substituted benzenesulfonyl groups for protection of the guanidino function of arginine.* Chem Pharm Bull, 1981. **29**: p. 2825-2831.

108. Moore, S.B., van der Hoek, J., de Capua, A., van Koetsveld, P.M., Hofland, L.J., Lamberts, S.W., and Goodman, M., *Discovery of iodinated somatostatin analogues selective for hsst2 and hsst5 with excellent inhibition of growth*

hormone and prolactin release from rat pituitary cells. J Med Chem, 2005. **48**(21): p. 6643-52.

109. Barany, G. and Merrifield, R.B., *The Peptides. Analysis, Synthesis, Biology*, ed. J. Meienhofer. Vol. 2. 1980, New York: Academic Press. 1-284.

110. Stewart, J.M. and Young, J.D., *Solid-Phase Peptide Synthesis.* Second ed. 1984, Rockford, Illinois: Pierce Chemical Company.

111. Fields, C.G., Lloyd, D.H., Macdonald, R.L., Otteson, K.M., and Noble, R.L., *HBTU activation for automated Fmoc solid-phase peptide synthesis.* Pept Res, 1991. **4**(2): p. 95-101.

112. Abrash, H.I. and Niemann, C., *Steric Hindrance in Alpha-Chymotrypsin-Catalyzed Reactions.* Biochemistry, 1963. **2**: p. 947-53.

113. Mahdi, F., Rehemtulla, A., Van Nostrand, W.E., Bajaj, S.P., and Schmaier, A.H., *Protease nexin-2/Amyloid beta-protein precursor regulates factor VIIa and the factor VIIa-tissue factor complex.* Thromb Res, 2000. **99**(3): p. 267-76.

114. Bieth, J.G., *In vivo significance of kinetic constants of protein proteinase inhibitors.* Biochem Med, 1984. **32**(3): p. 387-97.

115. Hasan, A.A., Cines, D.B., Zhang, J., and Schmaier, A.H., *The carboxyl terminus of bradykinin and amino terminus of the light chain of kininogens comprise an endothelial cell binding domain.* J Biol Chem, 1994. **269**(50): p. 31822-30.